GOBIERNO DE ESPAÑA
MINISTERIO DE CIENCIA, INNOVACIÓN Y UNIVERSIDADES
AGENCIA ESTATAL DE INVESTIGACIÓN
FEDER
Fondo Europeo de Desarrollo Regional
UNIÓN EUROPEA
"Una manera de hacer Europa"

Systematic nuclear potential for stable, weakly bound and exotic nuclei reactions

Dr. Juan Pablo Fernández García
Dpto. Física Atómica Molecular y Nuclear
Universidad de Sevilla

The International Research Collaborators

Argentina:
- Laboratorio Tandar - Comisión Nacional de Energía Atómica (CNEA)

Brazil:
- Laboratorio Aberto de Física Nuclear (LAFN) – Universidade de São Paulo (IFUSP)

Italy:
- Laboratori Nazionale del Sud (LNS) – Istituto Nazionale di Fisica Nucleare (INFN).
- Università degli Studi di Padova

Spain:
- Universidad de Sevilla (US)
- Universidad de Huelva (UHU)

Portugal:
- Faculty of Sciences of Lisbon (LIP)

Mexico:
- Universidad Nacional Autónoma de México (UNAM)

Costa Rica:
- Universidad de Costa Rica - CICANUM

1. The Laboratories and SETUP´s
2. The Theoretical Optical Model
3. Experimental Data x Theoretical Calculations
4. Conclusions

1. <u>The Laboratories and SETUP´s</u>

2. The Theoretical Optical Model

3. Experimental Data x Theoretical Calculations

4. Conclusions

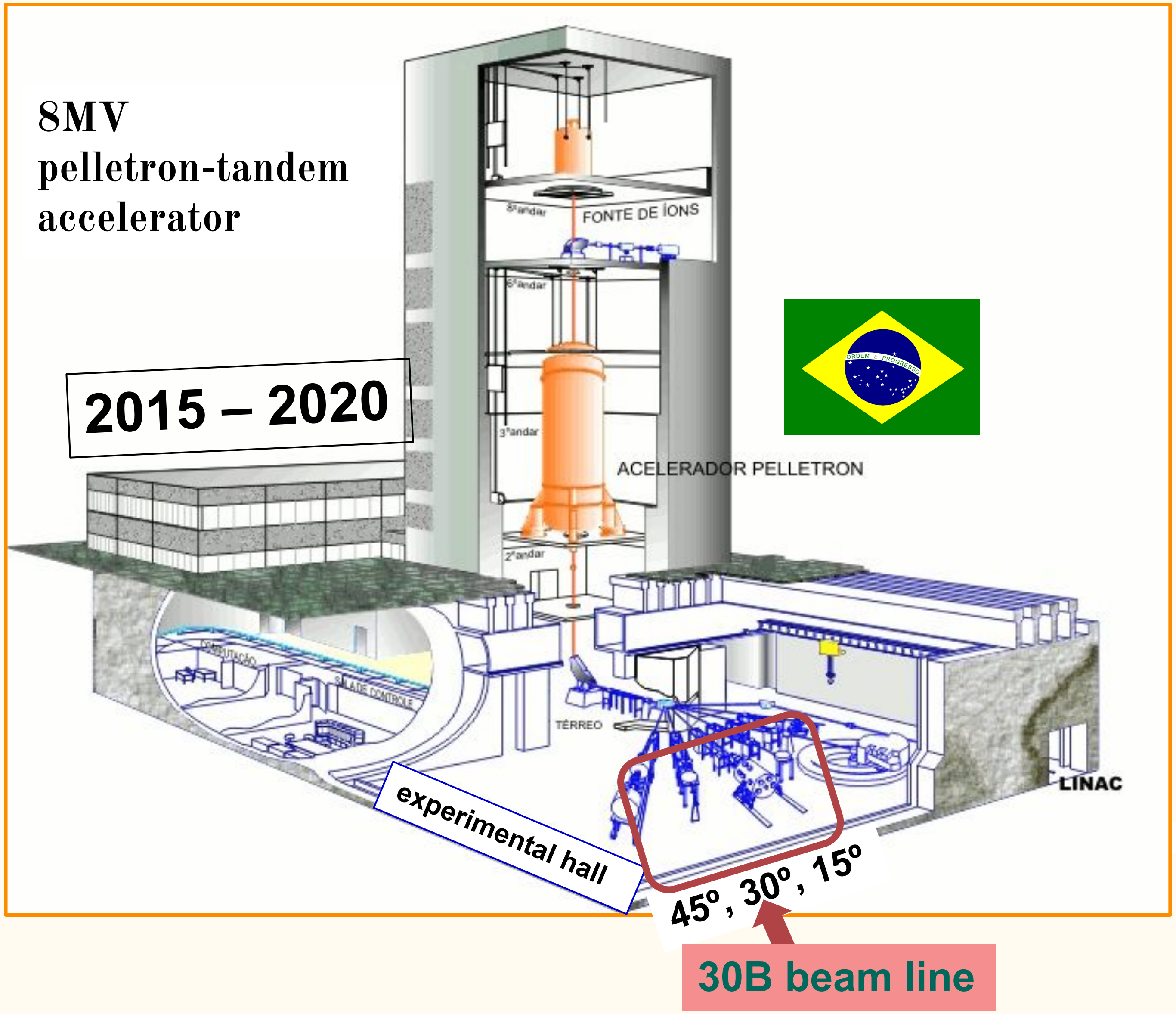

- **Open Laboratory of Nuclear Physics**

Experimental hall is divided into
two rooms: A and B
Room B: 3 experimental beam lines
15B; <u>30B</u> and 45B (RIBRAS)

Goals:

➢ **Permanent dedicated setup**

➢ **Long term experimental campaigns**

✓ beam time availability
✓ good statistics
✓ precise new data

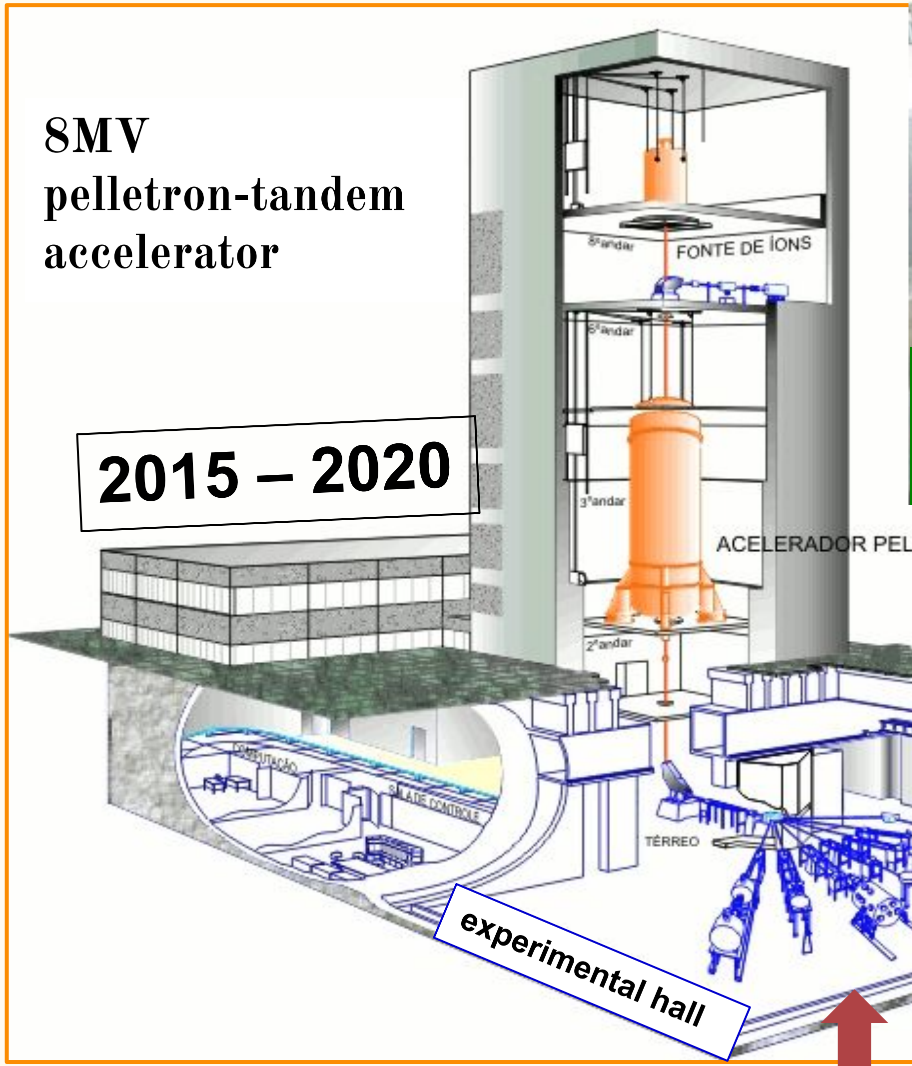

30B beam line

- ➢ Permanent dedicated setup
- ➢ Long term experimental campaigns
  - – ^{6,7}Li+^{120}Sn,^{197}Au (2017)
  - – ^{10,11}B+^{120}Sn,^{197}Au (2018-9)
  - – ^{12,13}C+^{120}Sn,^{197}Au (2020)

Local Research Team:

- ❑ Leandro Gasques
- ❑ Luiz Carlos Chamon
- ❑ Alinka Lèpine
- ❑ Valdir Scarduelli
- ❑ Vinicius Zagatto
- ❑ José Roberto Brandão

Theoretical Support:

- ❑ University of Seville (US) (M. R. Gallardo)
- ❑ Università degli Studi di Padova (J. Casal)

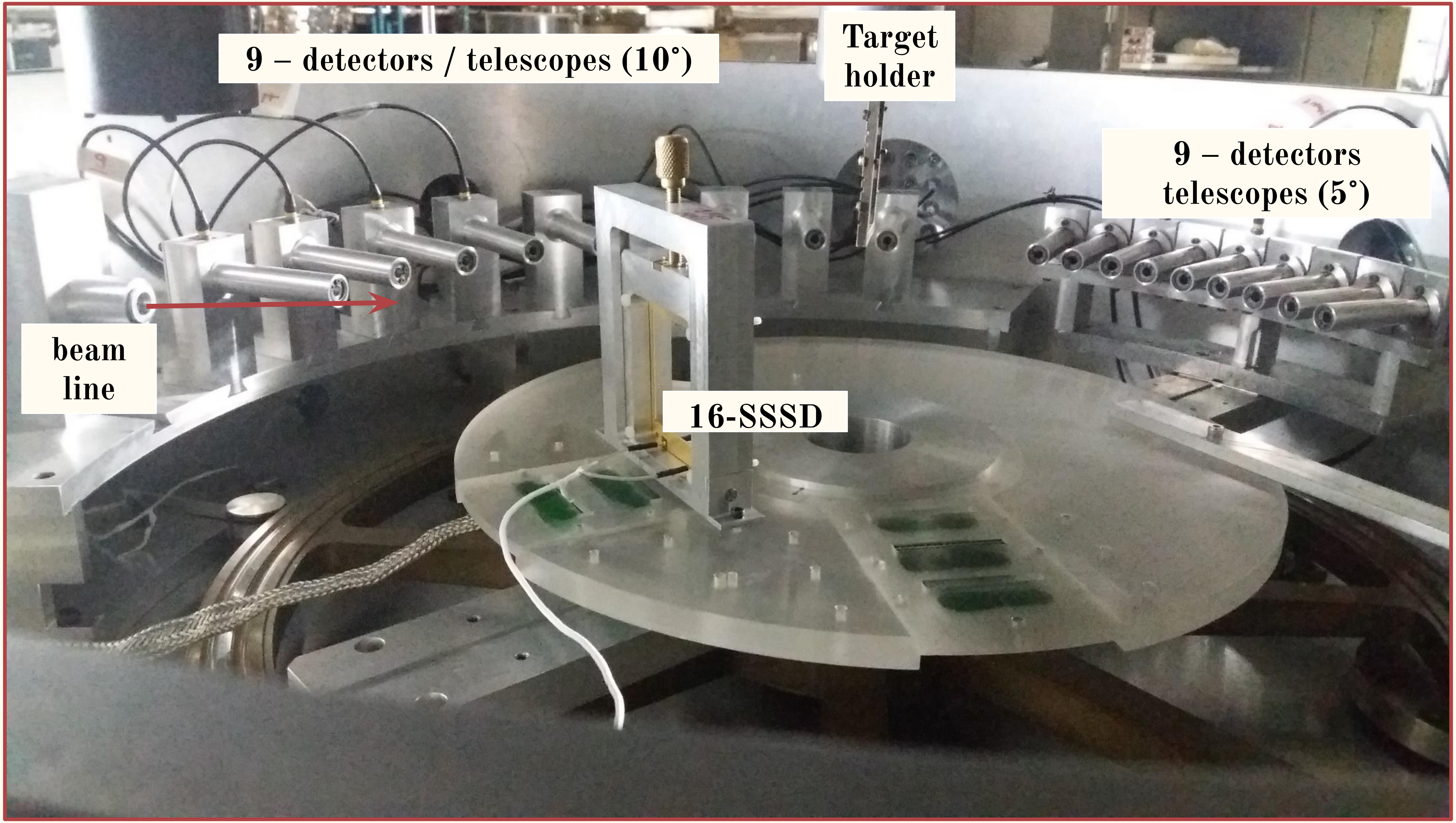
9 – detectors / telescopes (10°)
Target holder
9 – detectors telescopes (5°)
beam line
16-SSSD

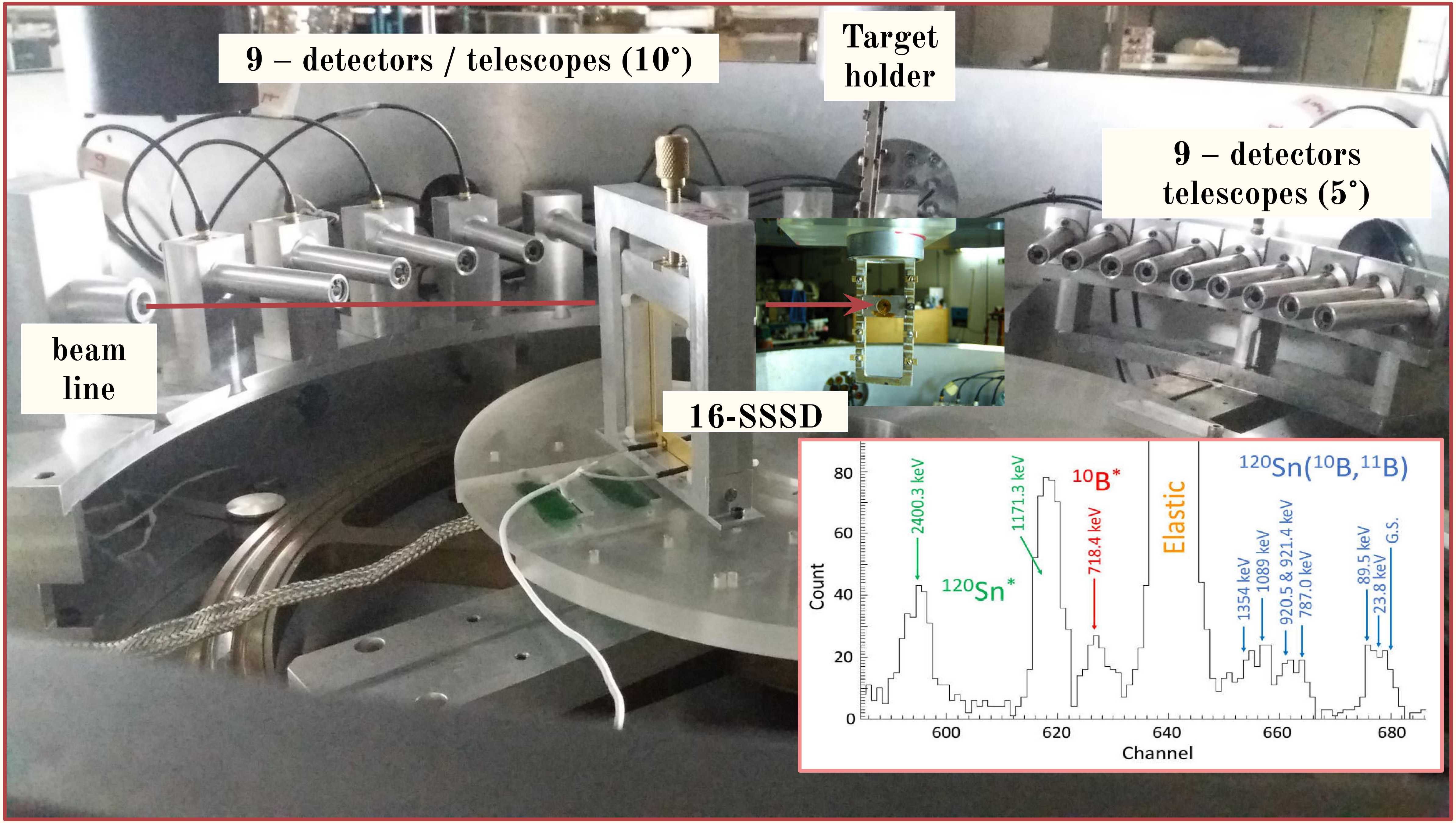
9 – detectors / telescopes (10°)
Target holder
9 – detectors telescopes (5°)
beam line
16-SSSD
120Sn(10B,11B)
10B*
Elastic
120Sn*
2400.3 keV
1171.3 keV
718.4 keV
1354 keV
1089 keV
920.5 & 921.4 keV
787.0 keV
89.5 keV
23.8 keV
G.S.
Count
Channel
0
20
40
60
80
600
620
640
660
680

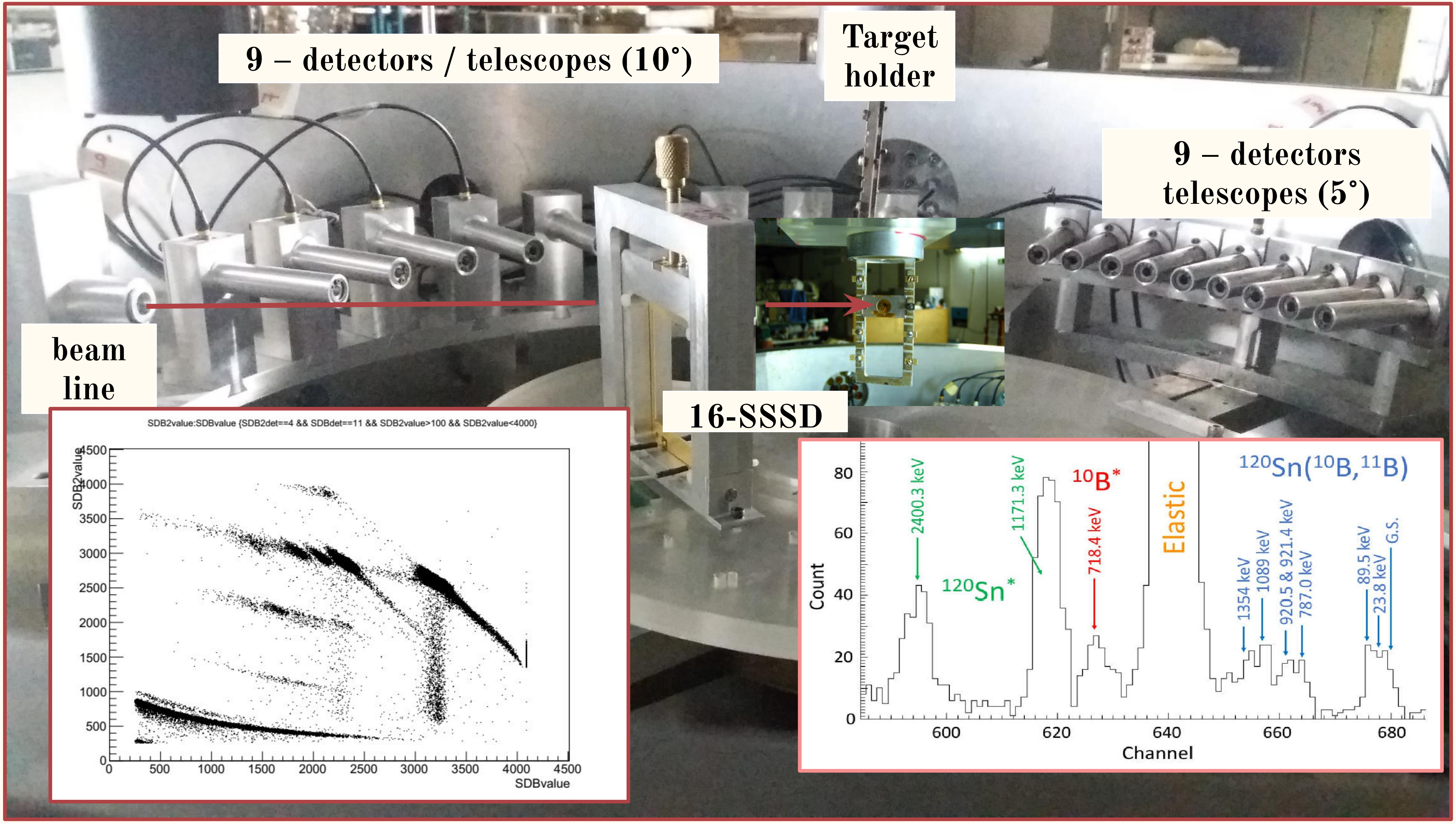
9 – detectors / telescopes (10°)
Target holder
9 – detectors telescopes (5°)
beam line
16-SSSD
SDB2value:SDBvalue {SDB2det==4 && SDBdet==11 && SDB2value>100 && SDB2value<4000}
SDB2value
SDBvalue
0
500
1000
1500
2000
2500
3000
3500
4000
4500
120Sn(10B,11B)
Count
Channel
600
620
640
660
680
0
20
40
60
80
2400.3 keV
1171.3 keV
120Sn*
10B*
718.4 keV
Elastic
1354 keV
1089 keV
920.5 & 921.4 keV
787.0 keV
89.5 keV
23.8 keV
G.S.

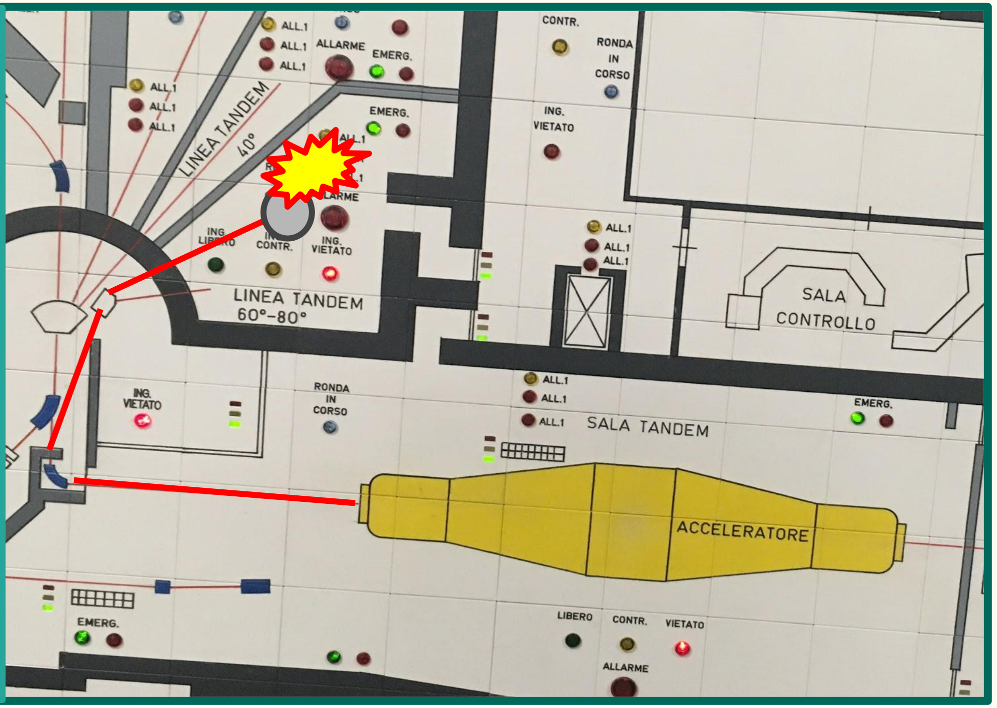

– $^{7}Li + ^{119}Sn$ (2017)

– $^{10}Be + ^{120}Sn$ (03/2020)

INFN Istituto Nazionale di Fisica Nucleare LNS -Catania

Local Research Team:

- A. Di Pietro
- P. Figuera
- R. Spartá
- D. Torresi
- M. La Cognata

Theoretical Support:

- University of Seville (US) (M. R. Gallardo)
- Università degli Studi di Padova (J.Casal)
- University of Seville (US) (A.M. Moro)
- INFN-Pisa (Jin Lei)

14MV pelletron-tandem accelerator

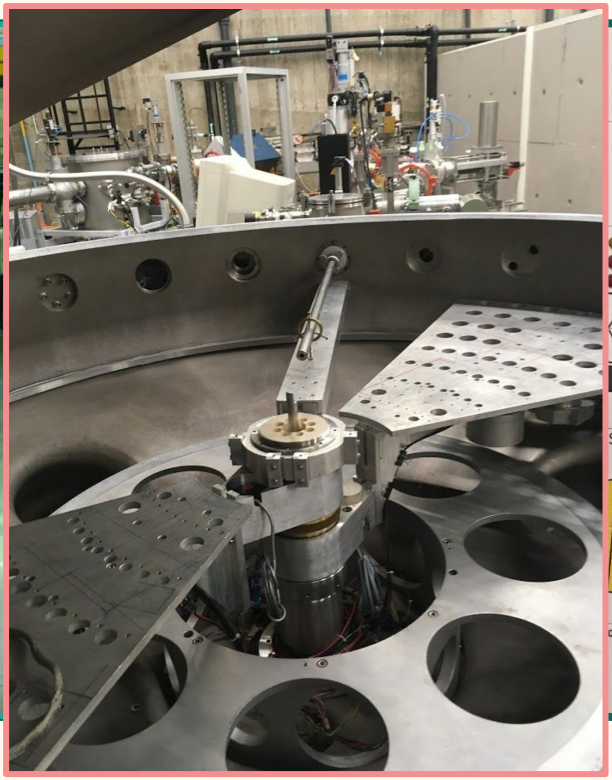

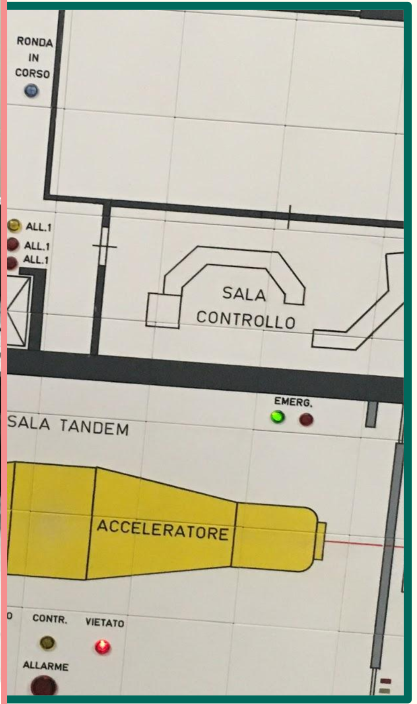

– $^{7}Li+^{119}Sn$ (2017)

– $^{10}Be+^{120}Sn$ (03/2020)

Istituto Nazionale di Fisica Nucleare
LNS -Catania

Local Research Team:

- A. Di Pietro
- P. Figuera
- R. Spartá
- D. Torresi
- M. La Cognata

Theoretical Support:

- University of Seville (US) (M. R. Gallardo)
- Università degli Studi di Padova (J.Casal)
- University of Seville (US) (A.M. Moro)
- INFN-Pisa (Jin Lei)

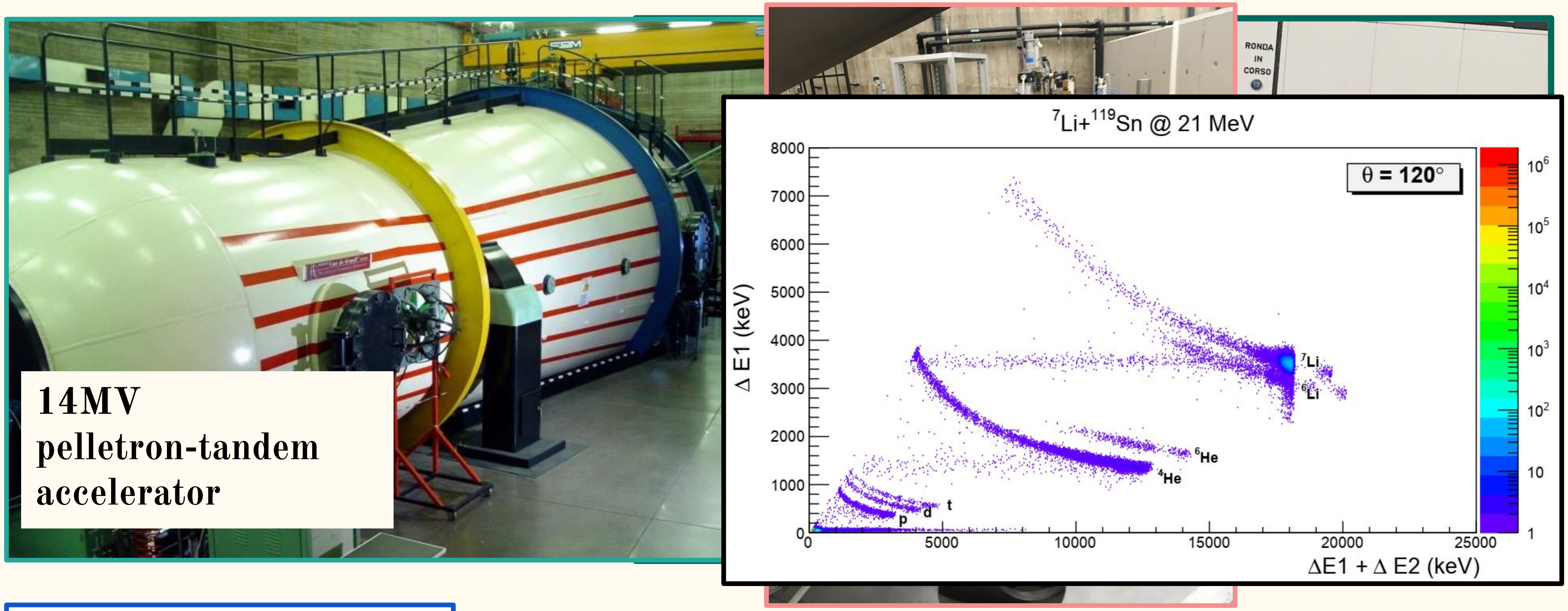

– ^{7}Li+^{119}Sn (2017)

– ^{10}Be+^{120}Sn (03/2020)

INFN
Istituto Nazionale di Fisica Nucleare
LNS -Catania

Local Research Team:

- A. Di Pietro
- P. Figuera
- R. Spartá
- D. Torresi
- M. La Cognata

Theoretical Support:

- University of Seville (US) (M. R. Gallardo)
- Università degli Studi di Padova (J.Casal)
- University of Seville (US) (A.M. Moro)
- INFN-Pisa (Jin Lei)

14MV pelletron-tandem accelerator

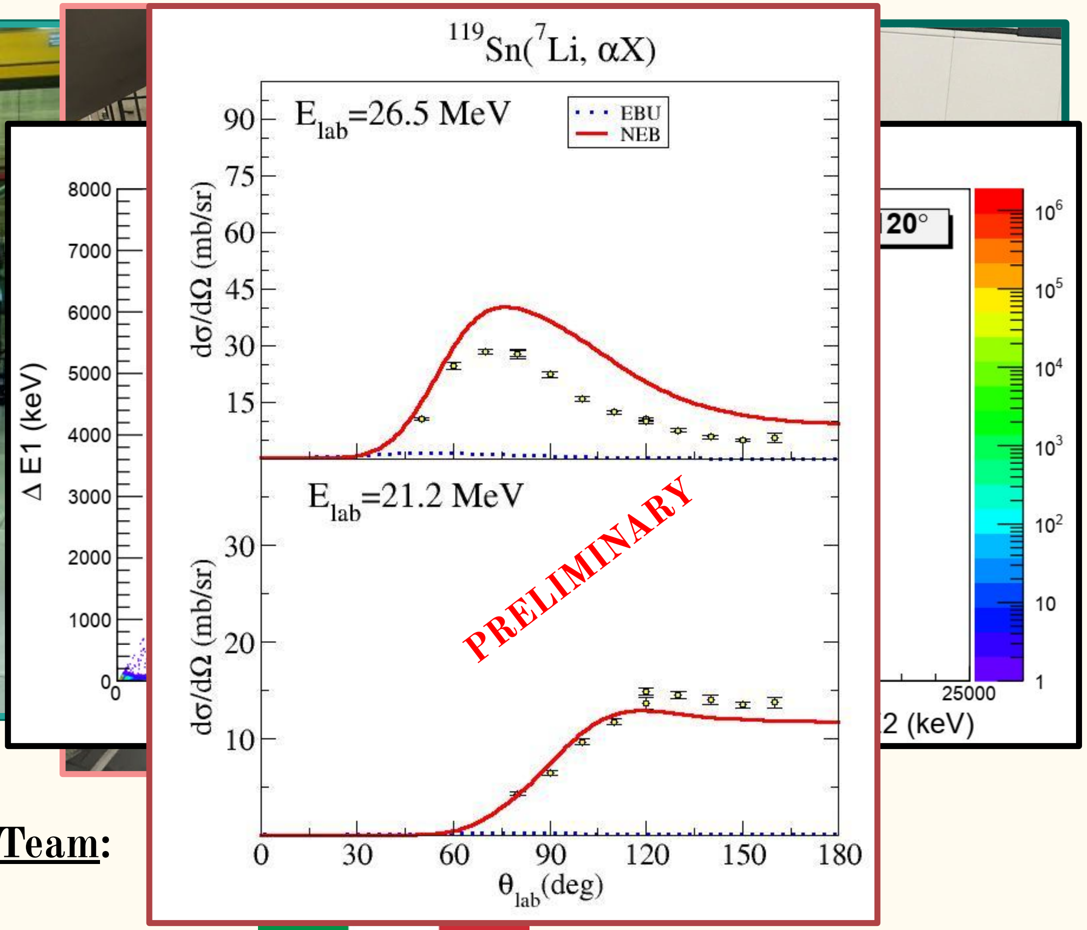

– $^{7}Li+^{119}Sn$ (2017)

– $^{10}Be+^{120}Sn$ (03/2020)

INFN
Istituto Nazionale di Fisica Nucleare
LNS -Catania

Local Research Team:

- A. Di Pietro
- P. Figuera
- R. Spartá
- D. Torresi
- M. La Cognata

Theoretical Support:

- University of Seville (US) (M. R. Gallardo)
- Università degli Studi di Padova (J.Casal)
- University of Seville (US) (A.M. Moro)
- INFN-Pisa (Jin Lei)

14MV pelletron-tandem accelerator

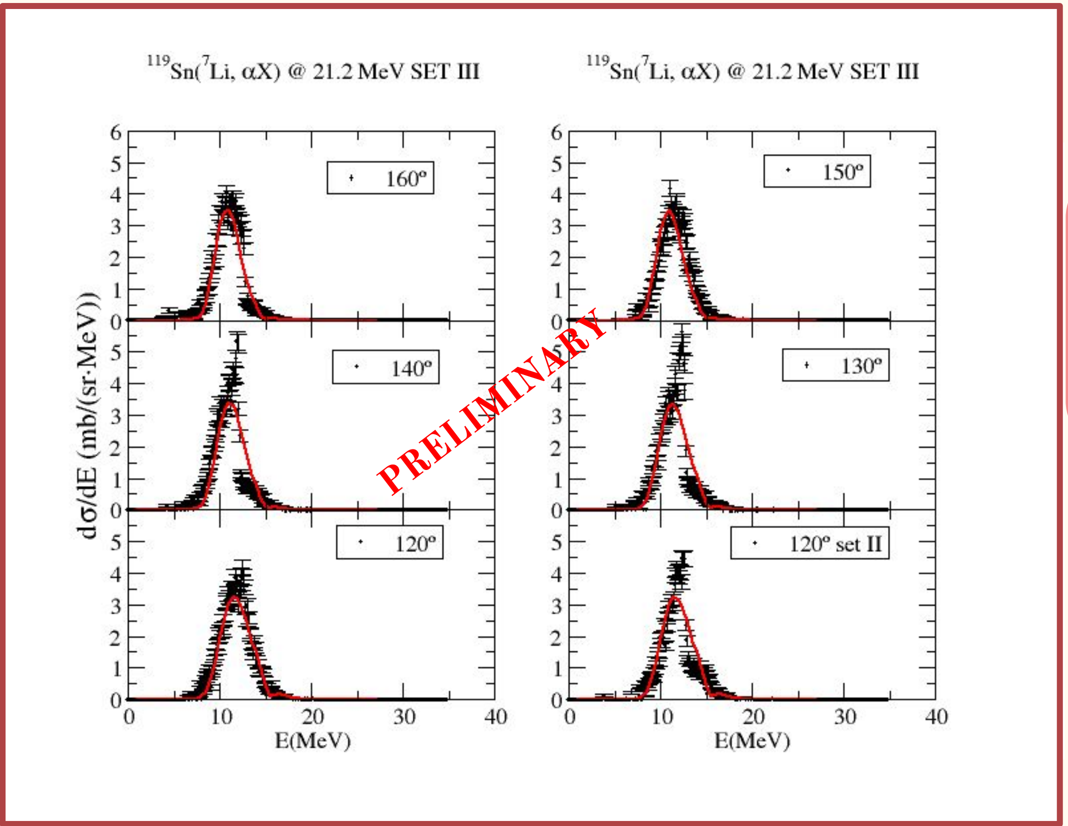

– ^{7}Li+^{119}Sn (2017)

– ^{10}Be+^{120}Sn (03/2020)

INFN
Istituto Nazionale
di Fisica Nucleare
LNS -Catania

Local Research Team:

- A. Di Pietro
- P. Figuera
- R. Spartá
- D. Torresi
- M. La Cognata

Theoretical Support:

- University of Seville (US) (M. R. Gallardo)
- Università degli Studi di Padova (J.Casal)
- University of Seville (US) (A.M. Moro)
- INFN-Pisa (Jin Lei)

14MV pelletron-tandem accelerator

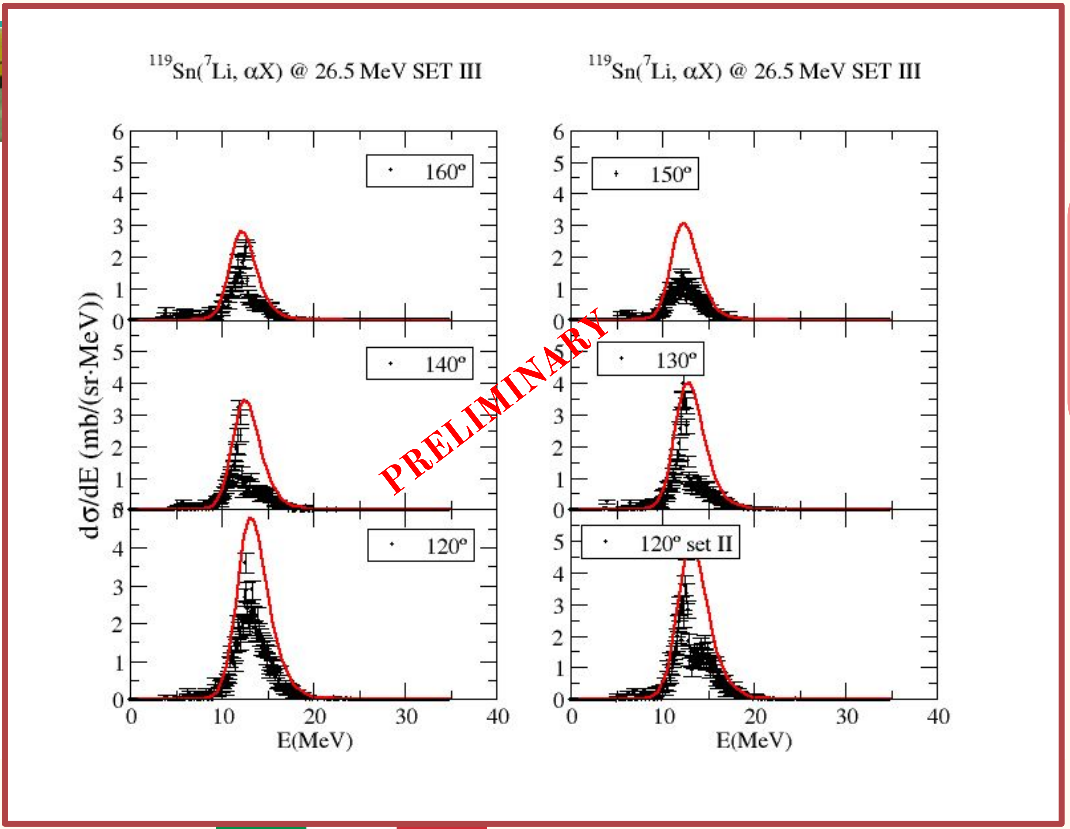

– $^{7}Li+^{119}Sn$ (2017)

– $^{10}Be+^{120}Sn$ (03/2020)

Local Research Team:

- A. Di Pietro
- P. Figuera
- R. Spartá
- D. Torresi
- M. La Cognata

Theoretical Support:

- University of Seville (US) (M. R. Gallardo)
- Università degli Studi di Padova (J.Casal)
- University of Seville (US) (A.M. Moro)
- INFN-Pisa (Jin Lei)

Istituto Nazionale di Fisica Nucleare LNS -Catania

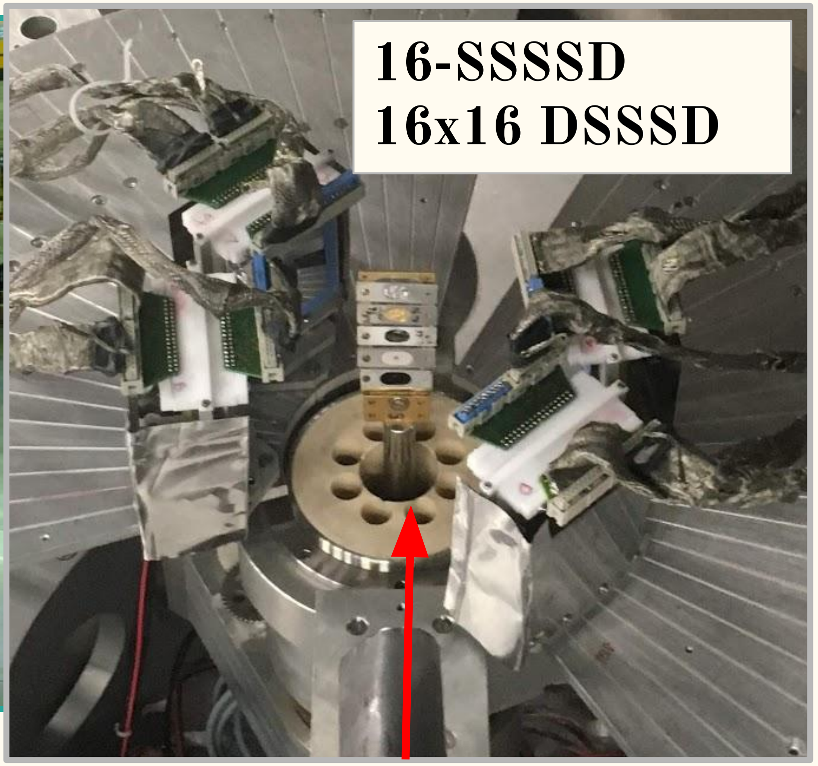

– $^{7}Li+^{119}Sn$ (2017)

→ – $^{10}Be+^{120}Sn$ (03/2020)

INFN
Istituto Nazionale di Fisica Nucleare
LNS -Catania

Local Research Team:

- A. Di Pietro
- P. Figuera
- R. Spartá
- D. Torresi
- M. La Cognata

Theoretical Support:

- University of Seville (US) (M. R. Gallardo)
- Università degli Studi di Padova (J.Casal)
- University of Seville (US) (A.M. Moro)
- INFN-Pisa (Jin Lei)

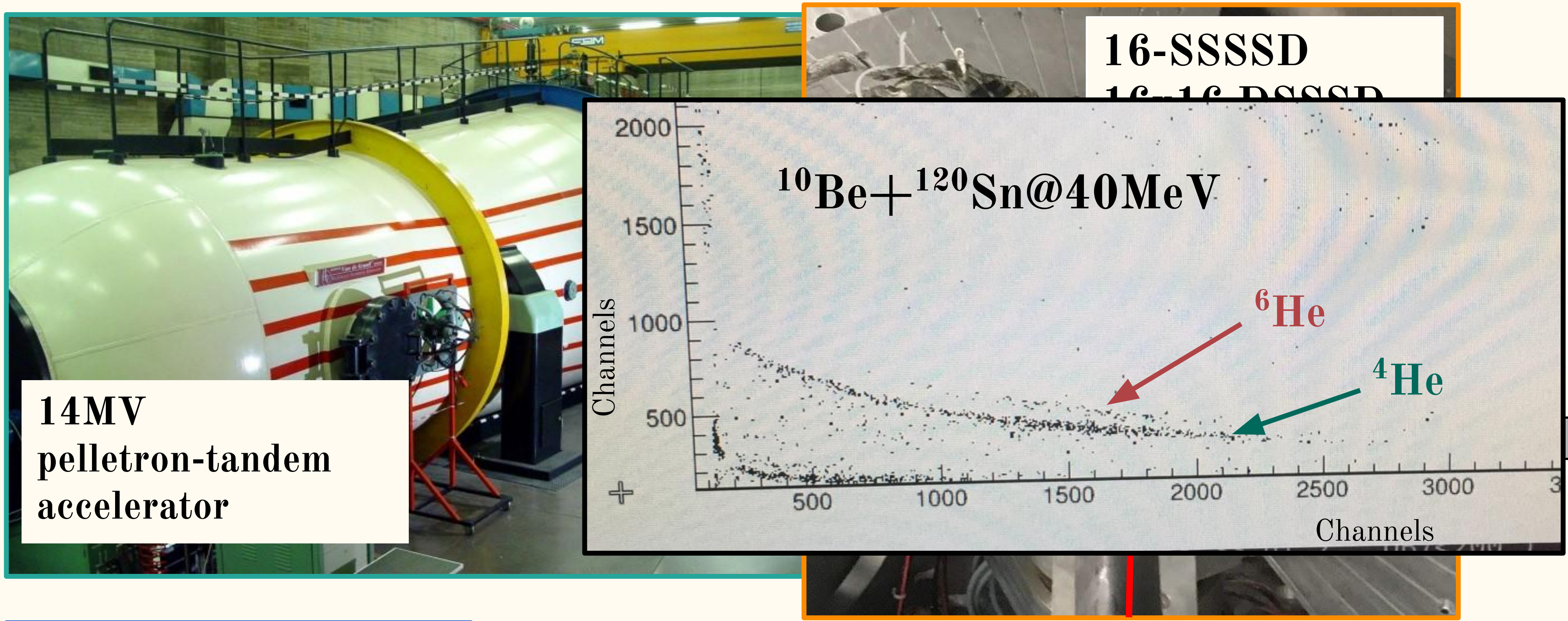

- $^{7}Li+^{119}Sn$ (2017)
- $^{10}Be+^{120}Sn$ (03/2020)

INFN Istituto Nazionale di Fisica Nucleare LNS -Catania

Local Research Team:

- A. Di Pietro
- P. Figuera
- R. Spartá
- D. Torresi
- M. La Cognata

Theoretical Support:

- University of Seville (US) (M. R. Gallardo)
- Università degli Studi di Padova (J.Casal)
- University of Seville (US) (A.M. Moro)
- INFN-Pisa (Jin Lei)

Comisión Nacional de Energía Atómica

20MV pelletron-tandem accelerator

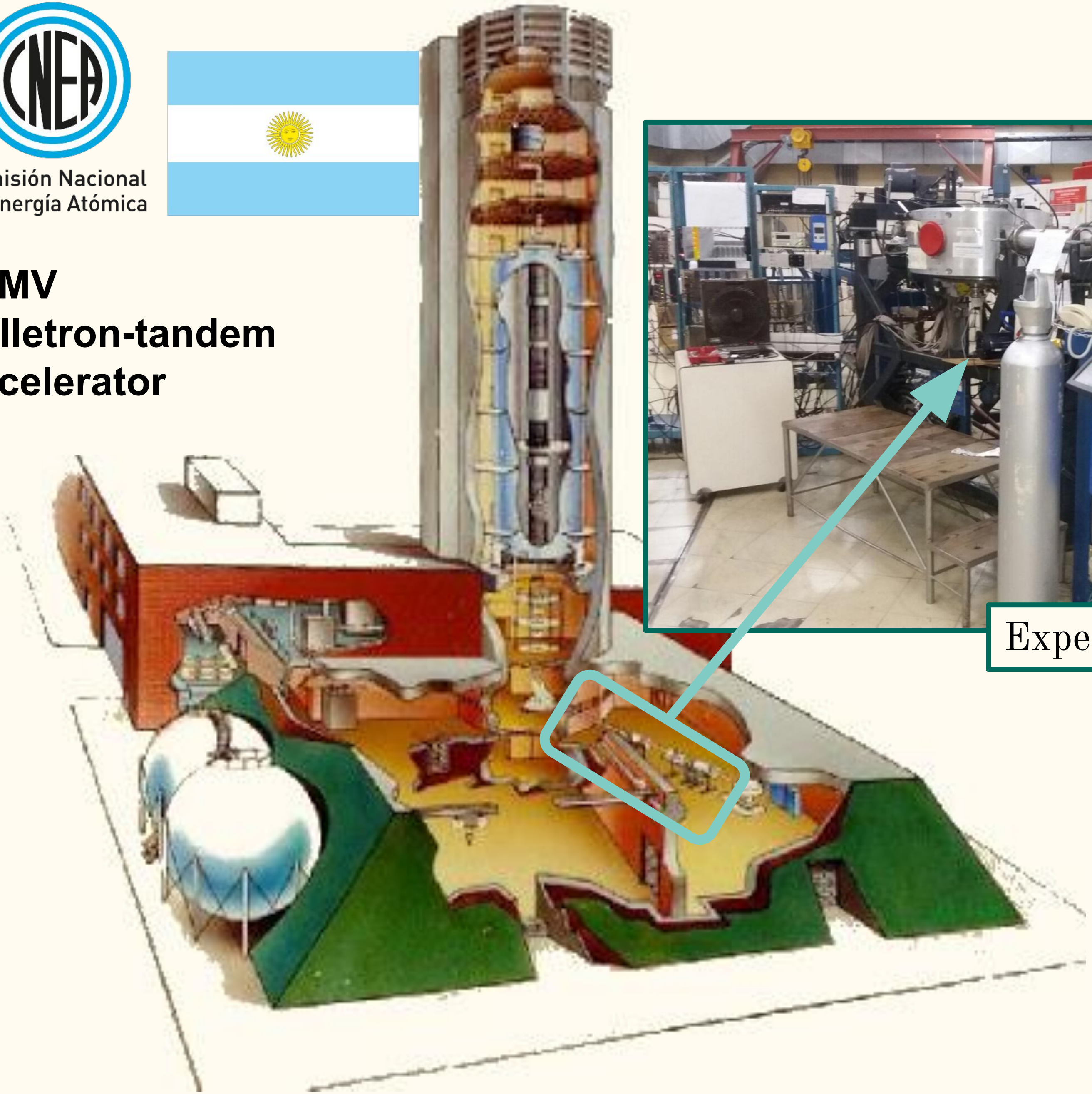

Experimental beam line

- Permanent dedicated setup
- Long term experimental campaigns

– $^{9}Be+^{120}Sn$ (2018)

– $^{9}Be+^{197}Au$ (2018)

– $^{10}B+^{197}Au$ (2019)

– $^{12,13}C+^{197}Au$ (2020)

Local Research Team:

- Daniel Abriola
- Andrés Arazi
- Daniel Hojman
- M. A. Carmona
- Ezequiel Cárdenas
- Guillermo Martín
- José Fernández Nielo

Theoretical Support:

- University of Seville (US) (M. R. Gallardo)
- Università degli Studi di Padova (J. Casal)

Comisión Nacional de Energía Atómica

- Permanent dedicated setup
- Long term experimental campaigns

20MV pelletron-tandem accelerator

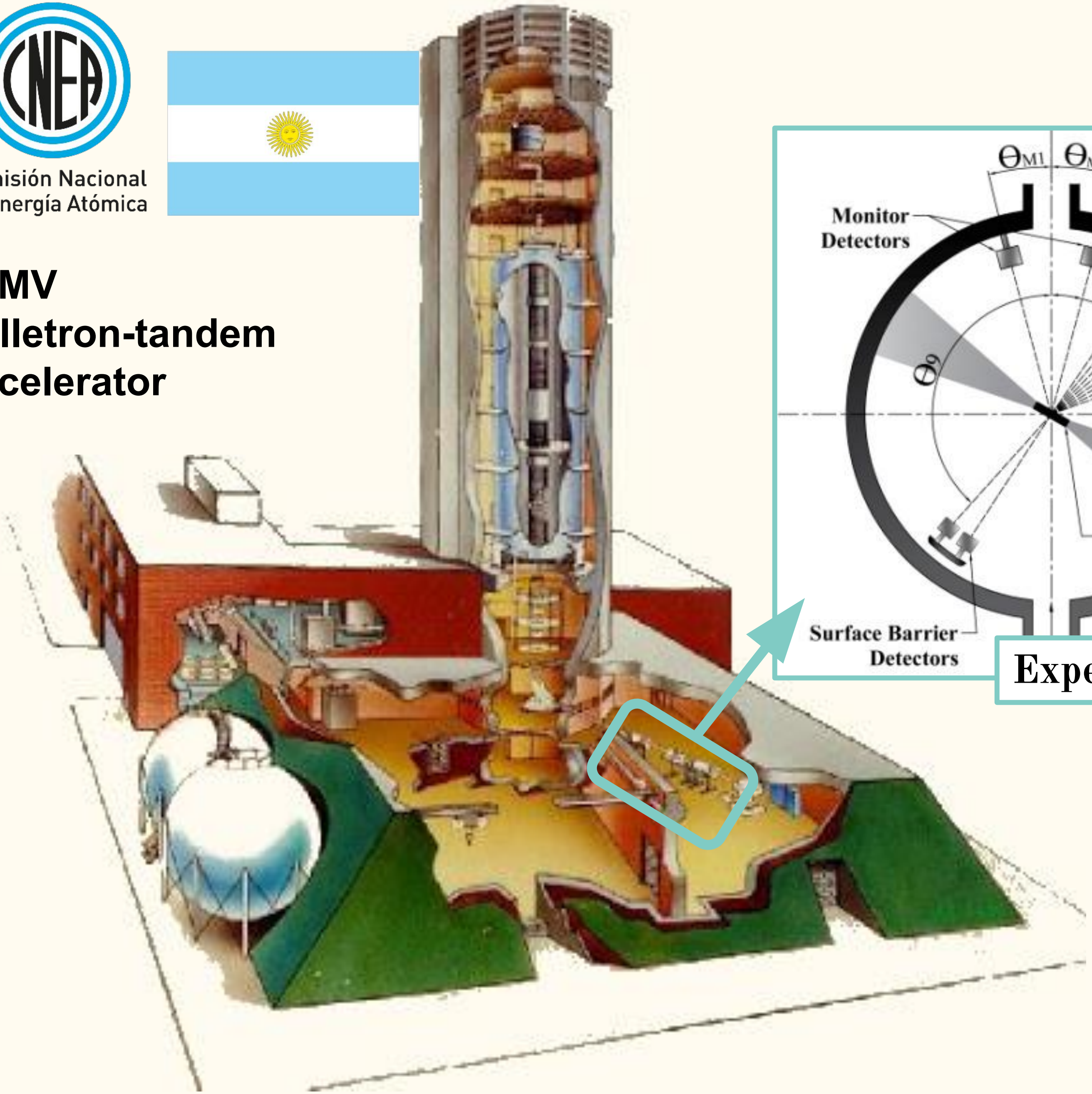

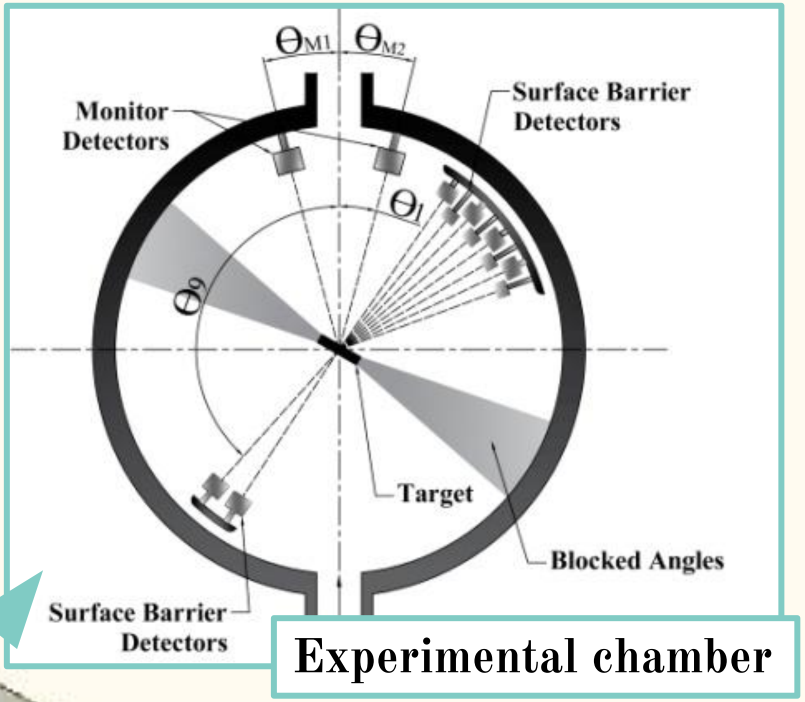

Experimental chamber

– $^{9}Be+^{120}Sn$ (2018)

– $^{9}Be+^{197}Au$ (2018)

– $^{10}B+^{197}Au$ (2019)

– $^{12,13}C+^{197}Au$ (2020)

Local Research Team:

- Daniel Abriola
- Andrés Arazi
- Daniel Hojman
- M. A. Carmona
- Ezequiel Cárdenas
- Guillermo Martín
- José Fernández Nielo

Theoretical Support:

- University of Seville (US) (M. R. Gallardo)
- Università degli Studi di Padova (J. Casal)

Comisión Nacional de Energía Atómica

20MV pelletron-tandem accelerator

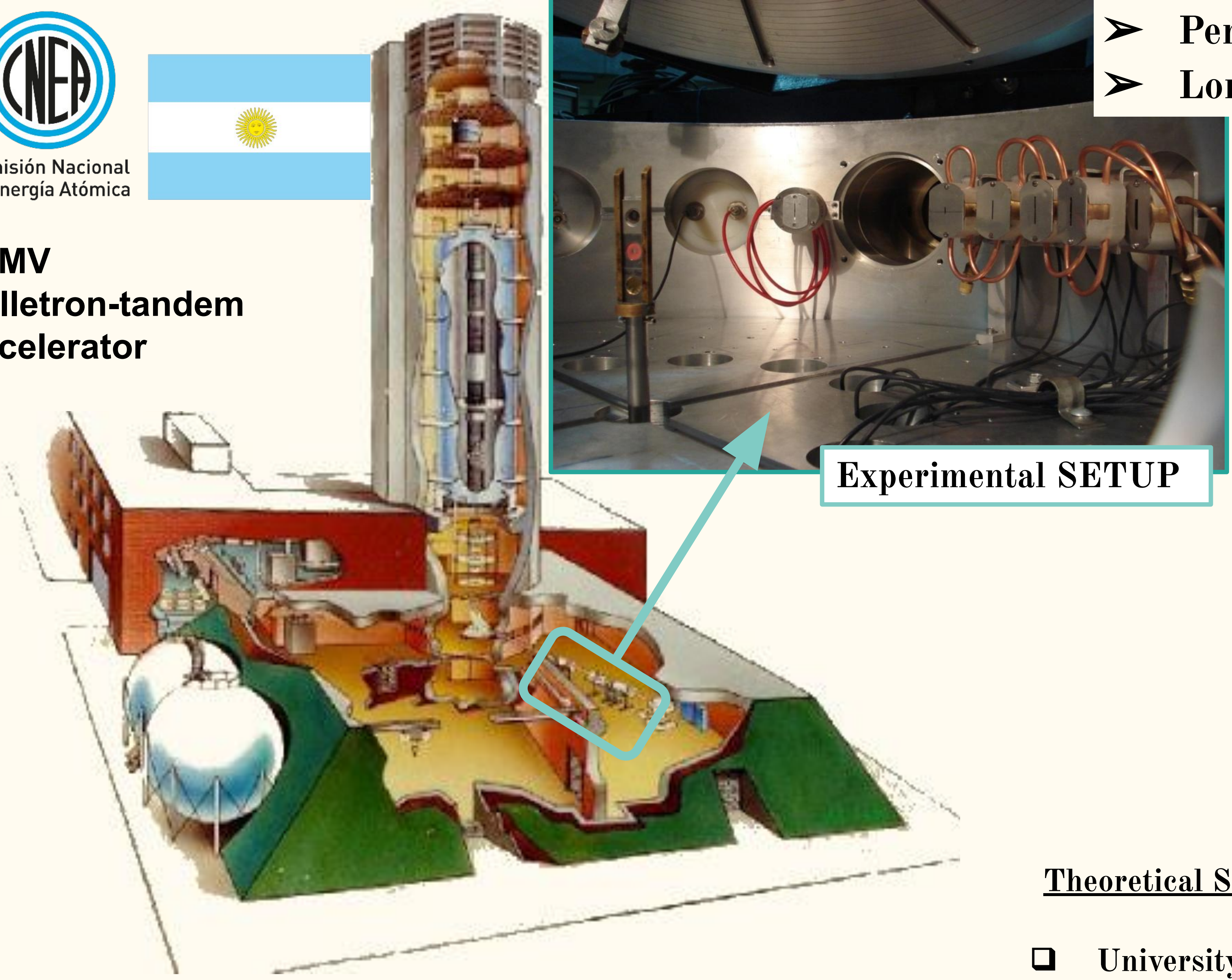

- ➢ Permanent dedicated setup
- ➢ Long term experimental campaigns

$-{}^{9}\mathrm{Be}+{}^{120}\mathrm{Sn}$ (2018)

$-{}^{9}\mathrm{Be}+{}^{197}\mathrm{Au}$ (2018)

$-{}^{10}\mathrm{B}+{}^{197}\mathrm{Au}$ (2019)

$-{}^{12,13}\mathrm{C}+{}^{197}\mathrm{Au}$ (2020)

<u>Local Research Team</u>:

- ❑ Daniel Abriola
- ❑ Andrés Arazi
- ❑ Daniel Hojman
- ❑ M. A. Carmona
- ❑ Ezequiel Cárdenas
- ❑ Guillermo Martín
- ❑ José Fernández Nielo

<u>Theoretical Support</u>:

- ❑ University of Seville (US) (M. R. Gallardo)
- ❑ Università degli Studi di Padova (J. Casal)

Comisión Nacional de Energía Atómica

20MV pelletron-tandem accelerator

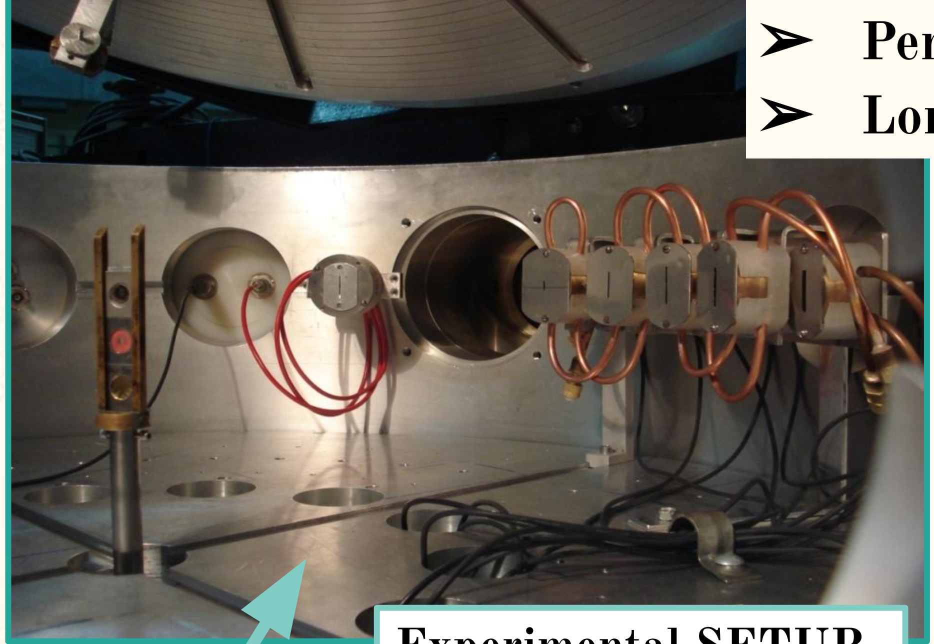

Experimental SETUP

- ➢ Permanent dedicated setup
- ➢ Long term experimental campaigns

$-{}^{9}Be+{}^{120}Sn$ (2018)

$-{}^{9}Be+{}^{197}Au$ (2018)

$-{}^{10}B+{}^{197}Au$ (2019)

$-{}^{12,13}C+{}^{197}Au$ (2020)

- ❑ ELASTIC SCATTERING
- ❑ INELASTIC EXCITATION
- ❑ NUCLEON TRANSFER

L. Gasques *et al.*PRC101 (4), 044604 (2020)

- ❑ FUSION

M. Aversa *et al.*, PRC101 (4), 044601 (2020)

Local Research Team:

- ❑ Daniel Abriola
- ❑ Andrés Arazi
- ❑ Daniel Hojman
- ❑ M. A. Carmona
- ❑ Ezequiel Cárdenas
- ❑ Guillermo Martín
- ❑ José Fernández Nielo

- ❑ ${}^{10}B+{}^{197}Au$ @ 38, 40, 42, 43, 44, 45, 46, 47, 48, 49, 50, 51, 52, 53, 54, 55, 56, 57, 58, 59, 61 MeV

Theoretical Support:

- ❑ University of Seville (US) (M. R. Gallardo)
- ❑ Università degli Studi di Padova (J. Casal)

Comisión Nacional de Energía Atómica

20MV pelletron-tandem accelerator

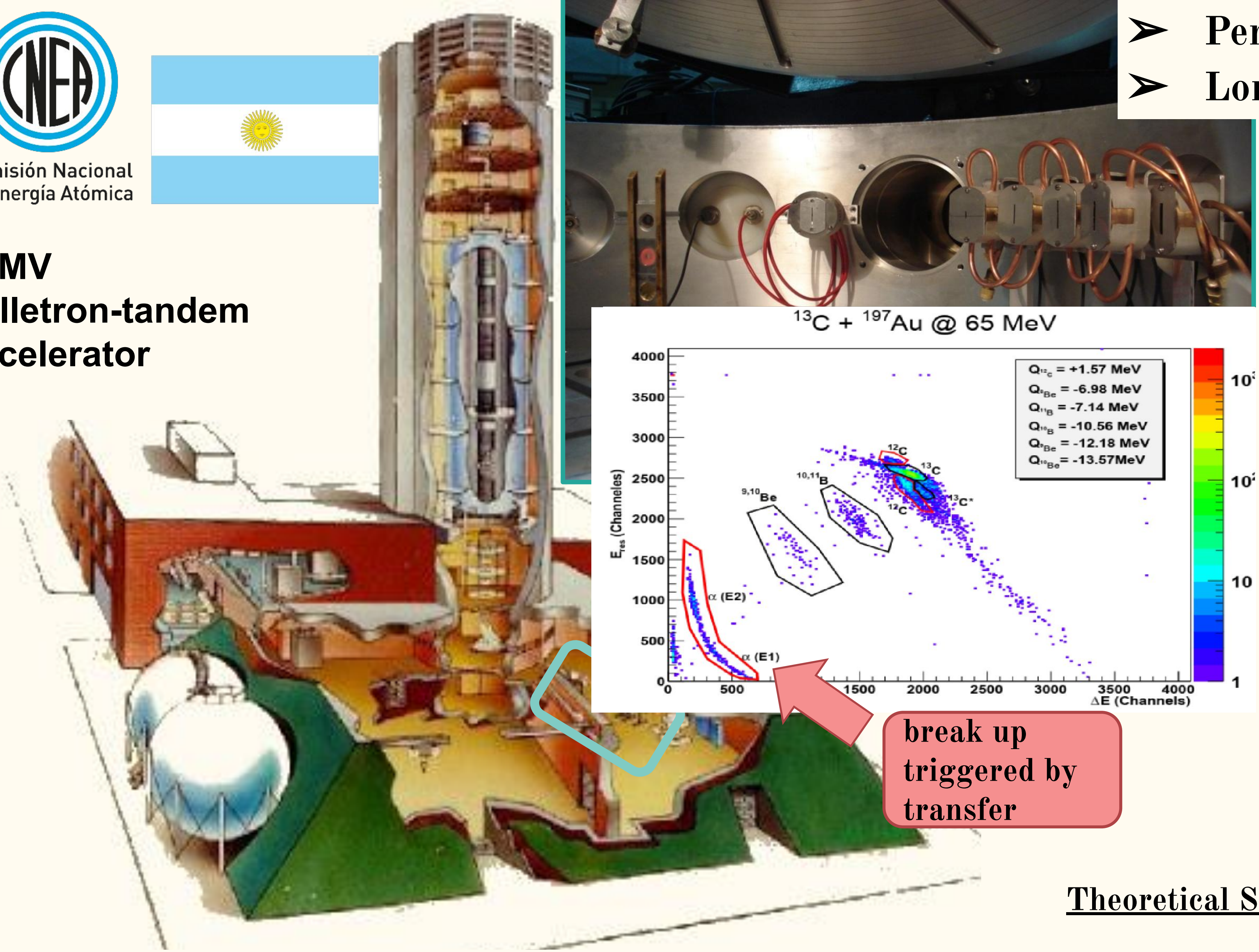

- ➢ Permanent dedicated setup
- ➢ Long term experimental campaigns

$-{}^{9}\text{Be}+{}^{120}\text{Sn}$ (2018)

$-{}^{9}\text{Be}+{}^{197}\text{Au}$ (2018)

$-{}^{10}\text{B}+{}^{197}\text{Au}$ (2019)

$-{}^{12,13}\text{C}+{}^{197}\text{Au}$ (2020)

break up triggered by transfer

Local Research Team:

- ❑ Daniel Abriola
- ❑ Andrés Arazi
- ❑ Daniel Hojman
- ❑ M. A. Carmona
- ❑ Ezequiel Cárdenas
- ❑ Guillermo Martín
- ❑ José Fernández Nielo

Theoretical Support:

- ❑ University of Seville (US) (M. R. Gallardo)
- ❑ Università degli Studi di Padova (J. Casal)

- ❑ $^{13}\text{C}+{}^{197}\text{Au}$ @ 60, 65 and 70 MeV (2018)

FROM AN EXPERIMENTAL POINT OF VIEW

We have four main TOOLS:

1. Access to the facilities.
2. High beam intensities.
3. Permanent/dedicated experimental setups.
4. Long term experimental campaigns.

RECENT GOOD EXPERIMENTAL DATA ARE AVAILABLE

1. The Laboratories and SETUP´s

2. The Theoretical Optical Model

3. Experimental Data x Theoretical Calculations

4. Conclusions

GOALS:

- ✔ How the weakly (**stable or exotic**) bound structures affect the dynamics of nuclei reactions?
- ✔ May theoretical models developed to study **stable nuclei** be applied to **weakly bound & exotic** ones?

CONCEPTS:

- ❑ The **elastic scattering** is the simplest process to test a **theoretical model.**
- ❑ The **optical model (OM)** is the most used theoretical approach for the corresponding **DATA** analysis.

$$U_N(R,E) \approx U_{opt}(R) = V(R) + iW(R)$$

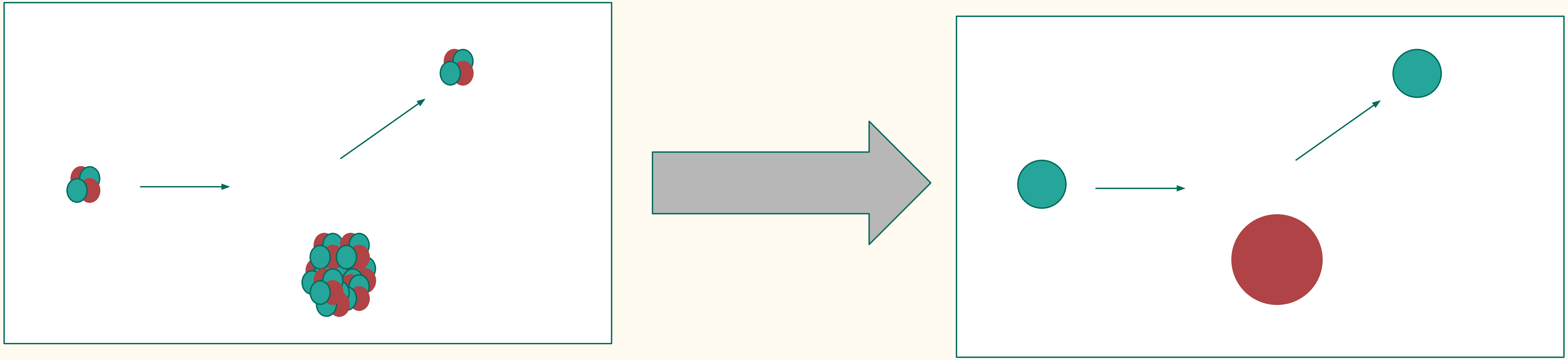

Optical Model

The imaginary part of the nuclear potential represents the absorption of the elastic channel.

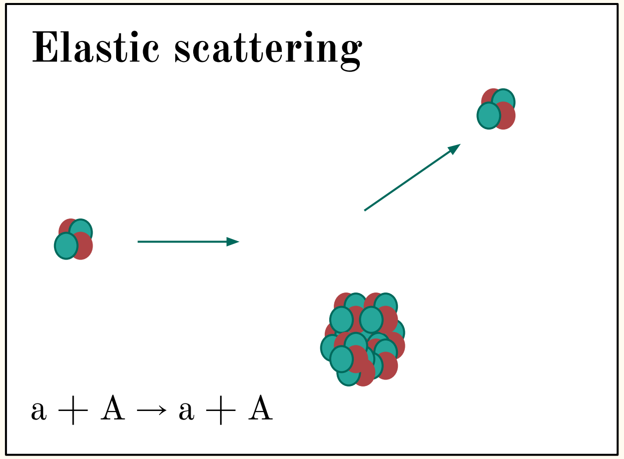

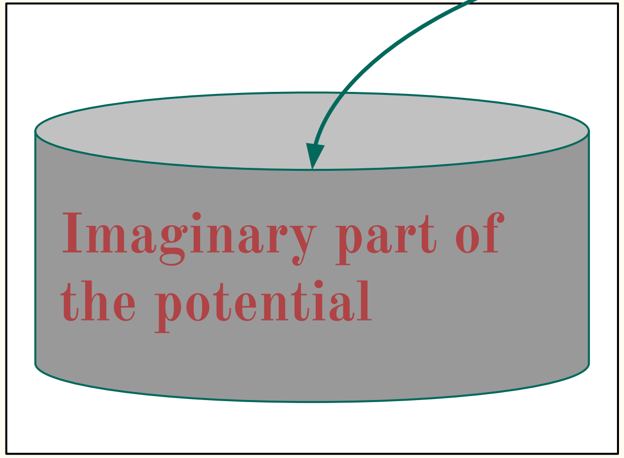

- Inelastic scattering
- Transfer reaction
- Breakup reaction
- Knock-out reaction
- Pick-up reaction
- Fusion

$$U_N(R, E) \approx U_{opt}(R) = V(R) + iW(R)$$

Double-folding nuclear São Paulo potential (SPP).

$$-\frac{\hbar^2}{2\mu}\nabla^2\Psi(R) + U(R,E)\Psi(R) = E\Psi(R)$$

Double-folding nuclear São Paulo potential (SPP).

$$-\frac{\hbar^2}{2\mu}\nabla^2\Psi(R) + U(R,E)\Psi(R) = E\Psi(R)$$

$$U(R,E) \approx U_N(R) + V_{Coul}(R) \approx U_{opt(R)} + V_{Coul}(R)$$

Double-folding nuclear São Paulo potential (SPP).

$$-\frac{\hbar^2}{2\mu}\nabla^2\Psi(R) + U(R,E)\Psi(R) = E\Psi(R)$$

$$U(R,E) \approx U_N(R) + V_{Coul}(R) \approx U_{opt(R)} + V_{Coul}(R)$$

$$U_{opt}(R) = V_{bare}(R) + V_{pol}(R) + i\,W_{pol}(R)$$

$$U_{opt}(R) = N_R V_{SPP}(R) + N_i V_{SPP}(R)$$

real potential

imaginary potential

Double-folding nuclear São Paulo potential (SPP).

$$U_{opt}(R) = N_R V_{SPP}(R) + N_i V_{SPP}(R)$$

$$V_{\mathrm{SPP}}(R) = V_{\mathrm{Fold}}(R) e^{-4v^2/c^2}$$

$$V_{\mathrm{Fold}}(R) = \int\int \rho_1(\vec{r}_1)\rho_2(\vec{r}_2)\nu_{NN}(\vec{R} - \vec{r}_1 + \vec{r}_2)\, d\vec{r}_1\, d\vec{r}_2$$

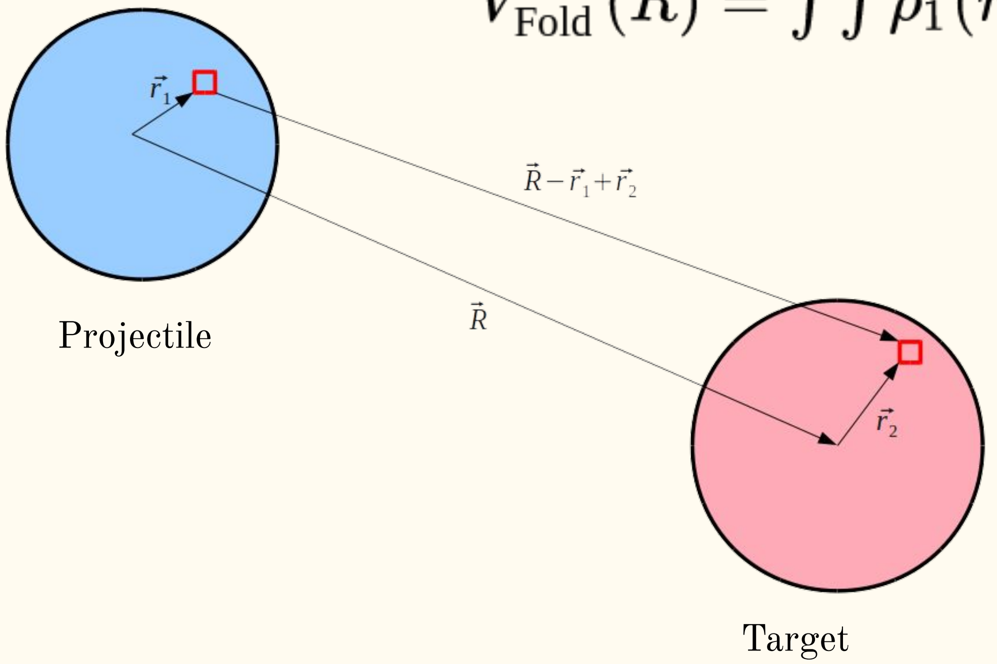

Zero-range interaction: $\nu_{NN} = V_0 \delta(\vec{R} - \vec{r_1} + \vec{r_2})$

The NN interaction range is negligible compared to nuclear density

V_0=-456 MeV fm^3 [1]

[1] L. C. Chamon et al. Phys.Rev. C66, 014610 (2002).

Double-folding nuclear São Paulo potential (SPP).

$$U_{opt}(R) = N_R V_{SPP}(R) + N_i V_{SPP}(R)$$

$$V_{\mathrm{SPP}}(R) = V_{\mathrm{Fold}}(R) e^{-4v^2/c^2}$$

$$V_{\mathrm{Fold}}(R) = \int\int \rho_1(\vec{r}_1)\rho_2(\vec{r}_2)\nu_{NN}(\vec{R} - \vec{r}_1 + \vec{r}_2)\, d\vec{r}_1\, d\vec{r}_2$$

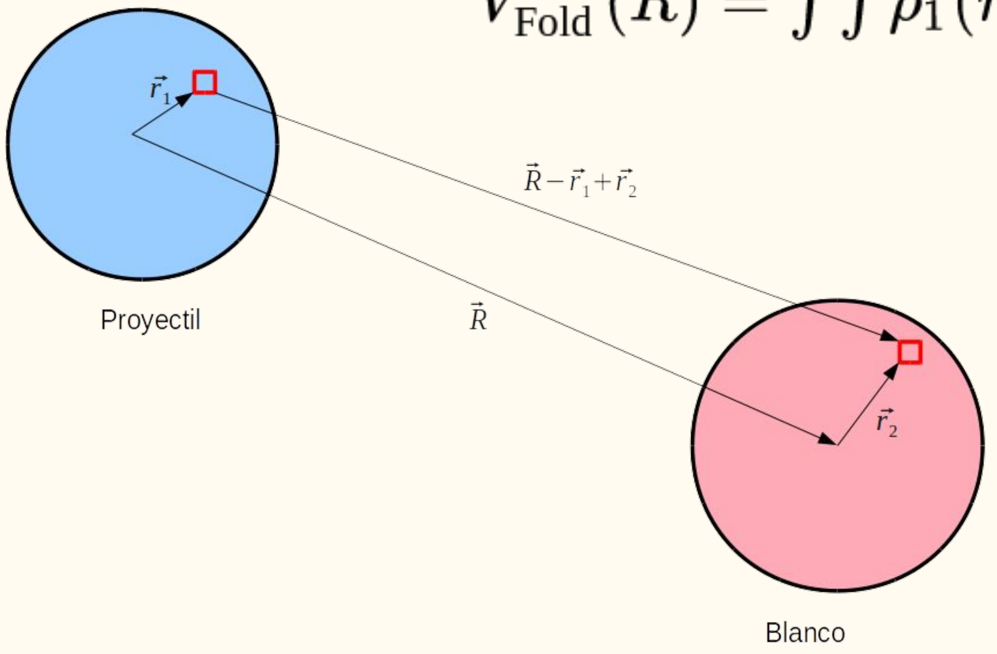

Zero-range interaction: $\nu_{NN} = V_0 \delta(\vec{R} - \vec{r_1} + \vec{r_2})$

The NN interaction range is negligible compared to nuclear density

V_0=-456 MeV fm^3 [1]

[1] L. C. Chamon et al. Phys.Rev. C66, 014610 (2002).

Double-folding nuclear São Paulo potential (SPP).

$$U_{opt}(R) = V_{SPP}(R) + iN_I V_{SPP}(R) + V_{pol}(R) + iW_{pol}(R)$$

$$U_{opt}(R) = V_{SPP}(R) + i0.78 V_{SPP}(R)$$

[2] M. A. G. Alvarez et al., Nucl. Phys. A723, 93 (2003).

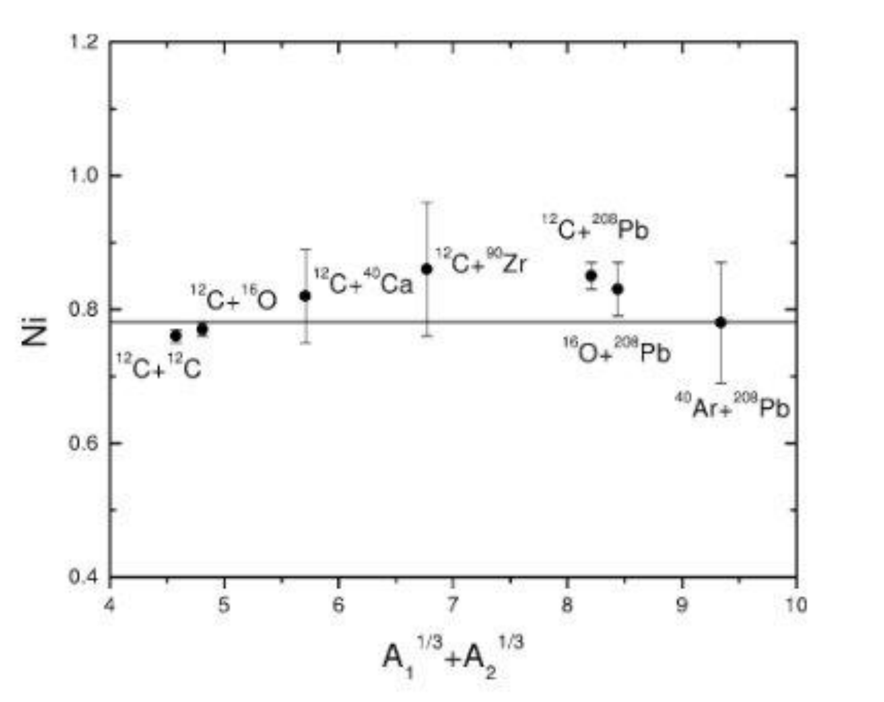

Stable nuclei reactions have been successfully described assuming the fundamental double-folding nuclear São Paulo potential (SPP).

Double-folding nuclear São Paulo potential (SPP).

$$U_{opt}(R) = V_{SPP}(R) + iN_I V_{SPP}(R) + V_{pol}(R) + iW_{pol}(R)$$

$$U_{opt}(R) = V_{SPP}(R) + i0.78 V_{SPP}(R)$$

black solid line

[2] M. A. G. Alvarez et al., Nucl. Phys. A723, 93 (2003).

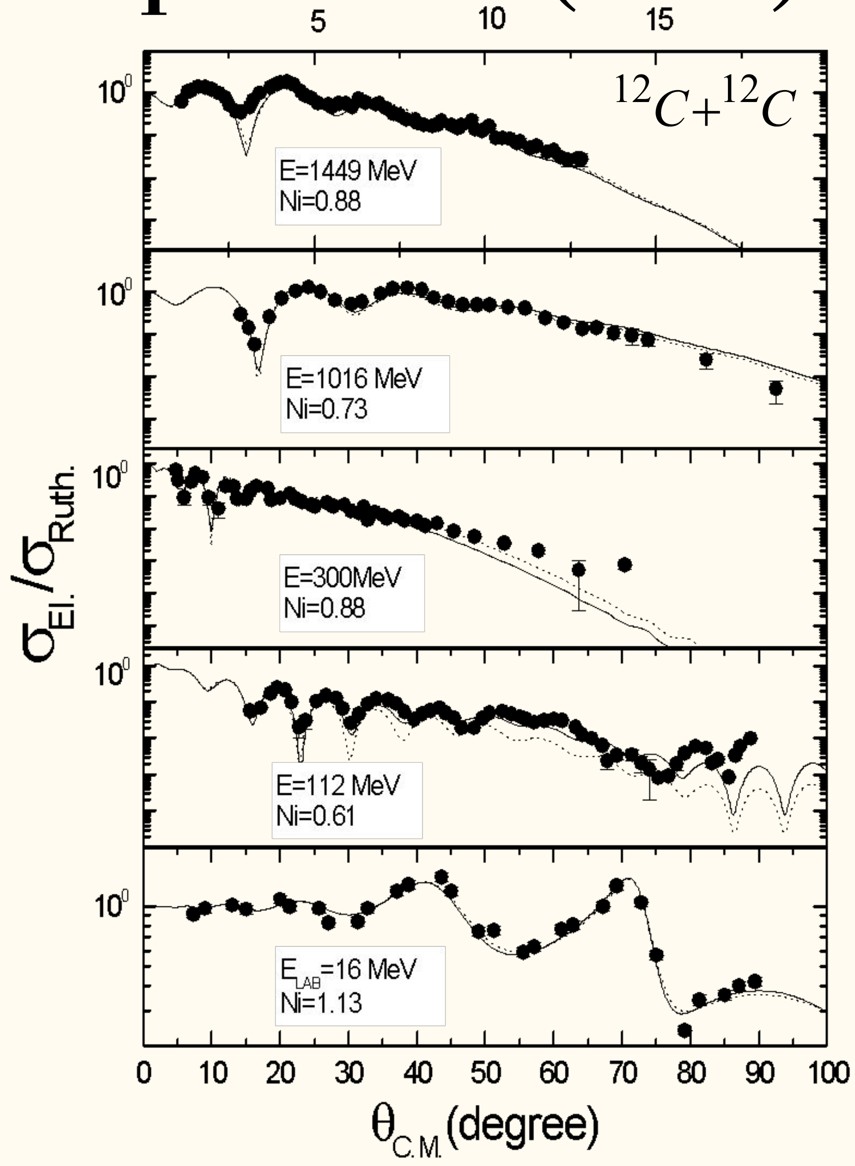

Stable nuclei reactions have been successfully described assuming the fundamental double-folding nuclear São Paulo potential (SPP).

Double-folding nuclear São Paulo potential (SPP).

$$U_{opt}(R) = V_{SPP}(R) + iN_I V_{SPP}(R) + V_{pol}(R) + iW_{pol}(R)$$

$$U_{opt}(R) = V_{SPP}(R) + i0.78 V_{SPP}(R)$$

black solid line

Reproduce more than 40 systems!!

[2] M. A. G. Alvarez et al., Nucl. Phys. A723, 93 (2003).

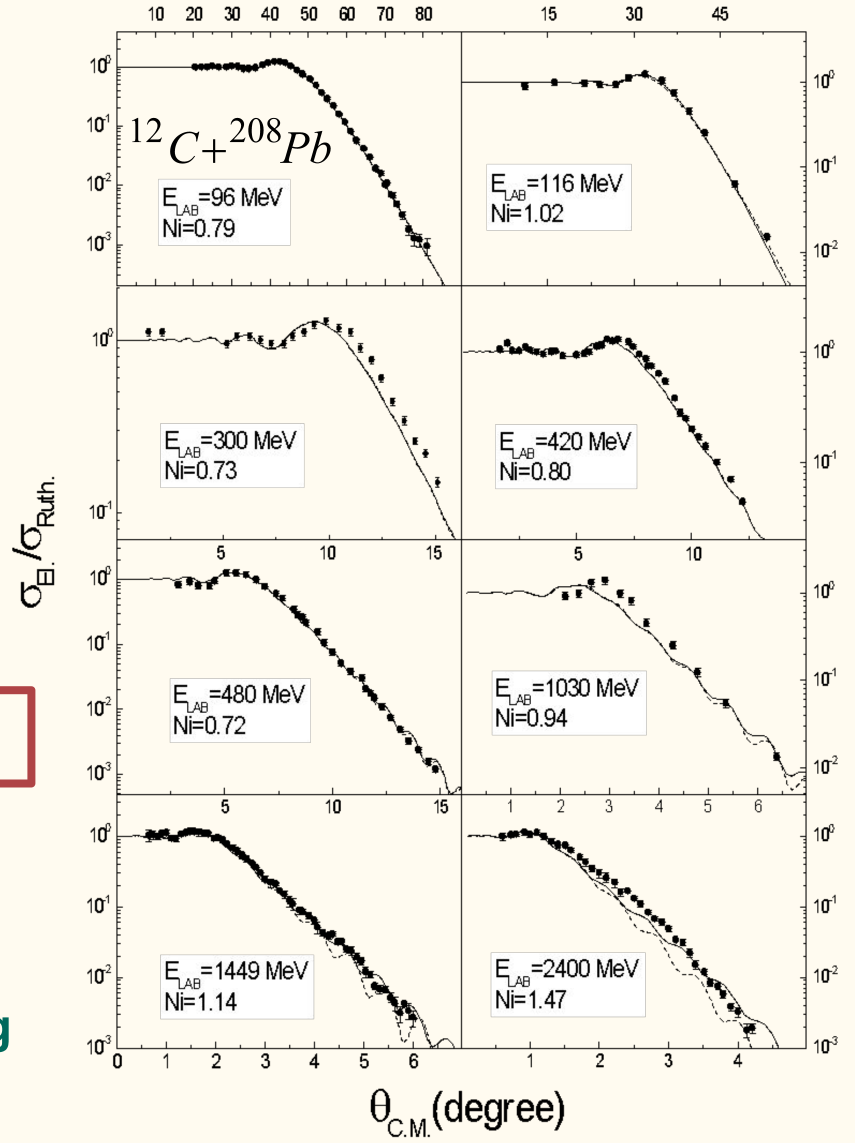

Stable nuclei reactions have been successfully described assuming the fundamental double-folding nuclear São Paulo potential (SPP).

1. The Laboratories and SETUP´s

2. The Theoretical Optical Model

3. Experimental Data x Theoretical Calculations

4. Conclusions

$$E_{Red} = E_{c.m.} - V_B$$

projectile	V_B(MeV)	R_B(fm)	$\hbar w$(MeV)
^{4}He	14.22	9.48	4.92
^{6}He	12.78	10.52	3.35
^{6}Li	19.76	10.16	4.20
^{7}Li	19.45	10.34	3.86
^{9}Be	25.78	10.40	3.93
^{10}B	32.38	10.34	4.17
^{16}O	50.79	10.56	4.14
^{18}O	50.05	10.74	3.86

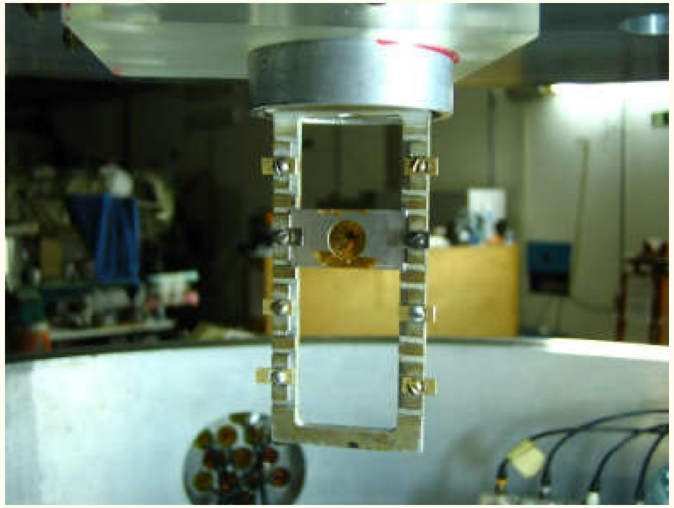

^{120}Sn target

- **Different projectiles + ^{120}Sn @ energies below, around and above the respective Coulomb barrier**

projectile	V_B(MeV)	R_B(fm)	$\hbar w$(MeV)
^{4}He	14.22	9.48	4.92
^{6}He	12.78	10.52	3.35
^{6}Li	19.76	10.16	4.20
^{7}Li	19.45	10.34	3.86
^{9}Be	25.78	10.40	3.93
^{10}B	32.38	10.34	4.17
^{16}O	50.79	10.56	4.14
^{18}O	50.05	10.74	3.86

$$E_{Red} = E_{c.m.} - V_B$$

$$U_{opt}(R) = V_{SPP} + iW(R) \quad \left\{ \begin{array}{l} U_{opt}(R) = V_{SPP} + iW_{fus}(R) \\ W_{fus} = W_0[1 + exp(\frac{R-R_o}{a_i}]^{-1} \\ W_0 = 100\ MeV\ a_i = 0.25\ fm \end{array} \right.$$

- Different projectiles + ^{120}Sn @ energies below, around and above the respective Coulomb barrier

$$E_{Red} = E_{c.m.} - V_B$$

projectile	V_B(MeV)	R_B(fm)	$\hbar w$(MeV)
^{4}He	14.22	9.48	4.92
^{6}He	12.78	10.52	3.35
^{6}Li	19.76	10.16	4.20
^{7}Li	19.45	10.34	3.86
^{9}Be	25.78	10.40	3.93
^{10}B	32.38	10.34	4.17
^{16}O	50.79	10.56	4.14
^{18}O	50.05	10.74	3.86

$$U_{opt}(R) = V_{SPP} + iW(R)$$

$$U_{opt}(R) = V_{SPP} + iW_{fus}(R)$$

$$W_{fus} = W_0[1 + exp(\frac{R-R_o}{a_i})]^{-1}$$

$$W_0 = 100\ MeV \quad a_i = 0.25\ fm$$

Only Internal Absorption (OIA)

- **Different projectiles + ^{120}Sn @ energies below, around and above the respective Coulomb barrier**

projectile	V_B(MeV)	R_B(fm)	$\hbar w$(MeV)
^{4}He	14.22	9.48	4.92
^{6}He	12.78	10.52	3.35
^{6}Li	19.76	10.16	4.20
^{7}Li	19.45	10.34	3.86
^{9}Be	25.78	10.40	3.93
^{10}B	32.38	10.34	4.17
^{16}O	50.79	10.56	4.14
^{18}O	50.05	10.74	3.86

$$E_{Red} = E_{c.m.} - V_B$$

$$U_{opt}(R) = V_{SPP} + iW(R)$$

$$U_{opt}(R) = V_{SPP} + iW_{fus}(R)$$

$$W_{fus} = W_0[1 + exp(\frac{R-R_o}{a_i})]^{-1}$$

$$W_0 = 100\ MeV\ a_i = 0.25\ fm$$

Only Internal Absorption (OIA)

$$U_{opt}(R) = V_{SPP} + iN_i V_{SPP}(R)$$

Strong Surface Absorption (SSA)

- **Different projectiles + ^{120}Sn @ energies below, around and above the respective Coulomb barrier**

$$E_{Red} = E_{c.m.} - V_B$$

projectile	V_B(MeV)	R_B(fm)	$\hbar w$(MeV)
^{4}He	14.22	9.48	4.92
^{6}He	12.78	10.52	3.35
^{6}Li	19.76	10.16	4.20
^{7}Li	19.45	10.34	3.86
^{9}Be	25.78	10.40	3.93
^{10}B	32.38	10.34	4.17
^{16}O	50.79	10.56	4.14
^{18}O	50.05	10.74	3.86

$$U_{opt}(R) = V_{SPP} + iW(R)$$

$$U_{opt}(R) = V_{SPP} + iW_{fus}(R)$$

$$W_{fus} = W_0[1 + exp(\frac{R-R_o}{a_i}]^{-1}$$

$$W_0 = 100\ MeV\ a_i = 0.25\ fm$$

Only Internal Absorption (OIA)

$$U_{opt}(R) = V_{SPP} + iN_i V_{SPP}(R)$$

N_i = **0.78**

Strong Surface Absorption (SSA)

- **Different projectiles + ^{120}Sn @ energies below, around and above the respective Coulomb barrier**

$$E_{Red} = E_{c.m.} - V_B$$

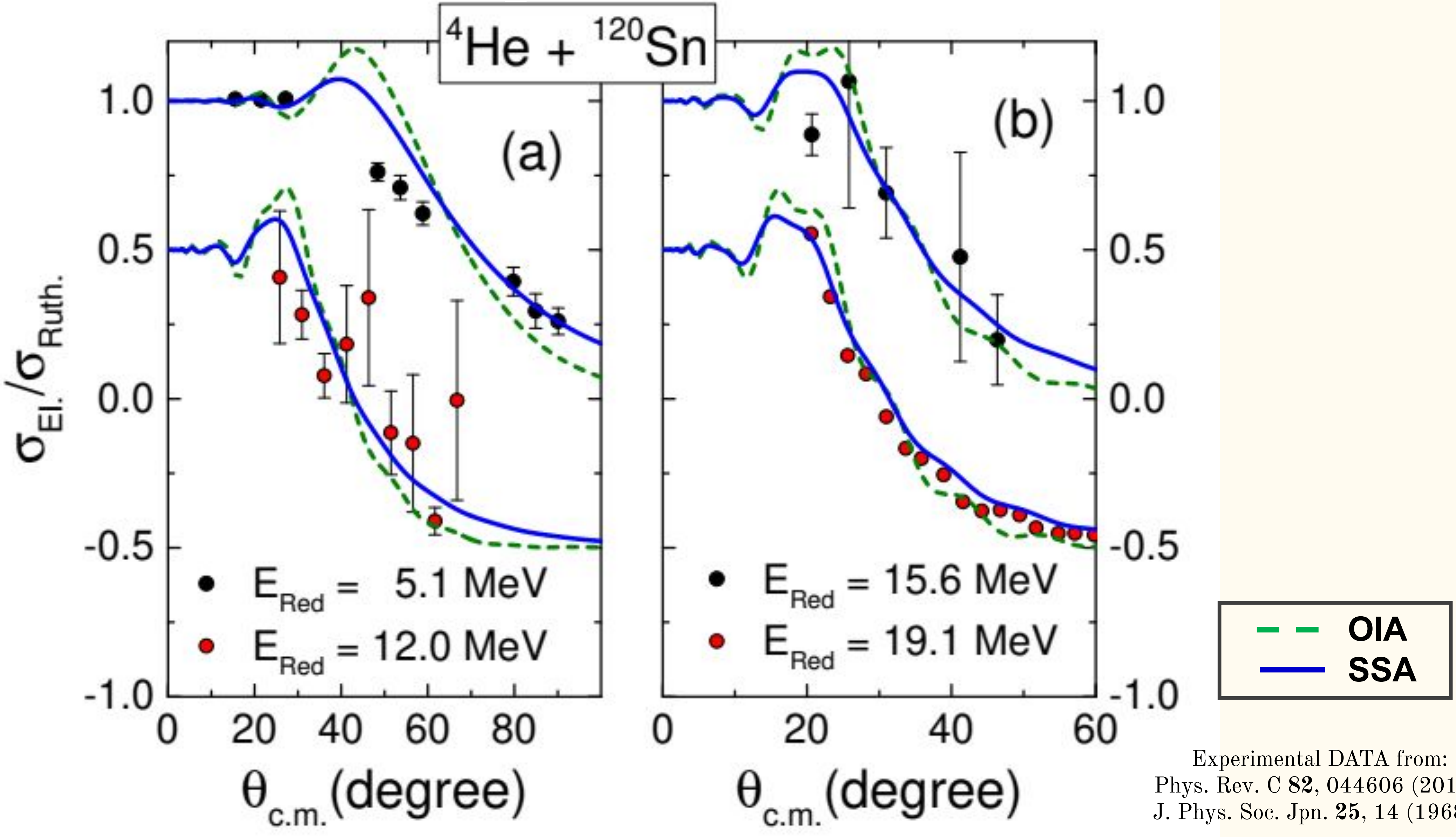

Experimental DATA from:
Phys. Rev. C **82**, 044606 (2010).
J. Phys. Soc. Jpn. **25**, 14 (1968) .

M. A. G. Alvarez et al., **PHYSICAL REVIEW C 100, 064602 (2019)**

$$E_{Red} = E_{c.m.} - V_B$$

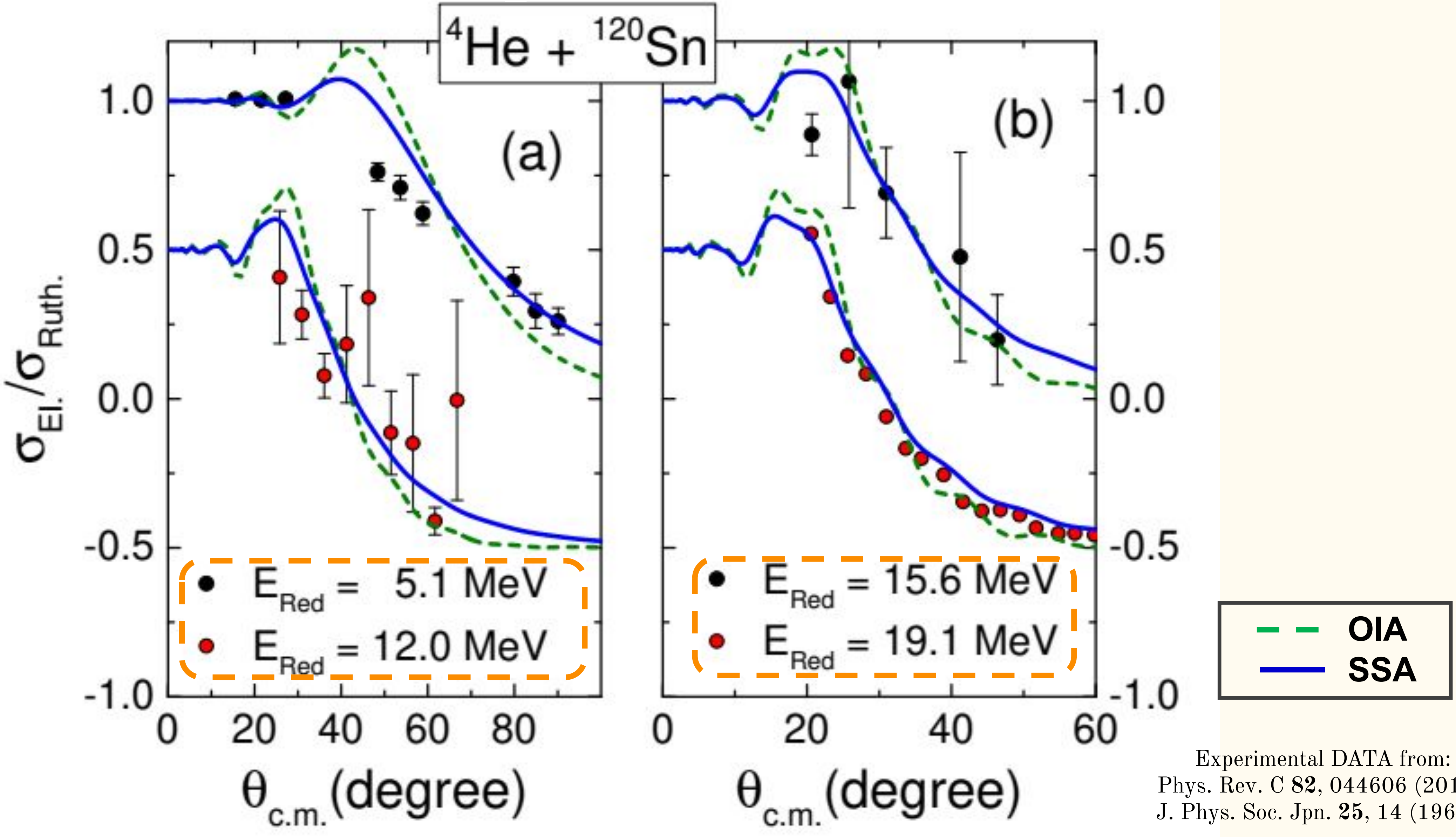

Experimental DATA from:
Phys. Rev. C **82**, 044606 (2010).
J. Phys. Soc. Jpn. **25**, 14 (1968) .

M. A. G. Alvarez et al., **PHYSICAL REVIEW C 100, 064602 (2019)**

$$E_{Red} = E_{c.m.} - V_B$$

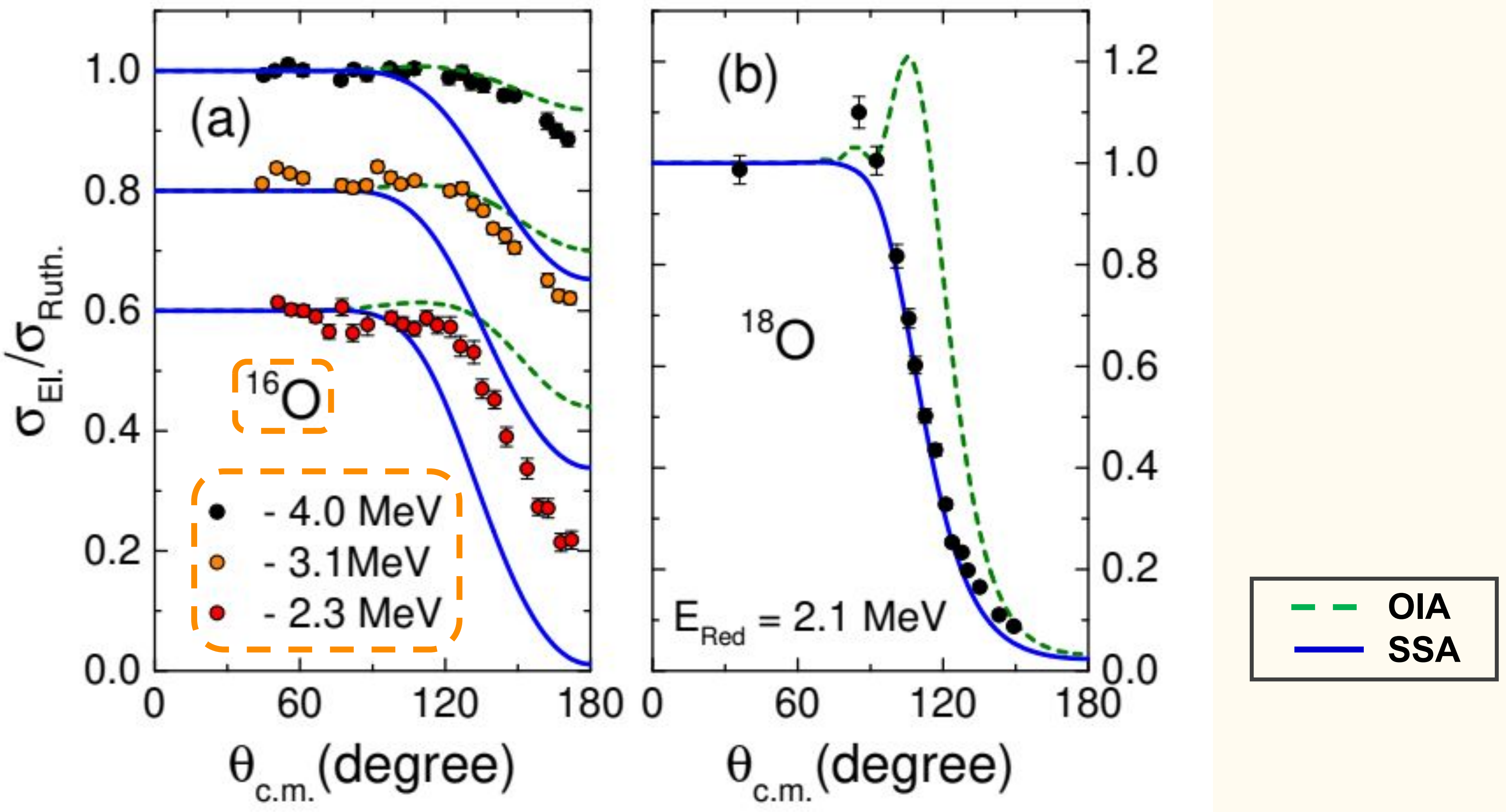

Experimental DATA from:
Nucl. Phys. A **679**, 287 (2001).

M. A. G. Alvarez et al., PHYSICAL REVIEW C 100, 064602 (2019)

$$E_{Red} = E_{c.m.} - V_B$$

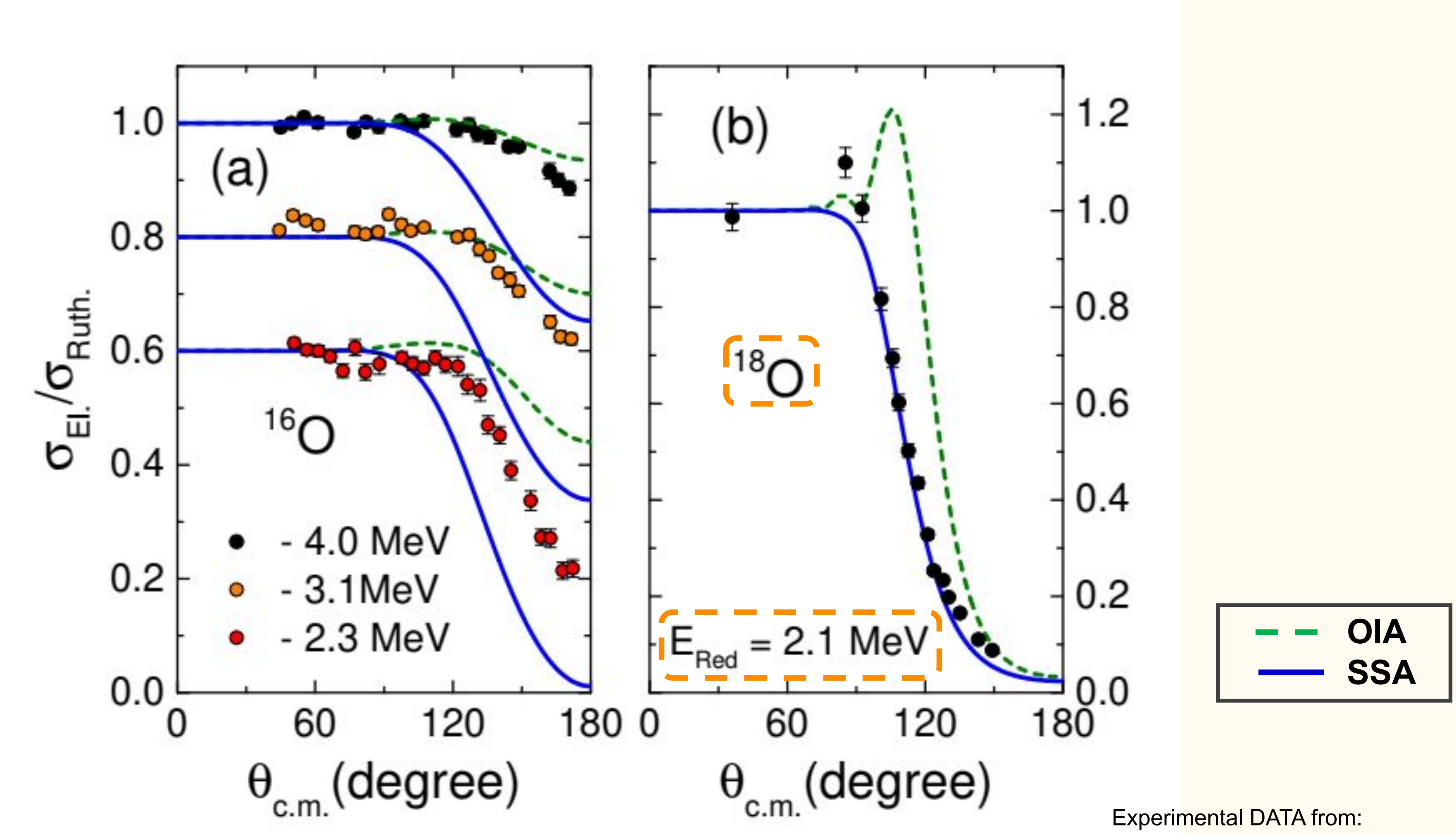

Experimental DATA from:
Z. Phys. A: At. Nucl. **273**, 211 (1975).

$$E_{Red} = E_{c.m.} - V_B$$

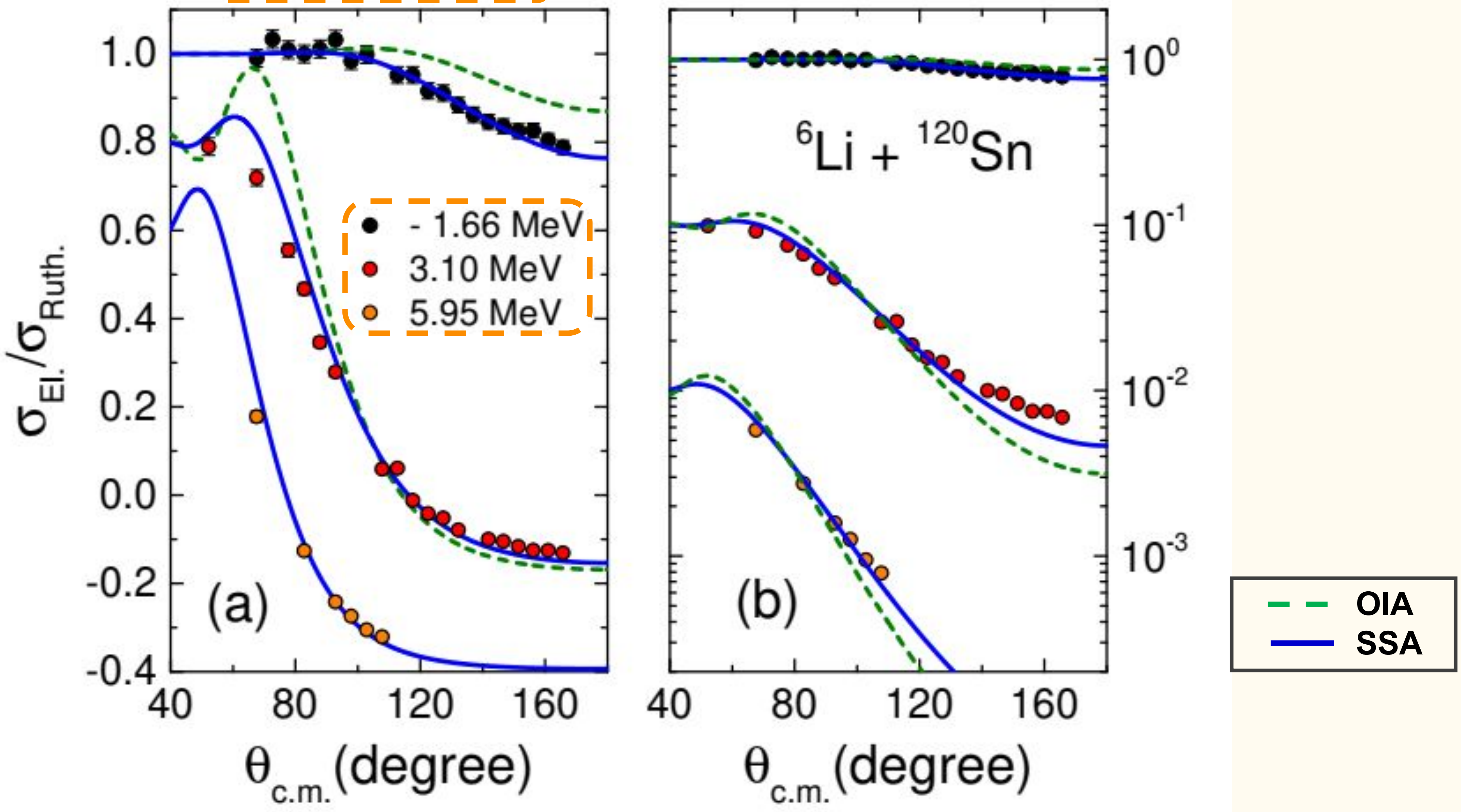

M. A. G. Alvarez et al., PHYSICAL REVIEW C 100, 064602 (2019)

$$E_{Red} = E_{c.m.} - V_B$$

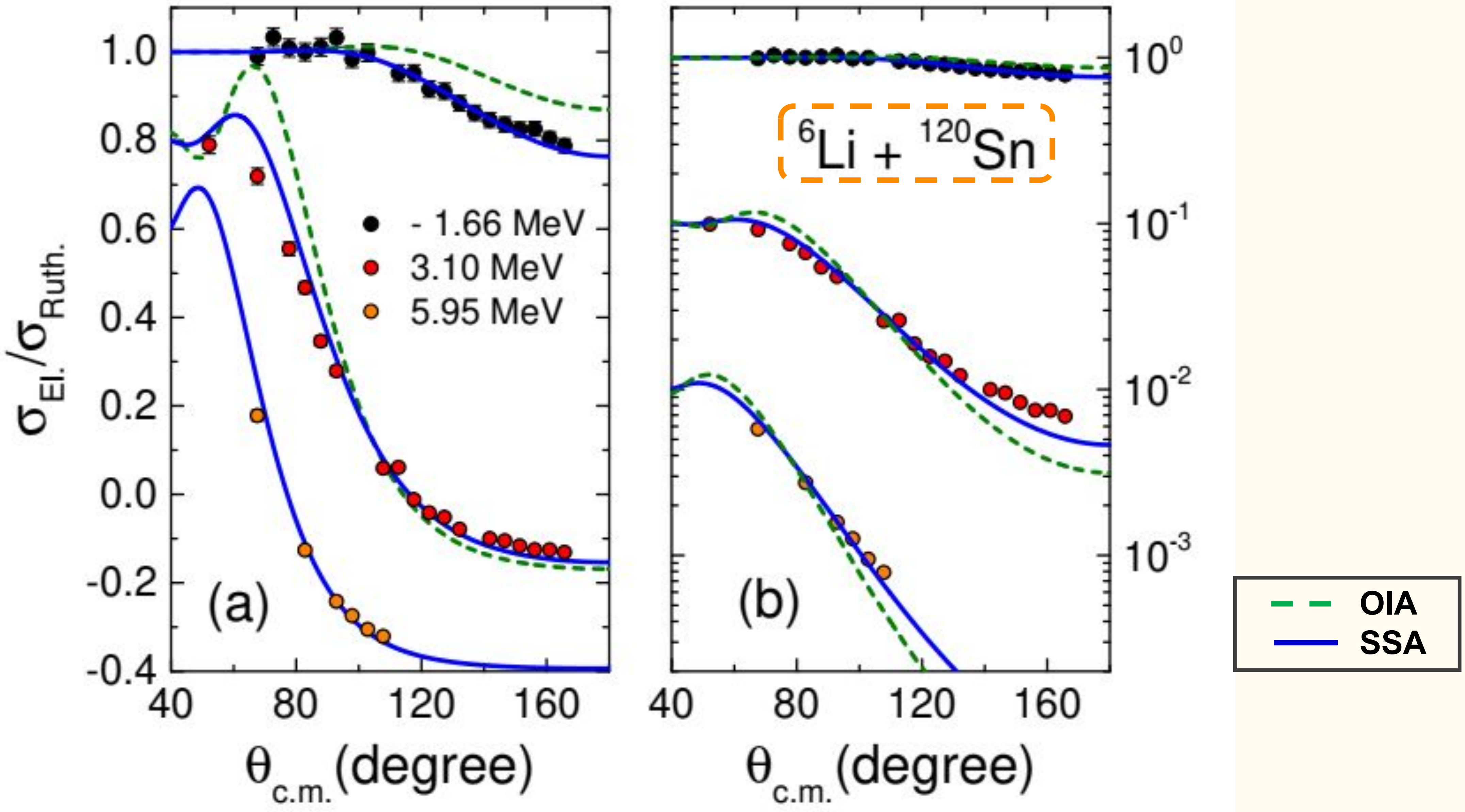

M. A. G. Alvarez et al., PHYSICAL REVIEW C 100, 064602 (2019)

$$E_{Red} = E_{c.m.} - V_B$$

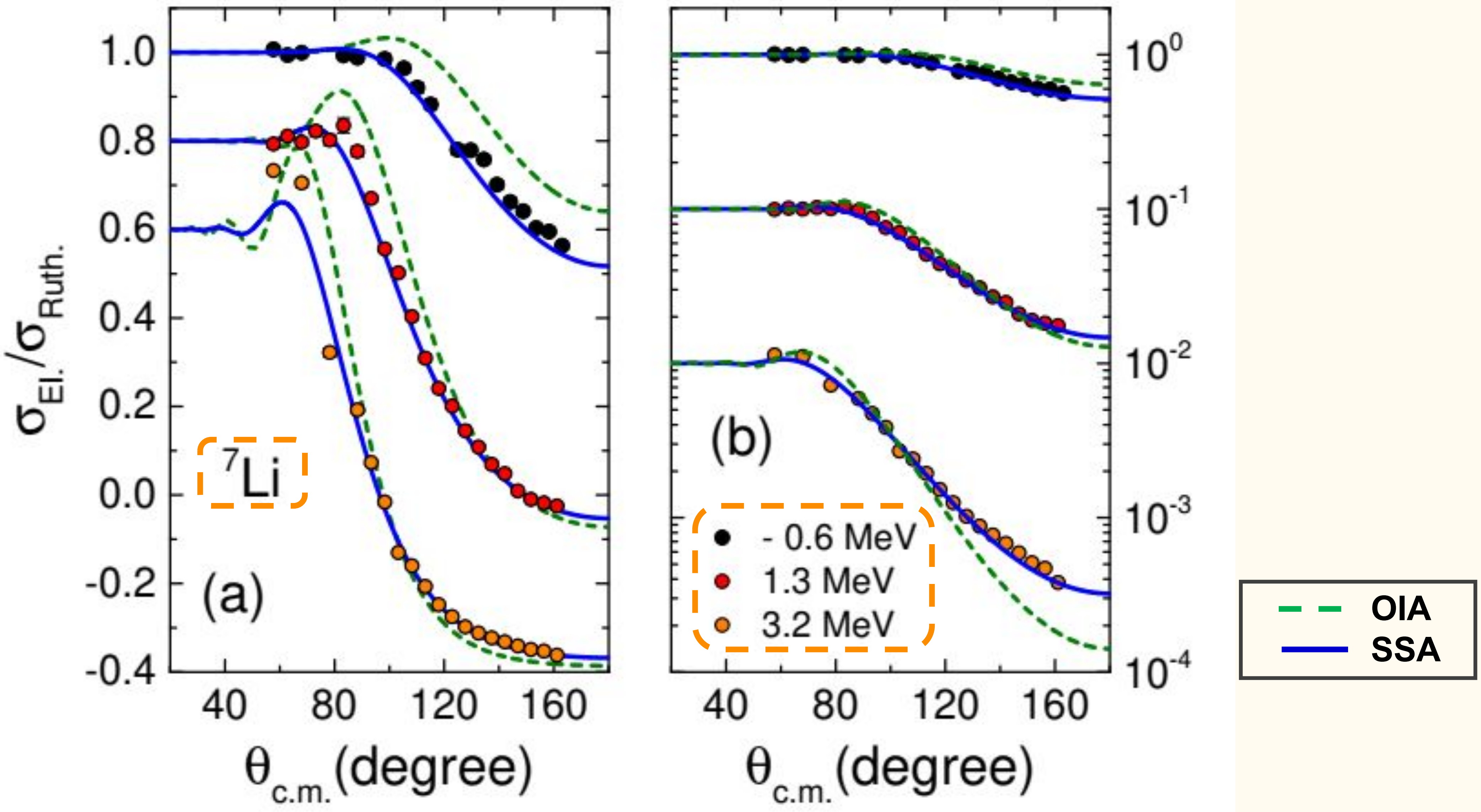

M. A. G. Alvarez et al., PHYSICAL REVIEW C 100, 064602 (2019)

$$E_{Red} = E_{c.m.} - V_B$$

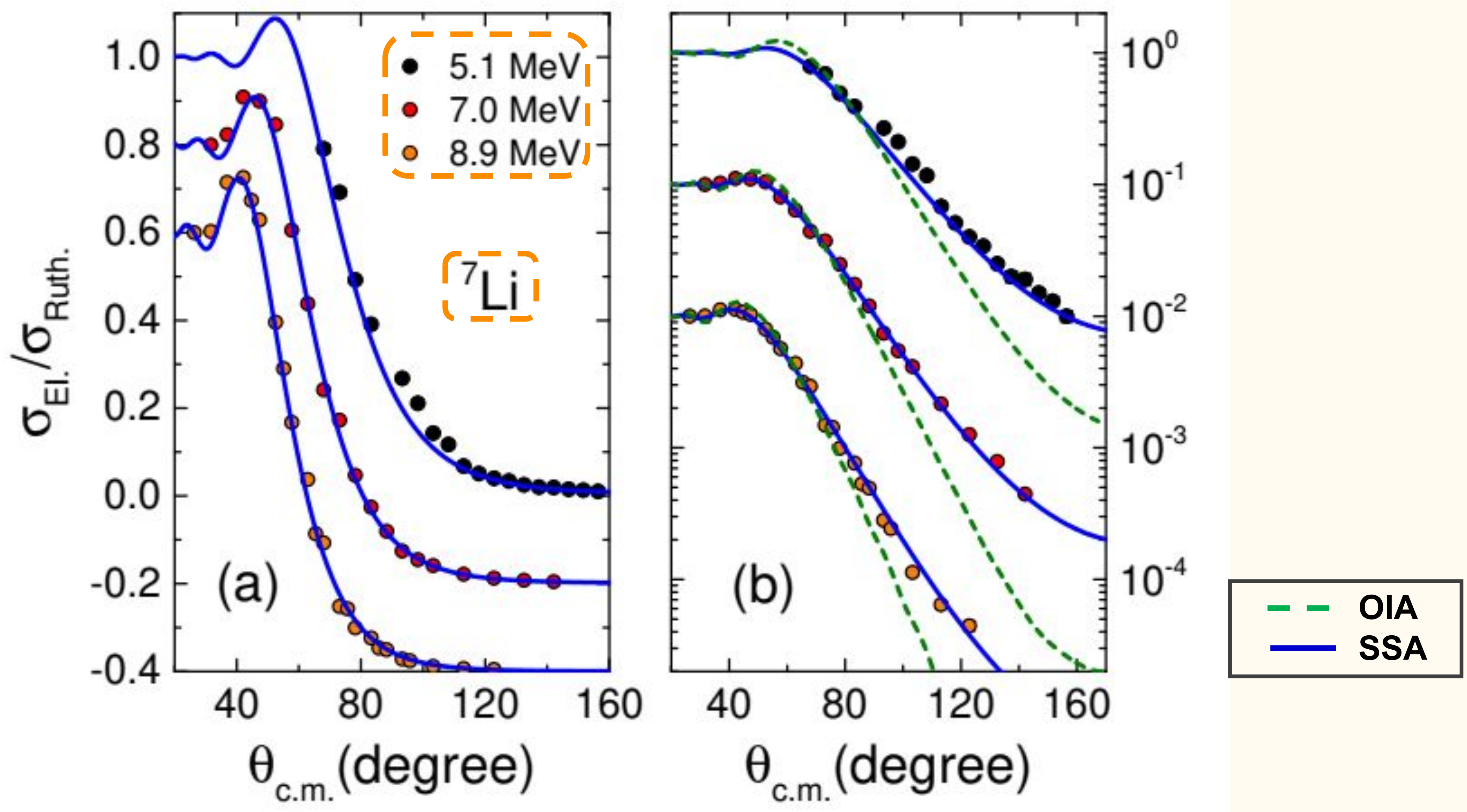

M. A. G. Alvarez et al., PHYSICAL REVIEW C 100, 064602 (2019)

$$E_{Red} = E_{c.m.} - V_B$$

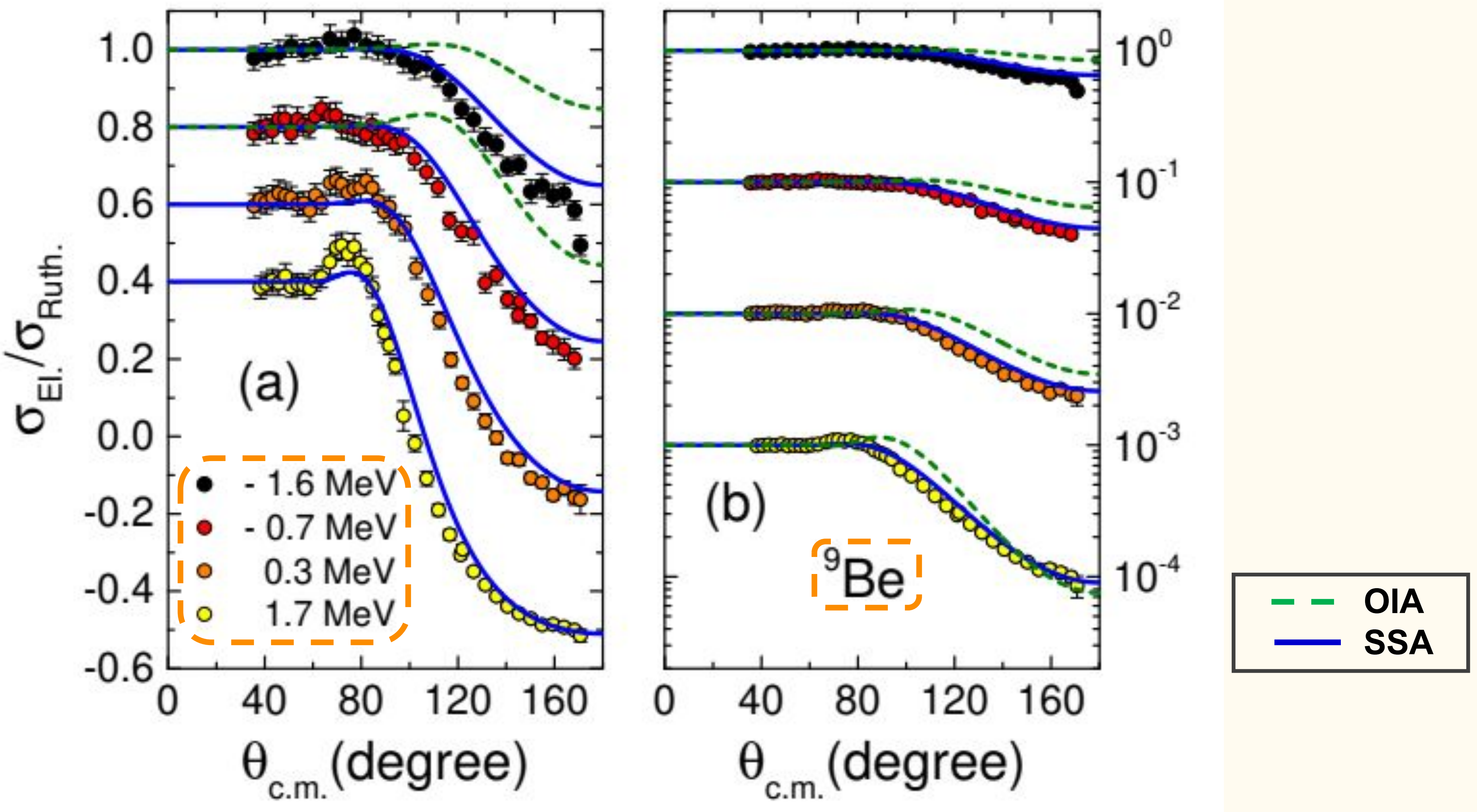

M. A. G. Alvarez et al., PHYSICAL REVIEW C 100, 064602 (2019)

$$E_{Red} = E_{c.m.} - V_B$$

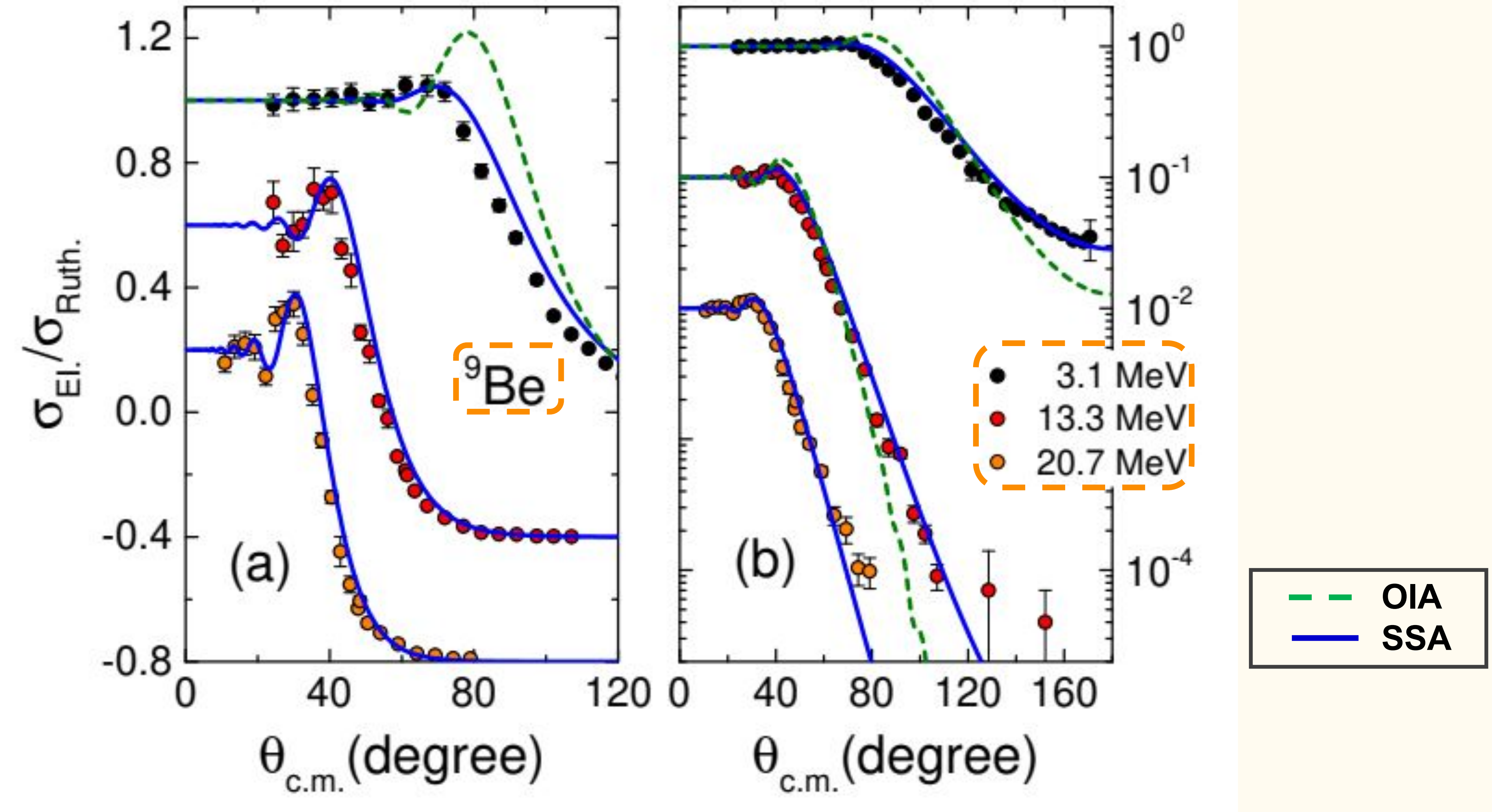

M. A. G. Alvarez et al., PHYSICAL REVIEW C 100, 064602 (2019)

$$E_{Red} = E_{c.m.} - V_B$$

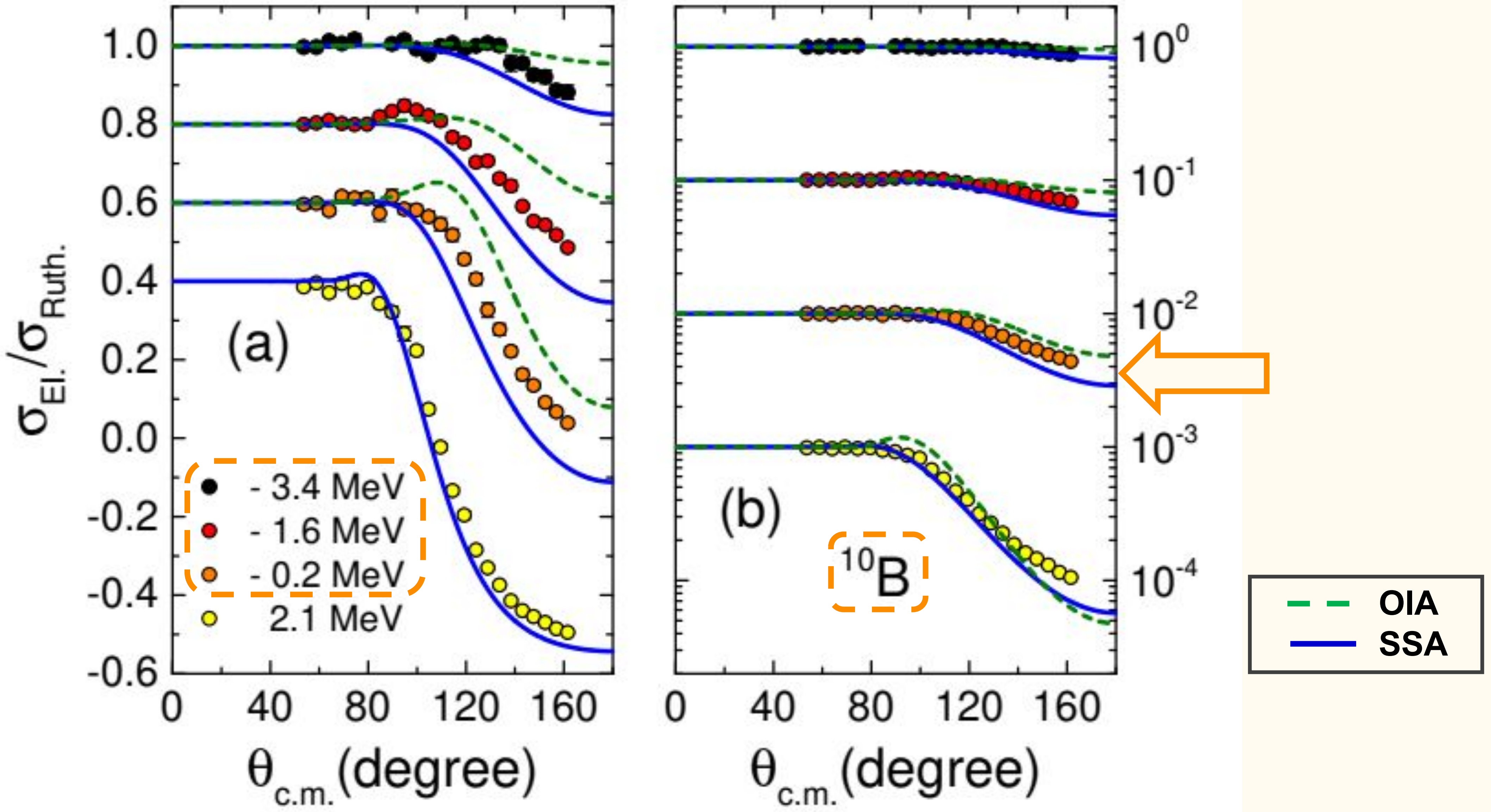

M. A. G. Alvarez et al., PHYSICAL REVIEW C 100, 064602 (2019)

$$E_{Red} = E_{c.m.} - V_B$$

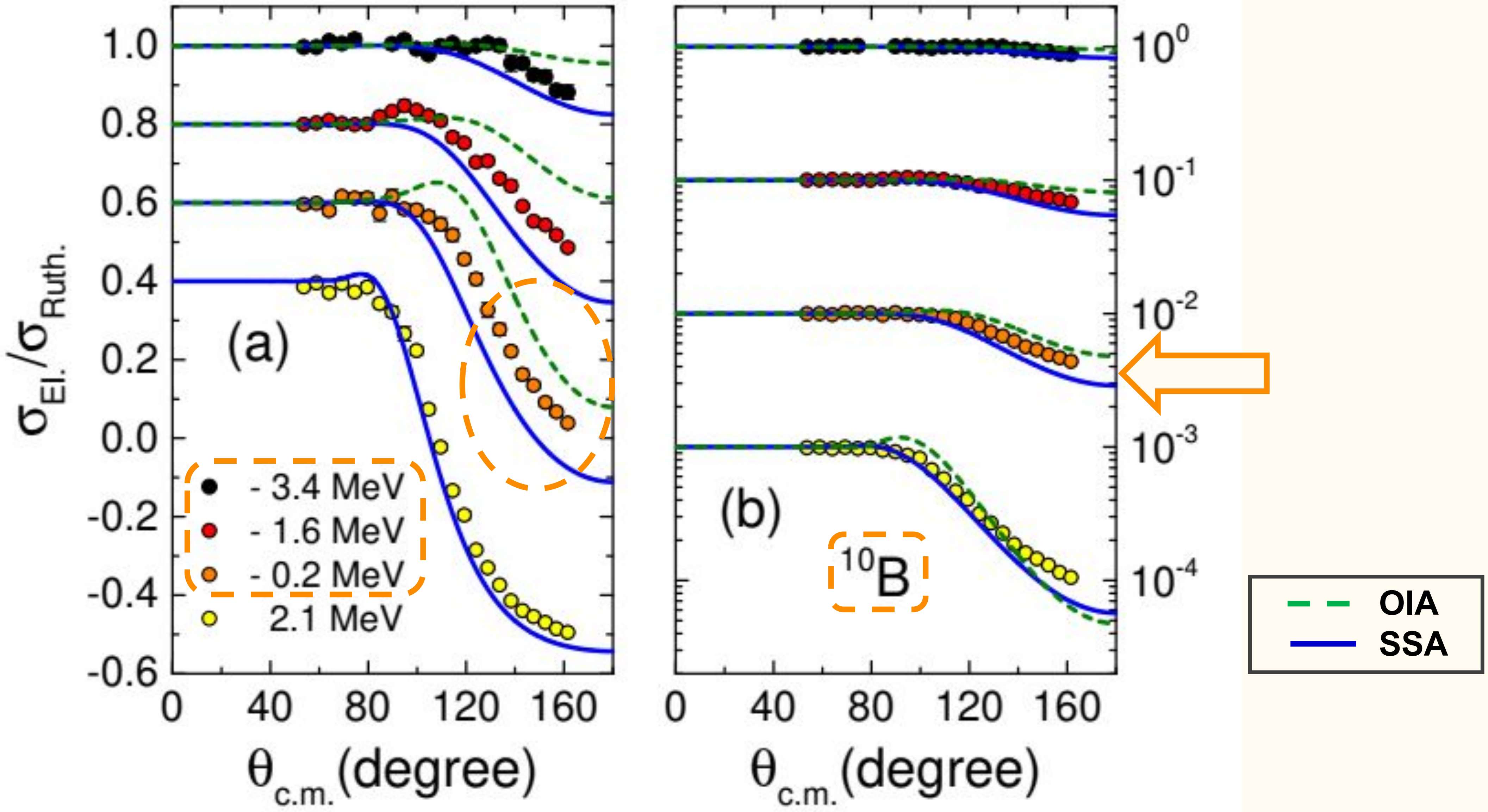

M. A. G. Alvarez et al., PHYSICAL REVIEW C 100, 064602 (2019)

$$E_{Red} = E_{c.m.} - V_B$$

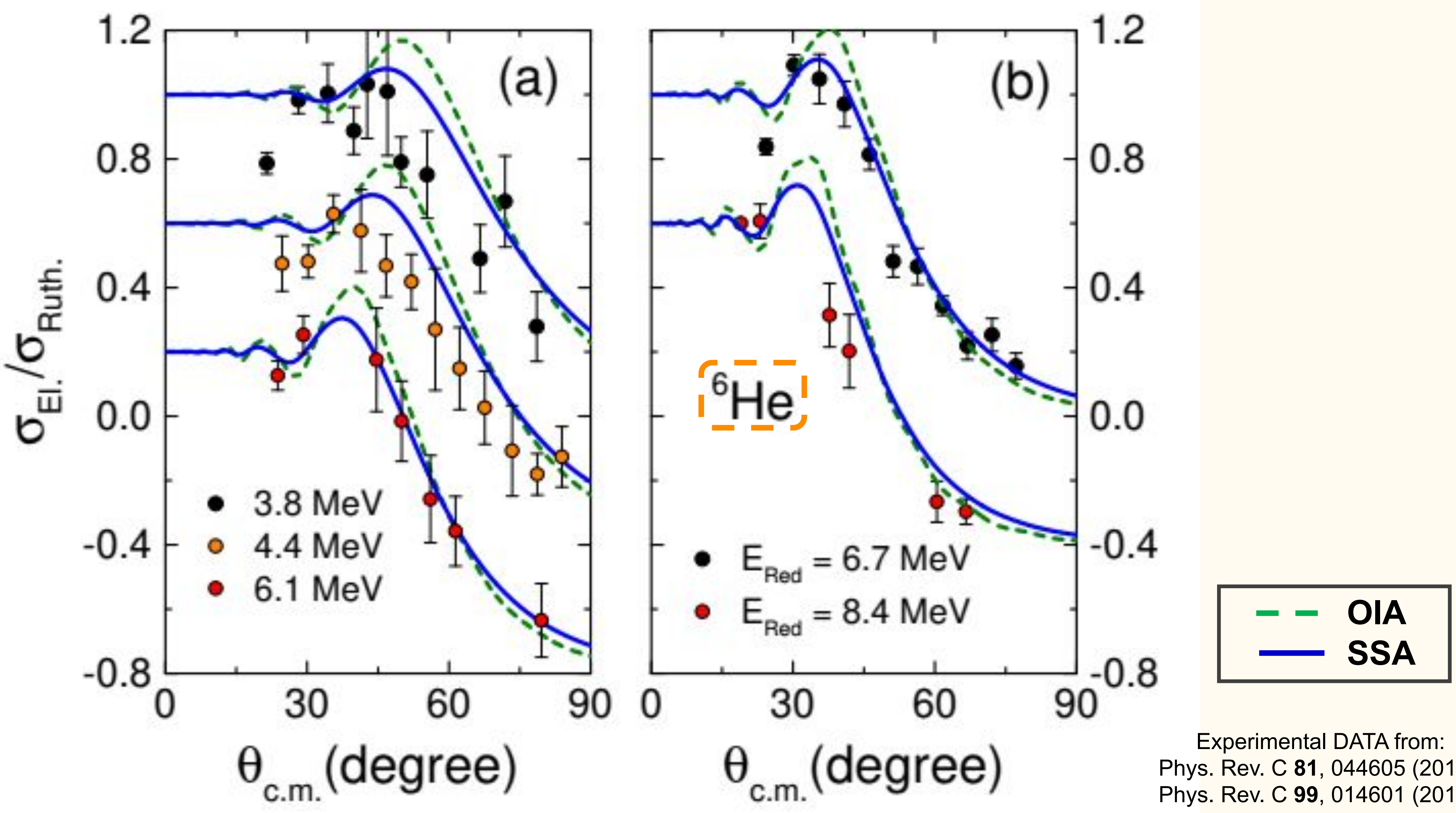

Experimental DATA from:
Phys. Rev. C **81**, 044605 (2010).
Phys. Rev. C **99**, 014601 (2019).

M. A. G. Alvarez et al., PHYSICAL REVIEW C 100, 064602 (2019)

$$E_{Red} = E_{c.m.} - V_B$$

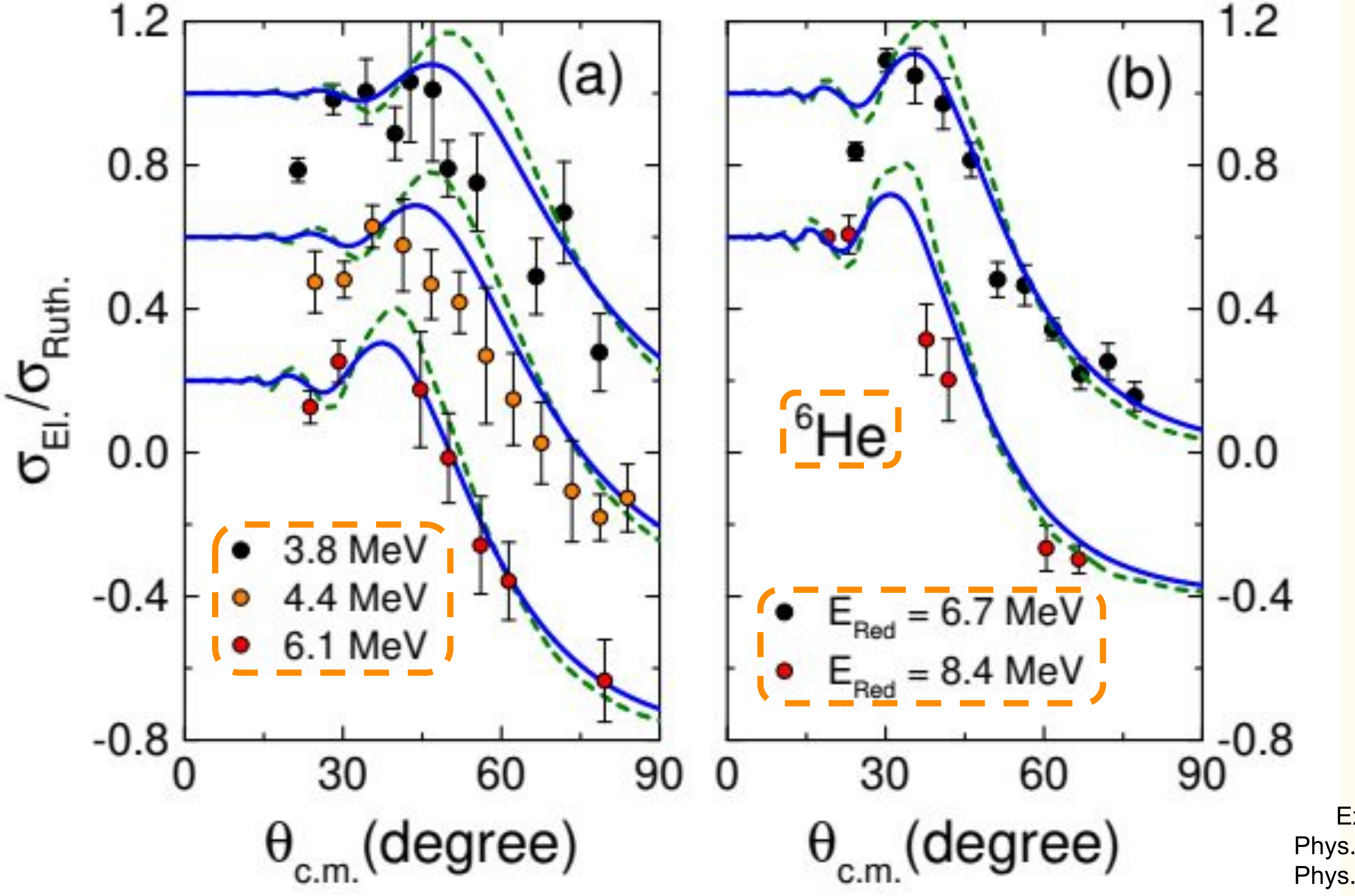

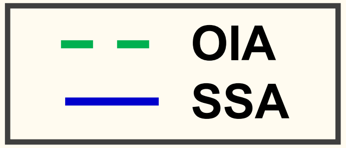

Experimental DATA from:
Phys. Rev. C **81**, 044605 (2010).
Phys. Rev. C **99**, 014601 (2019).

M. A. G. Alvarez et al., PHYSICAL REVIEW C 100, 064602 (2019)

Strong Surface Absorption (SSA)

$$U_{opt}(R) = V_{SPP} + iN_i V_{SPP}(R)$$

Studying the intensity of the imaginary potential

$$V_{\text{SPP}}(R) = V_{\text{Fold}}(R)e^{-4v^2/c^2}$$

$$V_{\text{Fold}}(R) = \int\int \rho_1(\vec{r}_1)\rho_2(\vec{r}_2)\nu_{NN}(\vec{R} - \vec{r}_1 + \vec{r}_2)\, d\vec{r}_1\, d\vec{r}_2$$

Sub-barrier region

$$E_{Red} = E_{c.m.} - V_B$$

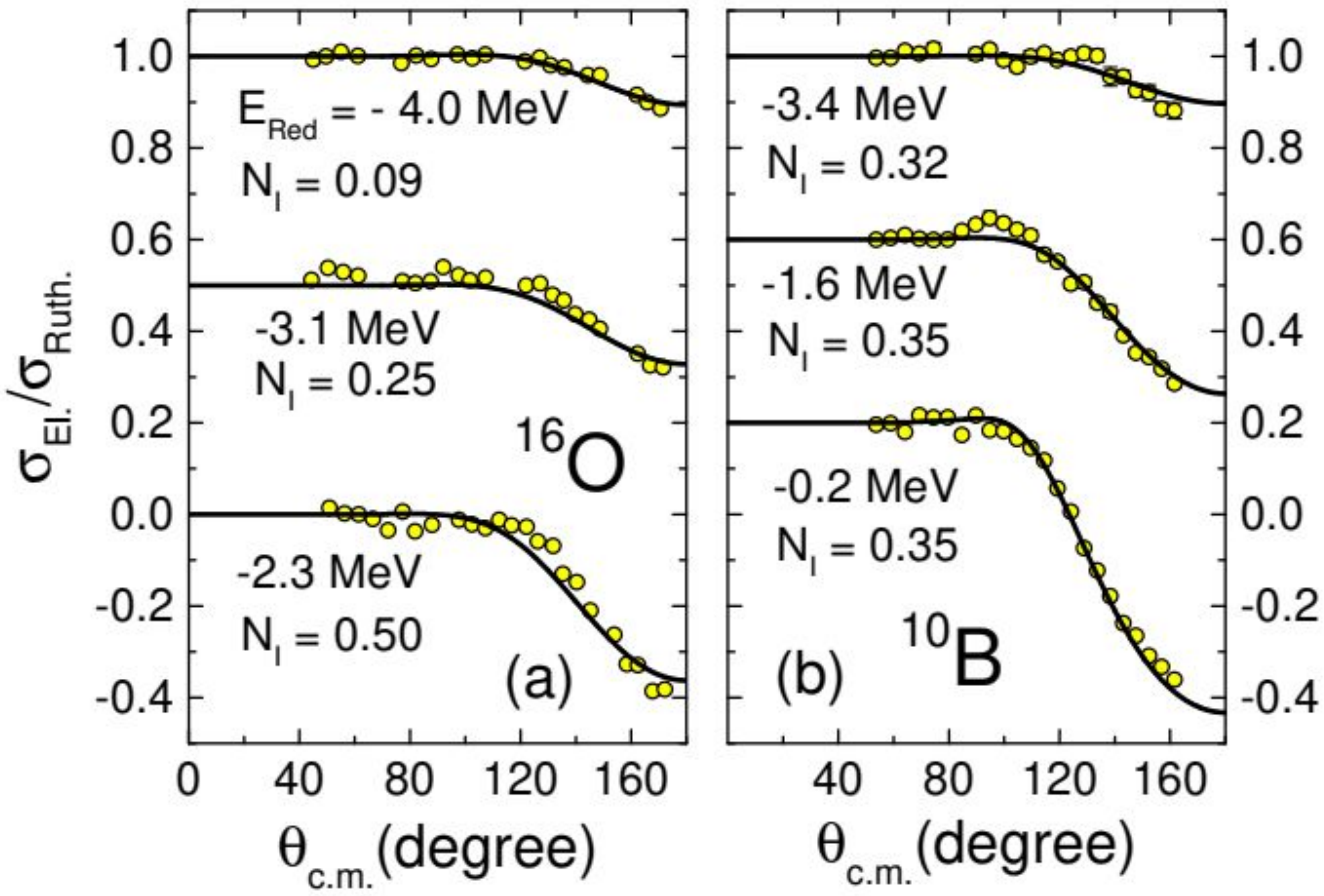

Sub-barrier region

$$E_{Red} = E_{c.m.} - V_B$$

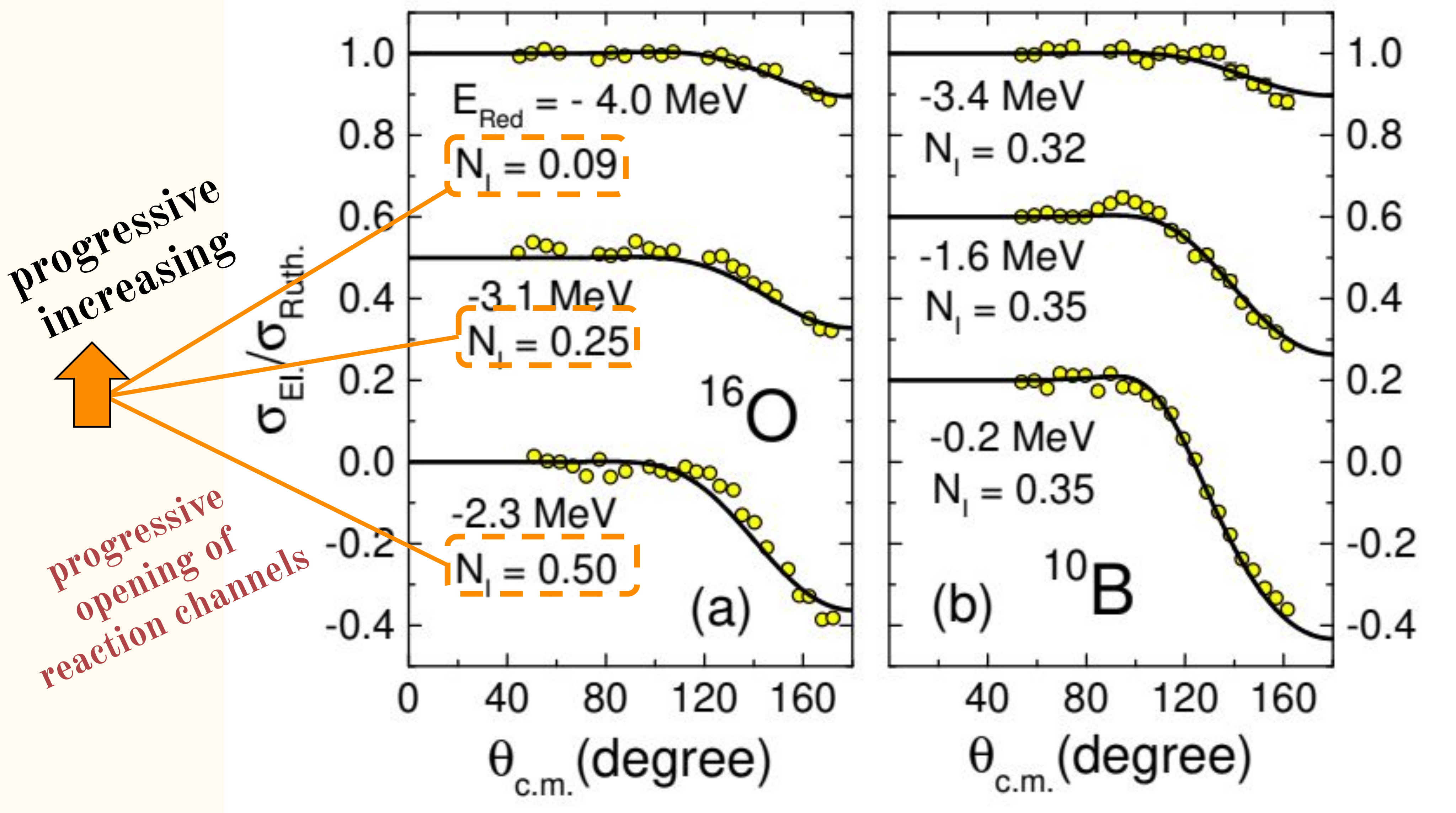

Sub-barrier region

$$E_{Red} = E_{c.m.} - V_B$$

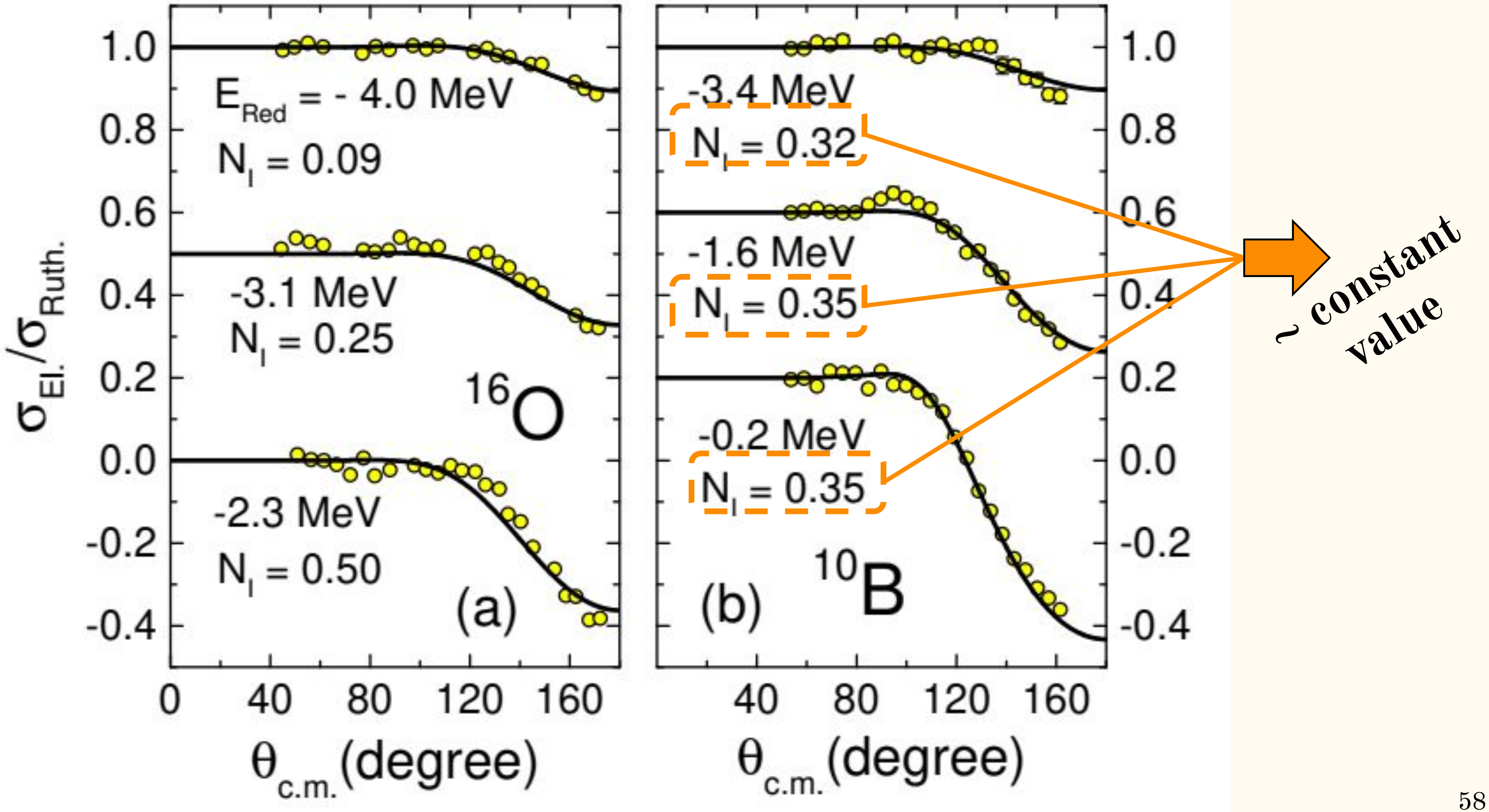

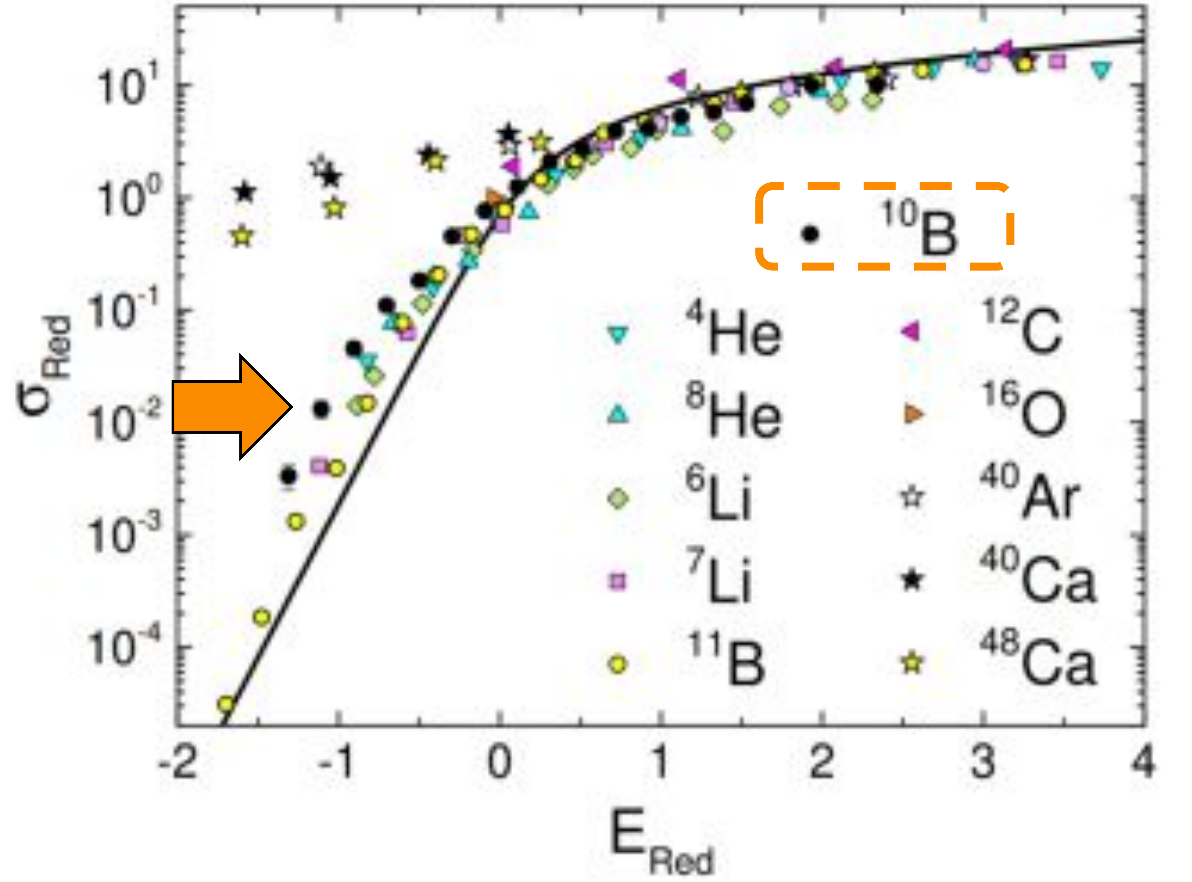

M. Aversa et al., Phys. Rev. C 101, 044601 (2020)

FIG. 9. (Color online) Experimental reduced fusion cross section as a function of the reduced energy, for several systems involving the same target nucleus: ^{197}Au. The solid lines represent the reduced BPM cross section.

Fusion is somehow favored for ^{10}B, while peripheral reaction channels, which are connected to strong surface absorption processes, are favored for the other weakly bound nuclei.

Sub-barrier region

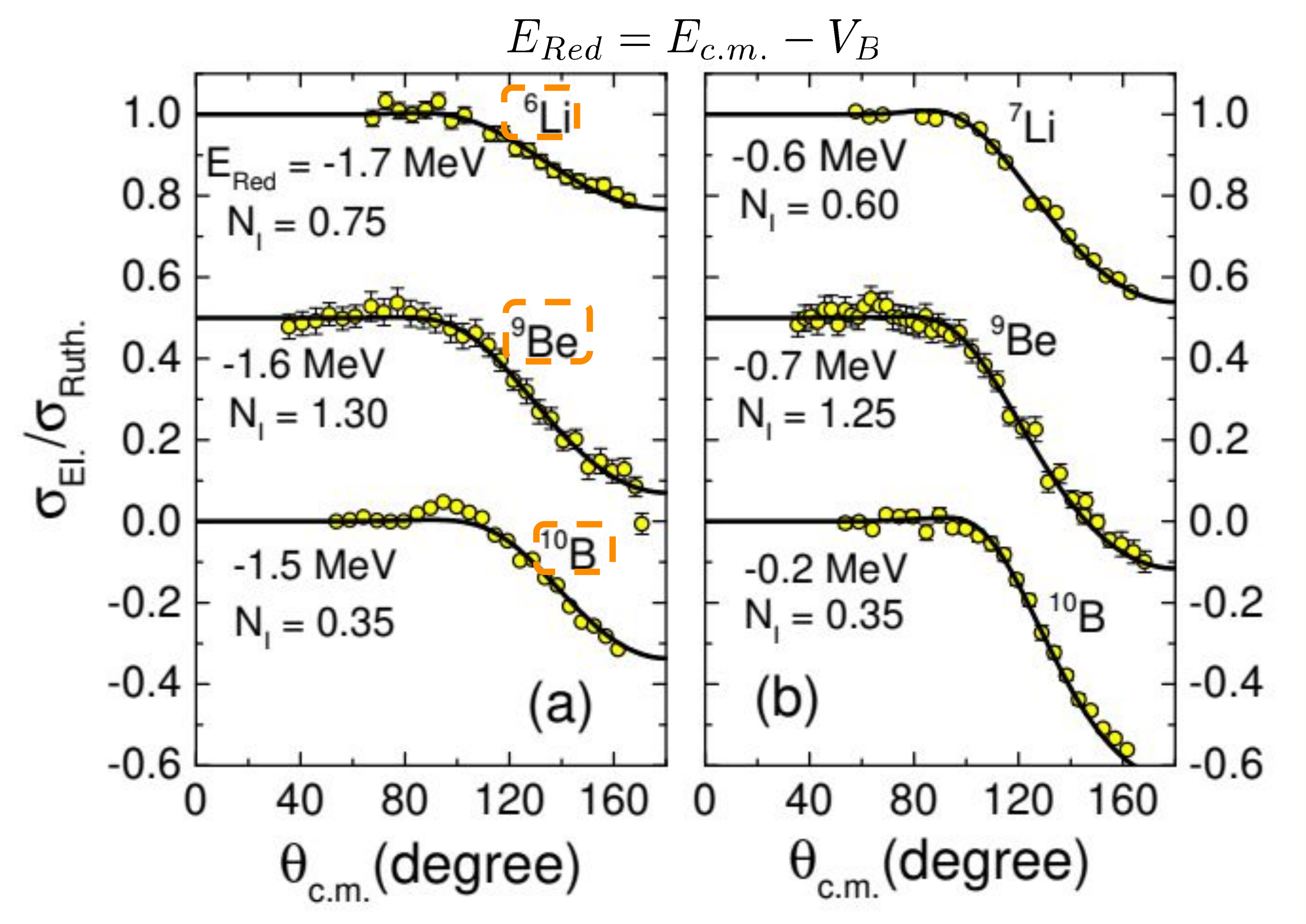

Sub-barrier region

progressive increasing

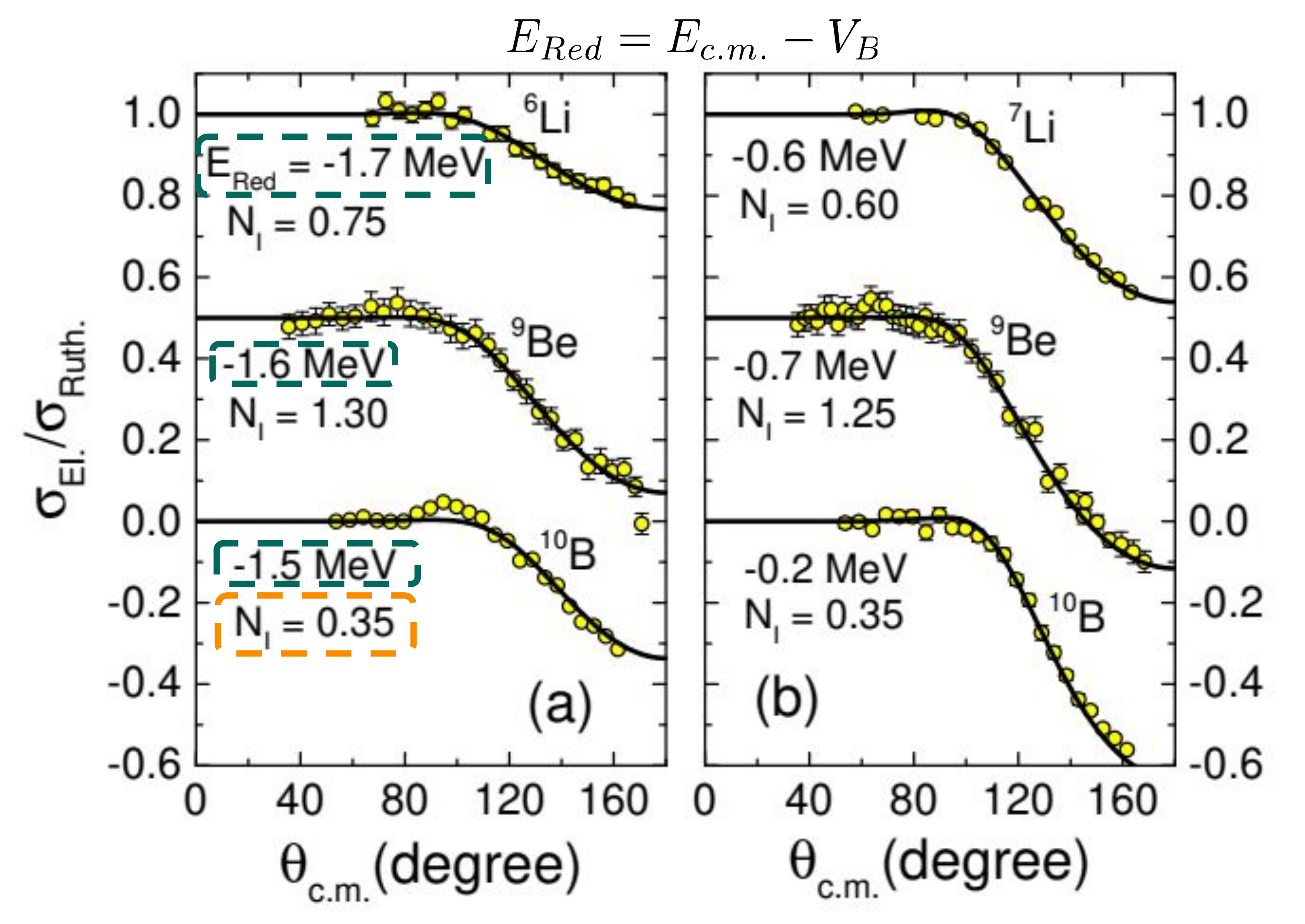

Sub-barrier region

progressive increasing

$$E_{Red} = E_{c.m.} - V_B$$

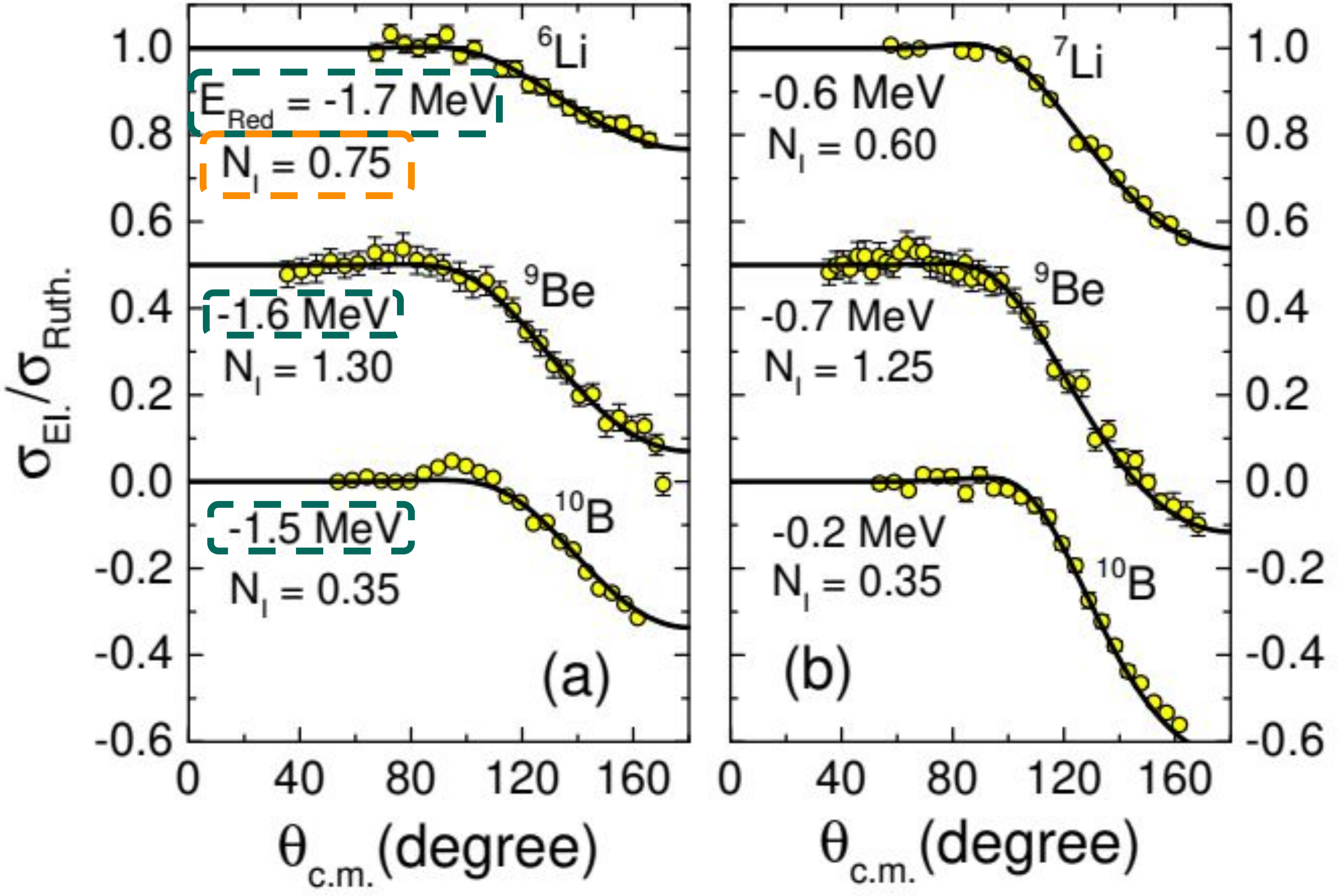

Sub-barrier region

progressive increasing

$$E_{Red} = E_{c.m.} - V_B$$

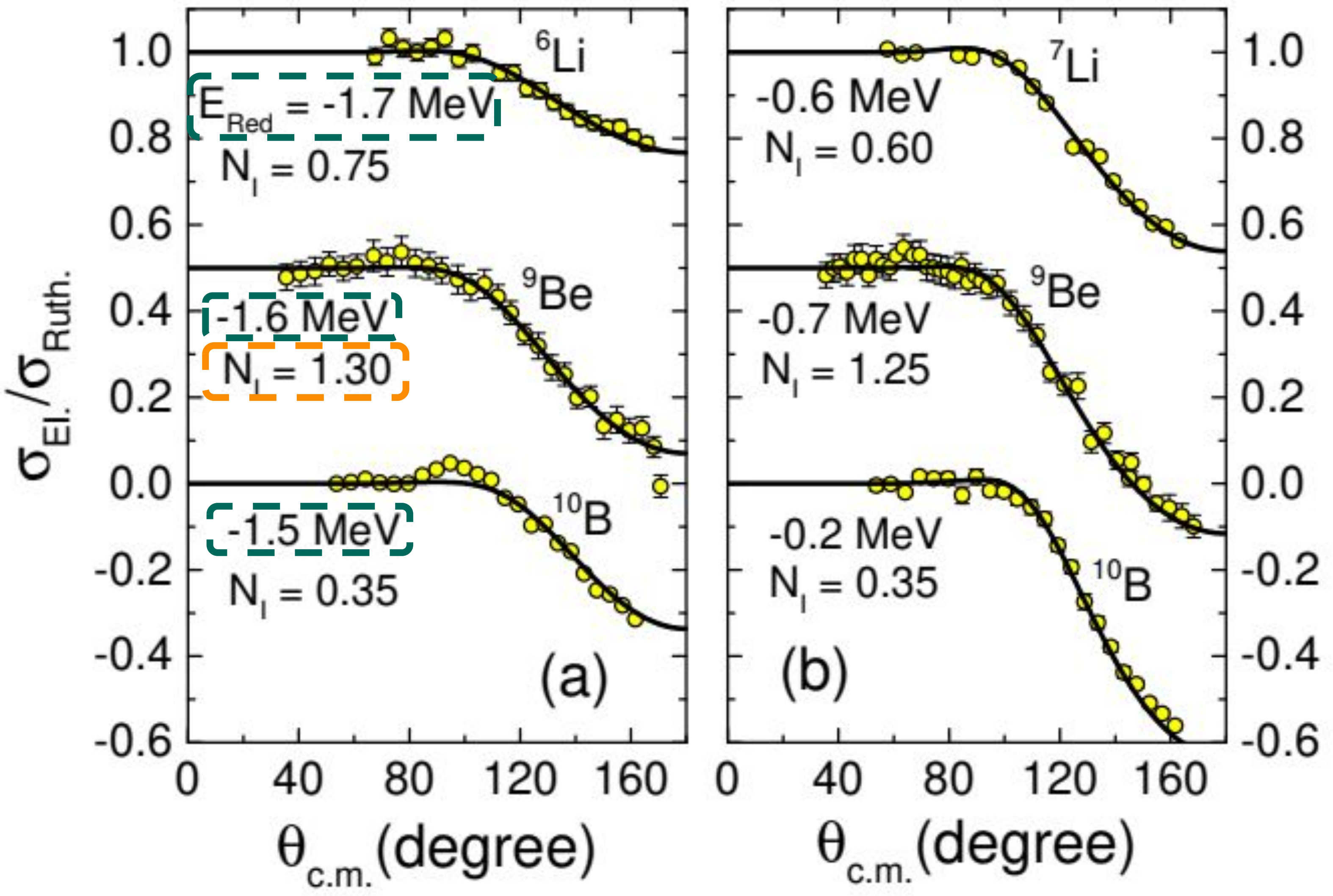

Sub-barrier region

$$E_{Red} = E_{c.m.} - V_B$$

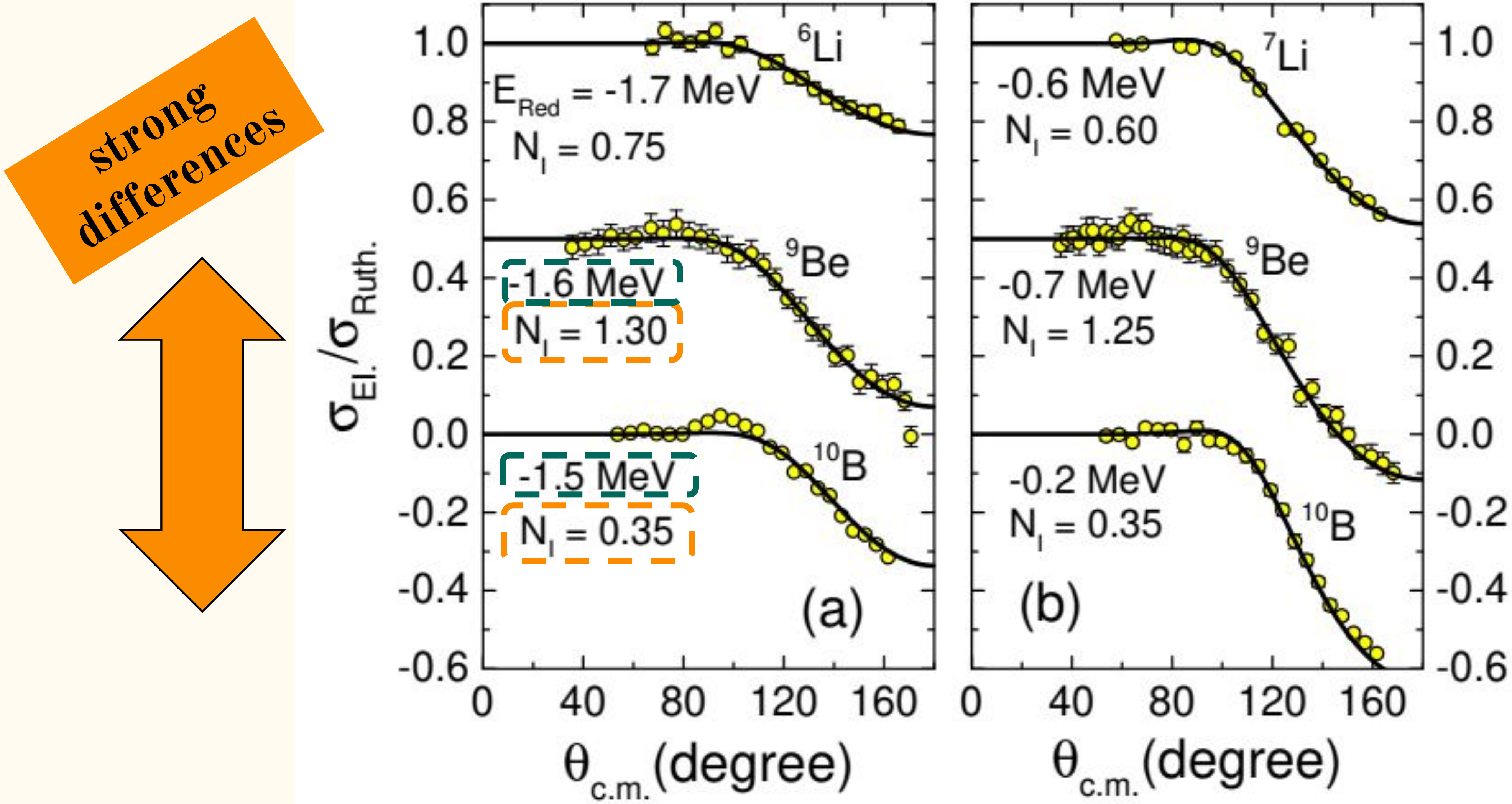

Sub-barrier region

$$E_{Red} = E_{c.m.} - V_B$$

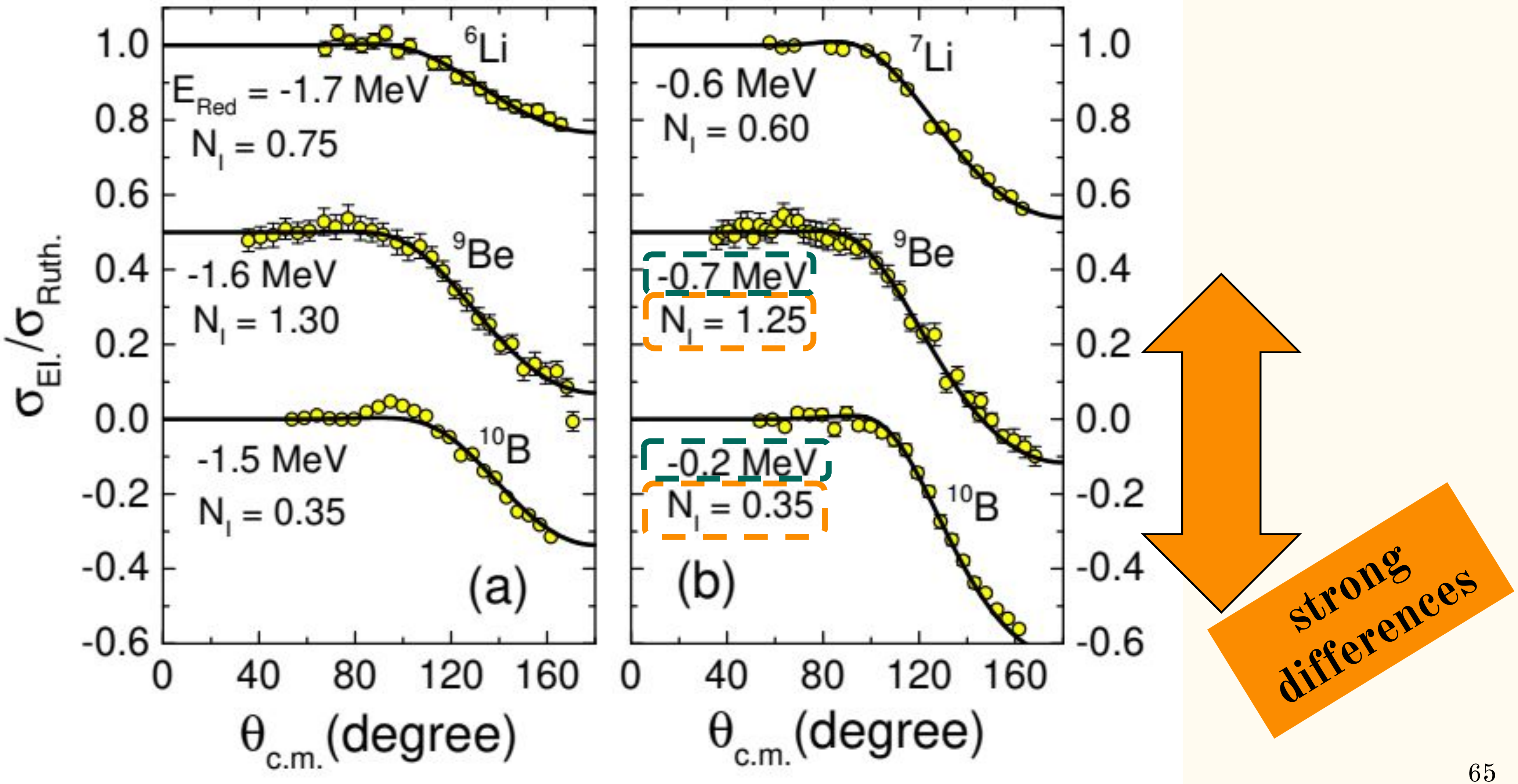

Above-barrier region

$$E_{Red} = E_{c.m.} - V_B$$

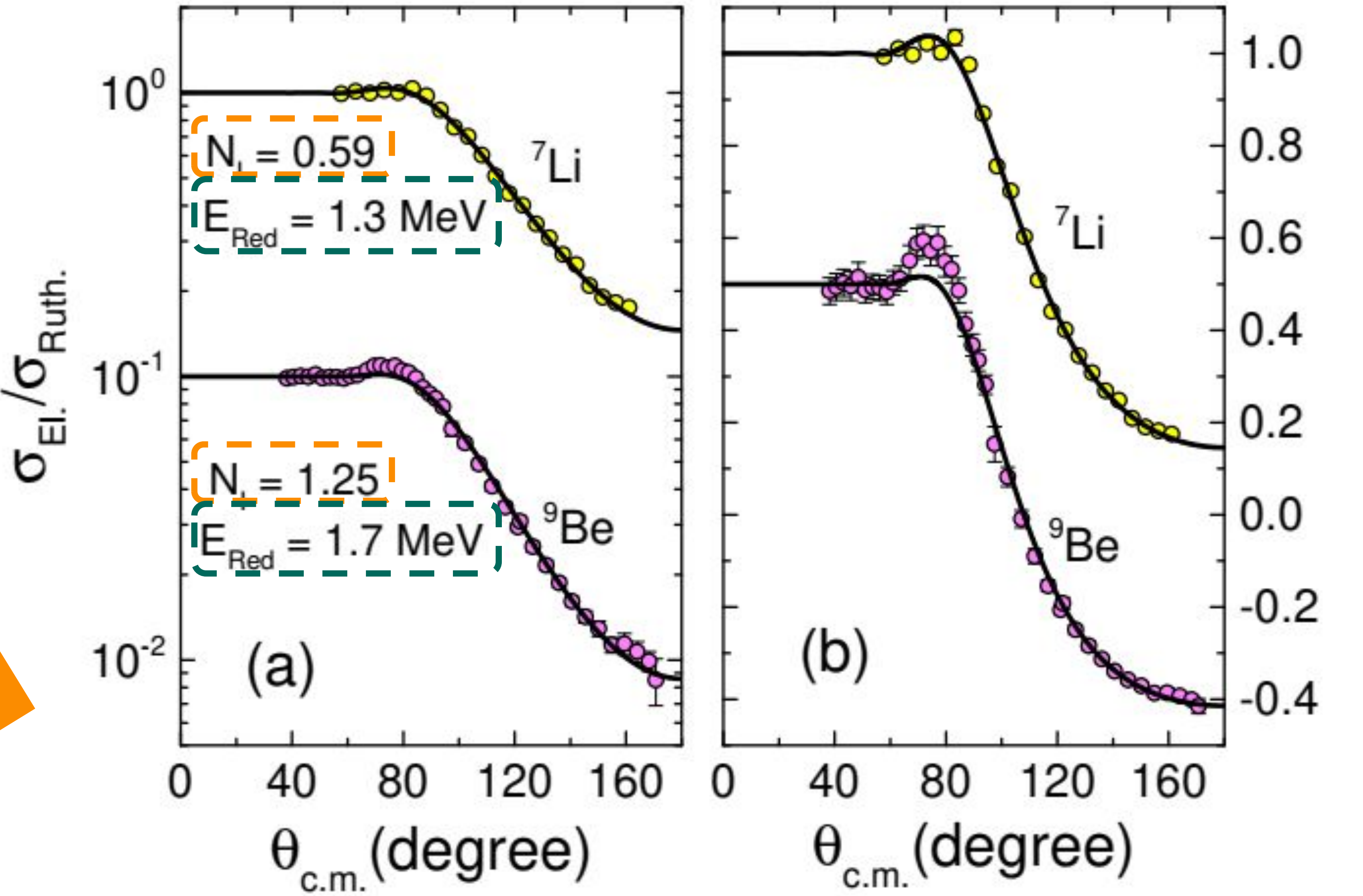

strong differences

Above-barrier region

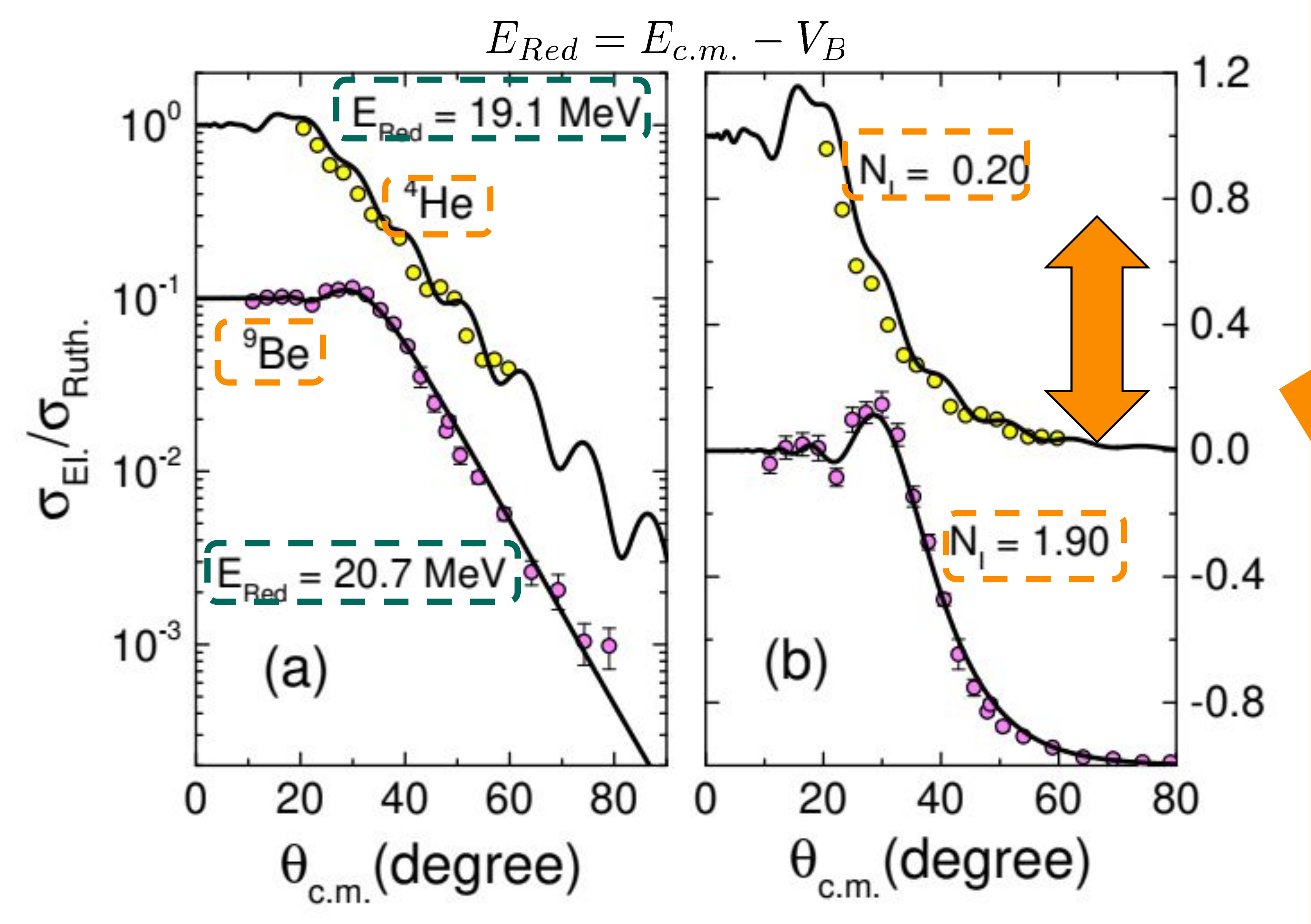

strong differences

Above-barrier region

$$E_{Red} = E_{c.m.} - V_B$$

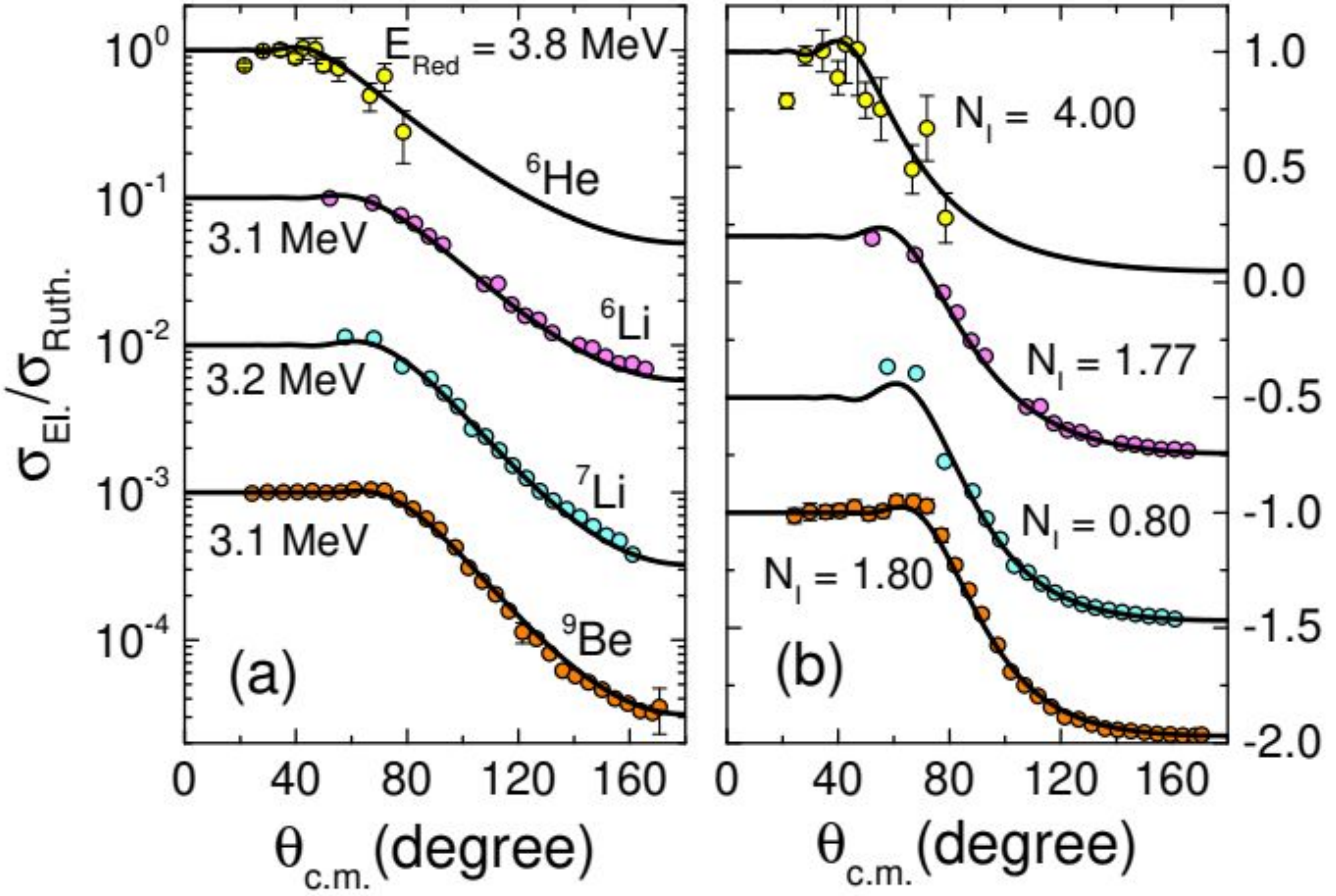

Above-barrier region

$$E_{Red} = E_{c.m.} - V_B$$

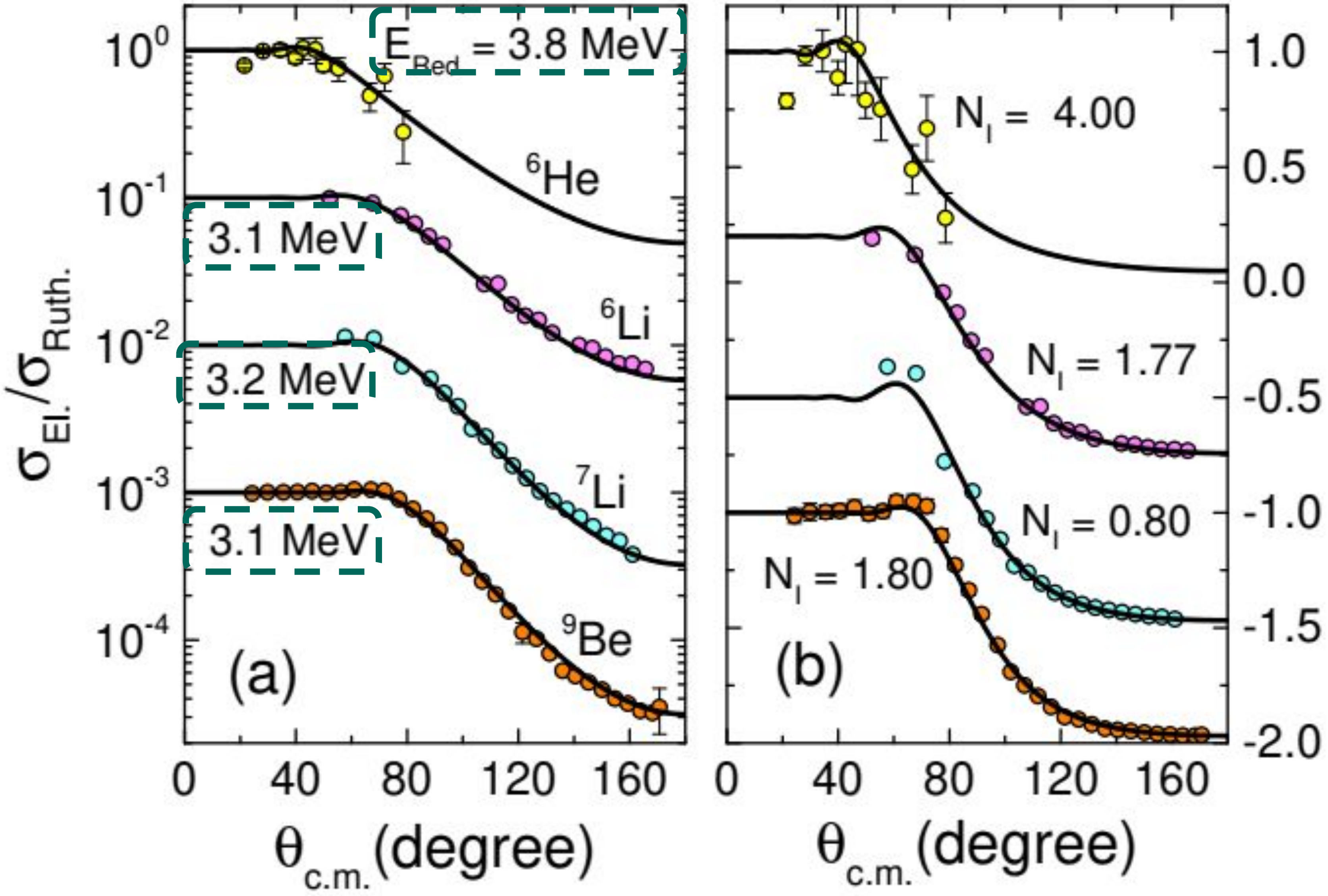

Above-barrier region

$$E_{Red} = E_{c.m.} - V_B$$

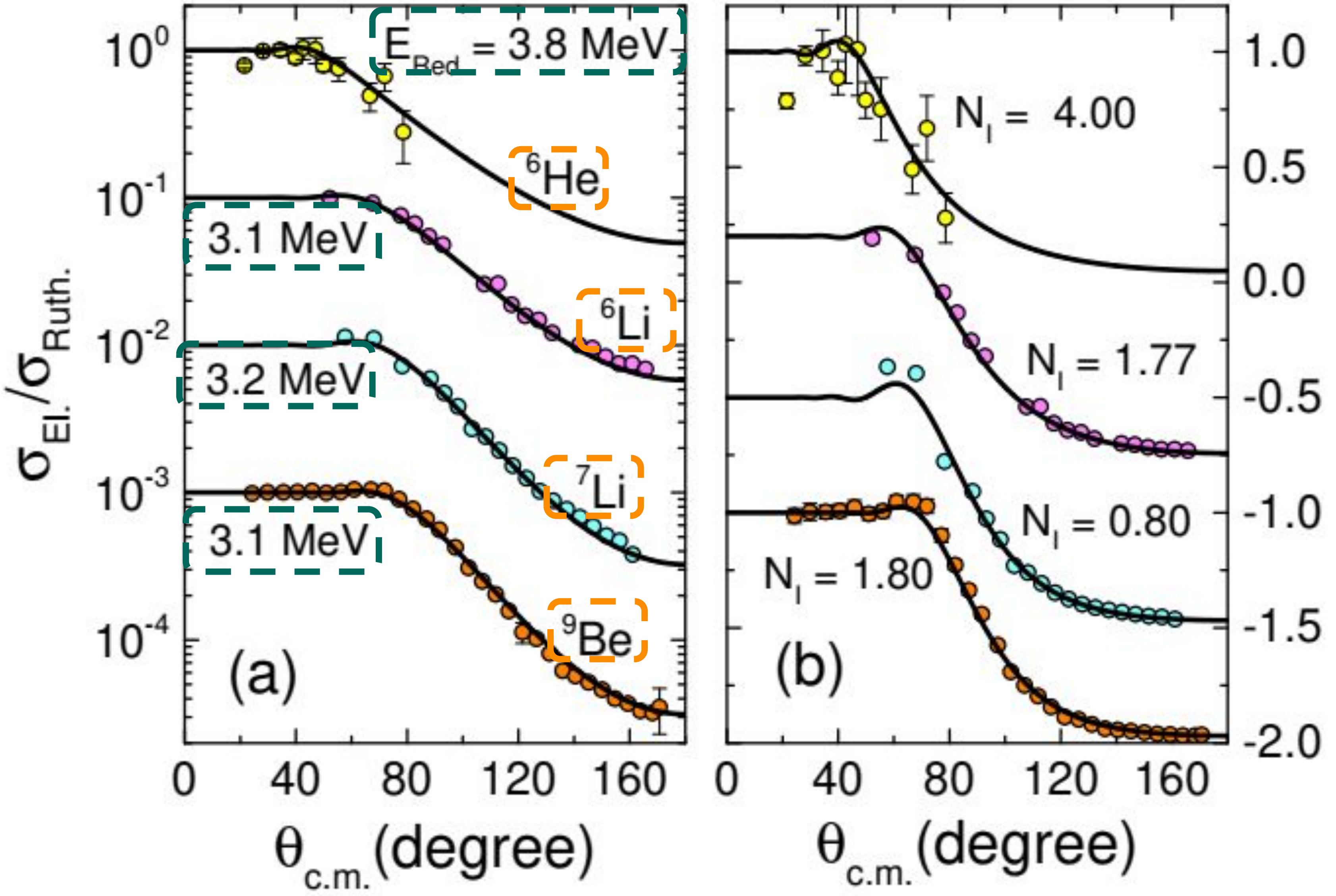

Above-barrier region

$$E_{Red} = E_{c.m.} - V_B$$

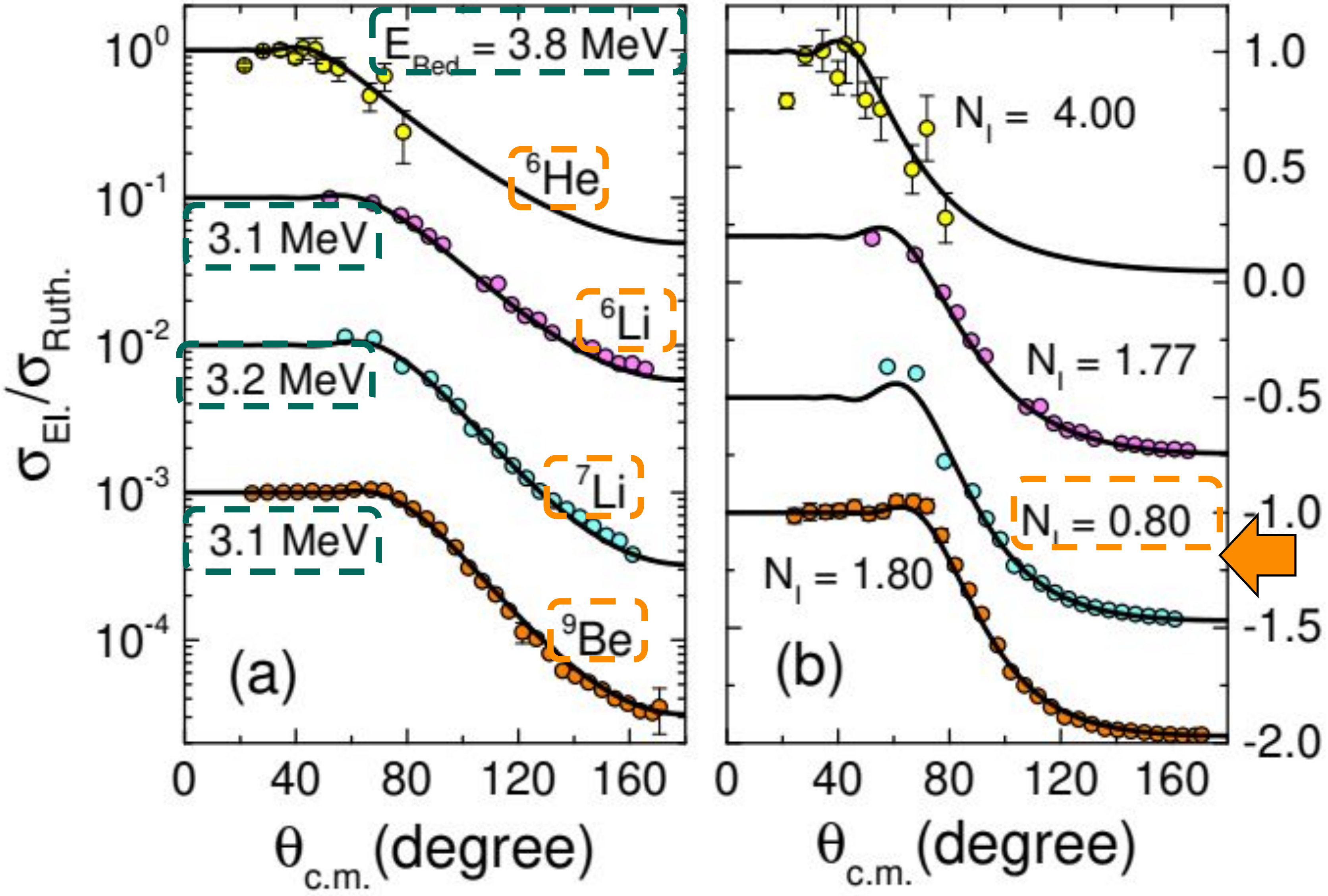

Above-barrier region

$$E_{Red} = E_{c.m.} - V_B$$

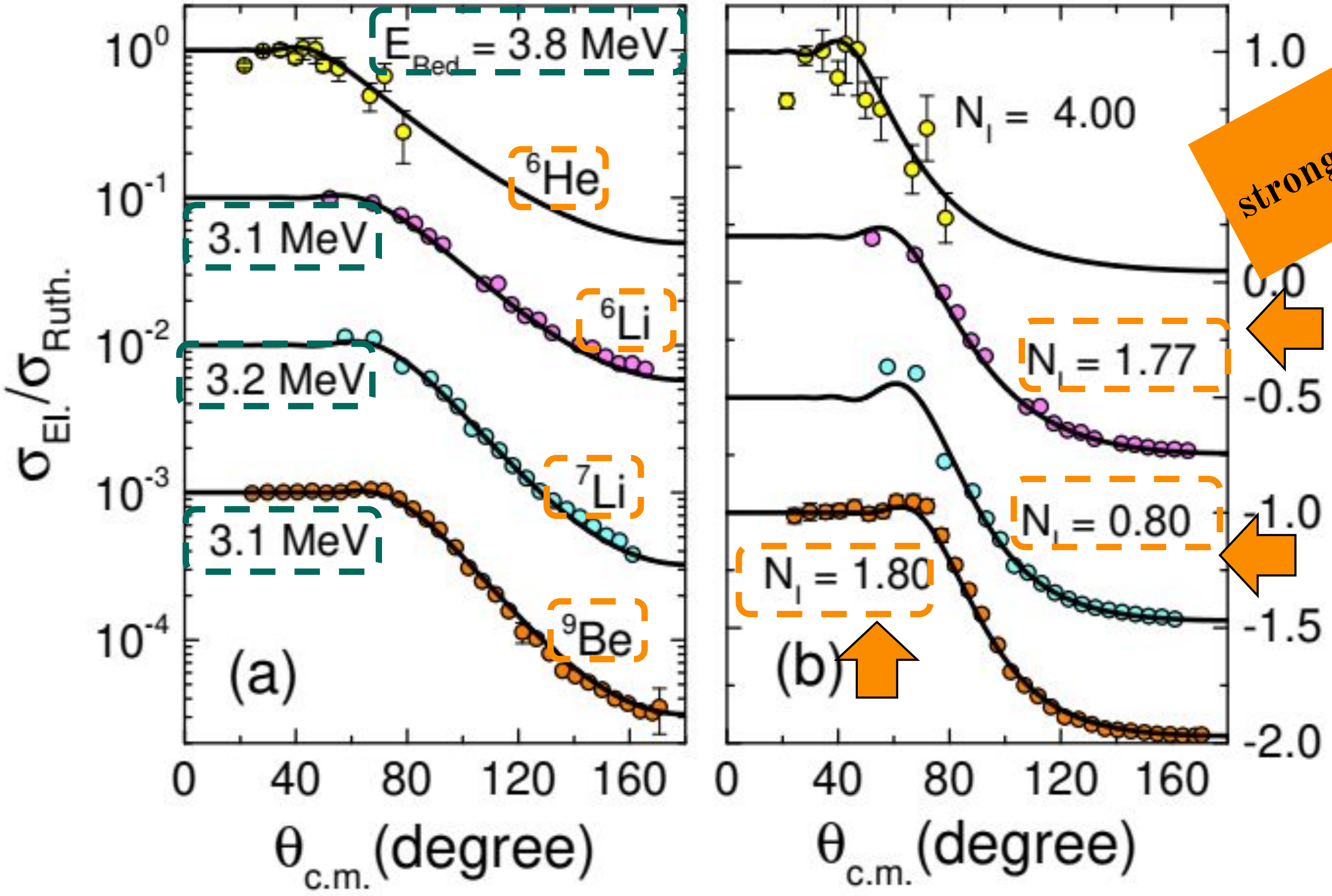

long range
strong surface absorption
SSA

Above-barrier region

$$E_{Red} = E_{c.m.} - V_B$$

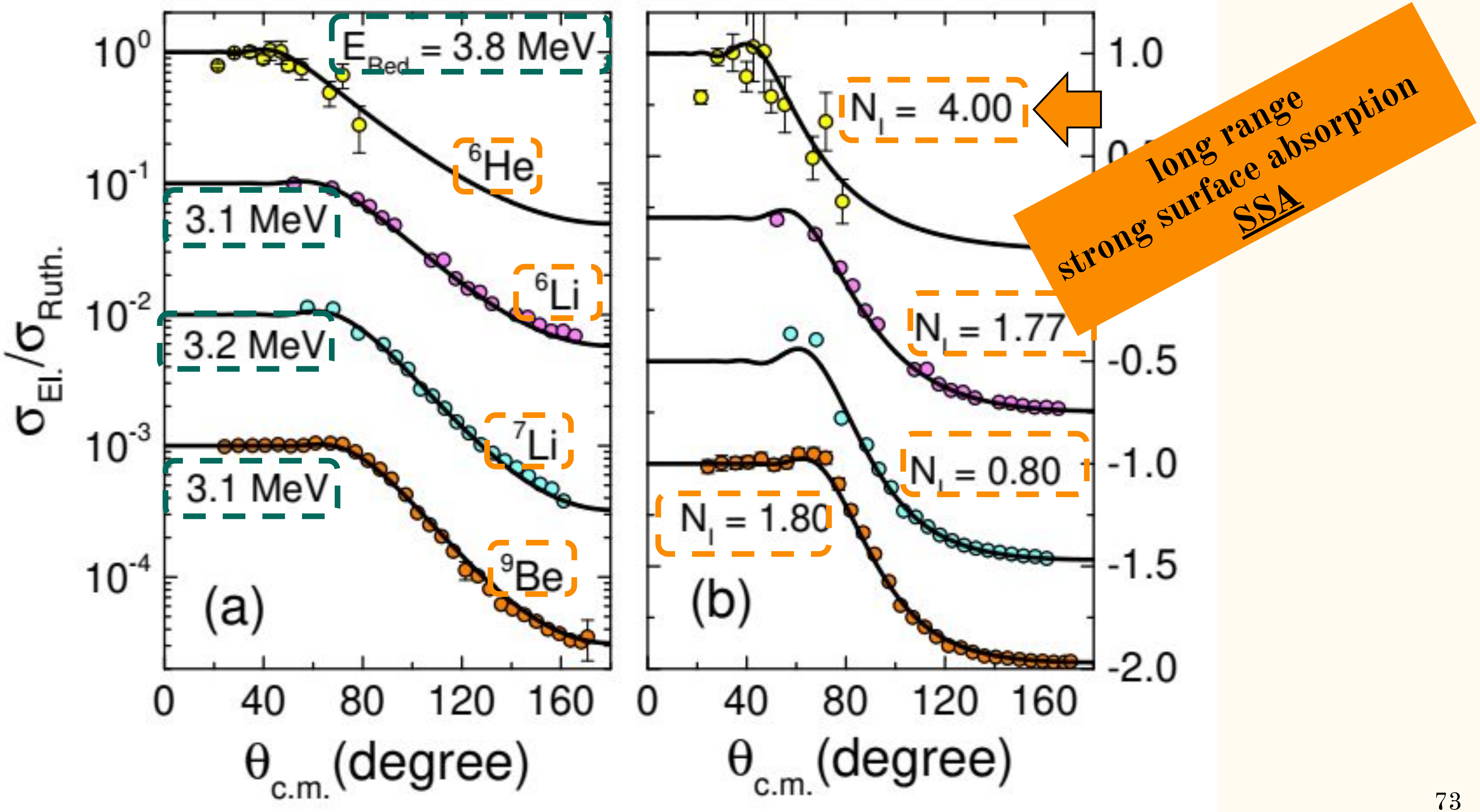

TABLE I. Break-up threshold of light stable and exotic nuclei.

system	cluster	ε_b (MeV)
^{11}Li	^{9}Li+2n	-0.396
^{11}Be	^{10}Be+1n	-0.501
^{6}He	^{4}He+2n	-0.975
^{6}Li	α+d	-1.473
^{9}Be	^{8}Be+1n	-1.574
^{9}Be	$\alpha+\alpha$+1n	-1.664
^{7}Li	α+t	-2.467
^{9}Li	^{7}Li+2n	-4.062
^{10}B	^{6}Li+α	-4.461
^{18}O	^{14}C+α	-6.228
^{16}O	^{12}C+α	-7.162
$^{12}C^{g.s.}$	^{8}Be+α	-7.367
$^{12}C^{H.s.}$	^{8}Be+α	-7.653
^{4}He	^{3}He+1n	-20.6

projectile	reaction products	Q(MeV)
^{6}Li	^{121}Sn + $\alpha + p$	2.472
^{6}Li	^{121}Sb + $\alpha + n$	2.092
^{7}Li	^{122}Sn + $\alpha + p$	4.036
^{7}Li	^{122}Sb + $\alpha + n$	1.247
^{9}Be	^{121}Sn + $\alpha + \alpha$	4.597
^{9}Be	^{120}Sn + ^{8}Be + n	4.505
^{10}B	^{121}Sn + $2\alpha + p$	-1.989
^{10}B	^{121}Sb + $2\alpha + n$	-2.368

TABLE I. Break-up threshold of light stable and exotic nuclei.

system	cluster	ε_b (MeV)
^{11}Li	^{9}Li+2n	-0.396
^{11}Be	^{10}Be+1n	-0.501
^{6}He	^{4}He+2n	-0.975
^{6}Li	α+d	-1.473
^{9}Be	^{8}Be+1n	-1.574
^{9}Be	$\alpha+\alpha$+1n	-1.664
^{7}Li	α+t	-2.467
^{9}Li	^{7}Li+2n	-4.062
^{10}B	^{6}Li+α	-4.461
^{18}O	^{14}C+α	-6.228
^{16}O	^{12}C+α	-7.162
$^{12}C^{g.s.}$	^{8}Be+α	-7.367
$^{12}C^{H.s.}$	^{8}Be+α	-7.653
^{4}He	^{3}He+1n	-20.6

projectile	reaction products	Q(MeV)
^{6}Li	^{121}Sn + $\alpha + p$	2.472
^{6}Li	^{121}Sb + $\alpha + n$	2.092
^{7}Li	^{122}Sn + $\alpha + p$	4.036
^{7}Li	^{122}Sb + $\alpha + n$	1.247
^{9}Be	^{121}Sn + $\alpha + \alpha$	4.597
^{9}Be	^{120}Sn + ^{8}Be + n	4.505
^{10}B	^{121}Sn + $2\alpha + p$	-1.989
^{10}B	^{121}Sb + $2\alpha + n$	-2.368

TABLE I. Break-up threshold of light stable and exotic nuclei.

system	cluster	ε_b (MeV)
^{11}Li	^{9}Li+2n	-0.396
^{11}Be	^{10}Be+1n	-0.501
^{6}He	^{4}He+2n	-0.975
^{6}Li	α+d	-1.473
^{9}Be	^{8}Be+1n	-1.574
^{9}Be	$\alpha+\alpha$+1n	-1.664
^{7}Li	α+t	-2.467
^{9}Li	^{7}Li+2n	-4.062
^{10}B	^{6}Li+α	-4.461
^{18}O	^{14}C+α	-6.228
^{16}O	^{12}C+α	-7.162
$^{12}C^{g.s.}$	^{8}Be+α	-7.367
$^{12}C^{H.s.}$	^{8}Be+α	-7.653
^{4}He	^{3}He+1n	-20.6

projectile	reaction products	Q(MeV)
^{6}Li	^{121}Sn $+ \alpha + p$	2.472
^{6}Li	^{121}Sb $+ \alpha + n$	2.092
^{7}Li	^{122}Sn $+ \alpha + p$	4.036
^{7}Li	^{122}Sb $+ \alpha + n$	1.247
^{9}Be	^{121}Sn $+ \alpha + \alpha$	4.597
^{9}Be	^{120}Sn + ^{8}Be $+ n$	4.505
^{10}B	^{121}Sn $+ 2\alpha + p$	-1.989
^{10}B	^{121}Sb $+ 2\alpha + n$	-2.368

TABLE I. Break-up threshold of light stable and exotic nuclei.

system	cluster	ε_b (MeV)
^{11}Li	^{9}Li+2n	-0.396
^{11}Be	^{10}Be+1n	-0.501
^{6}He	^{4}He+2n	-0.975
^{6}Li	α+d	-1.473
^{9}Be	^{8}Be+1n	-1.574
^{9}Be	$\alpha+\alpha$+1n	-1.664
^{7}Li	α+t	-2.467
^{9}Li	^{7}Li+2n	-4.062
^{10}B	^{6}Li+α	-4.461
^{18}O	^{14}C+α	-6.228
^{16}O	^{12}C+α	-7.162
^{12}C$^{g.s.}$	^{8}Be+α	-7.367
^{12}C$^{H.s.}$	^{8}Be+α	-7.653
^{4}He	^{3}He+1n	-20.6

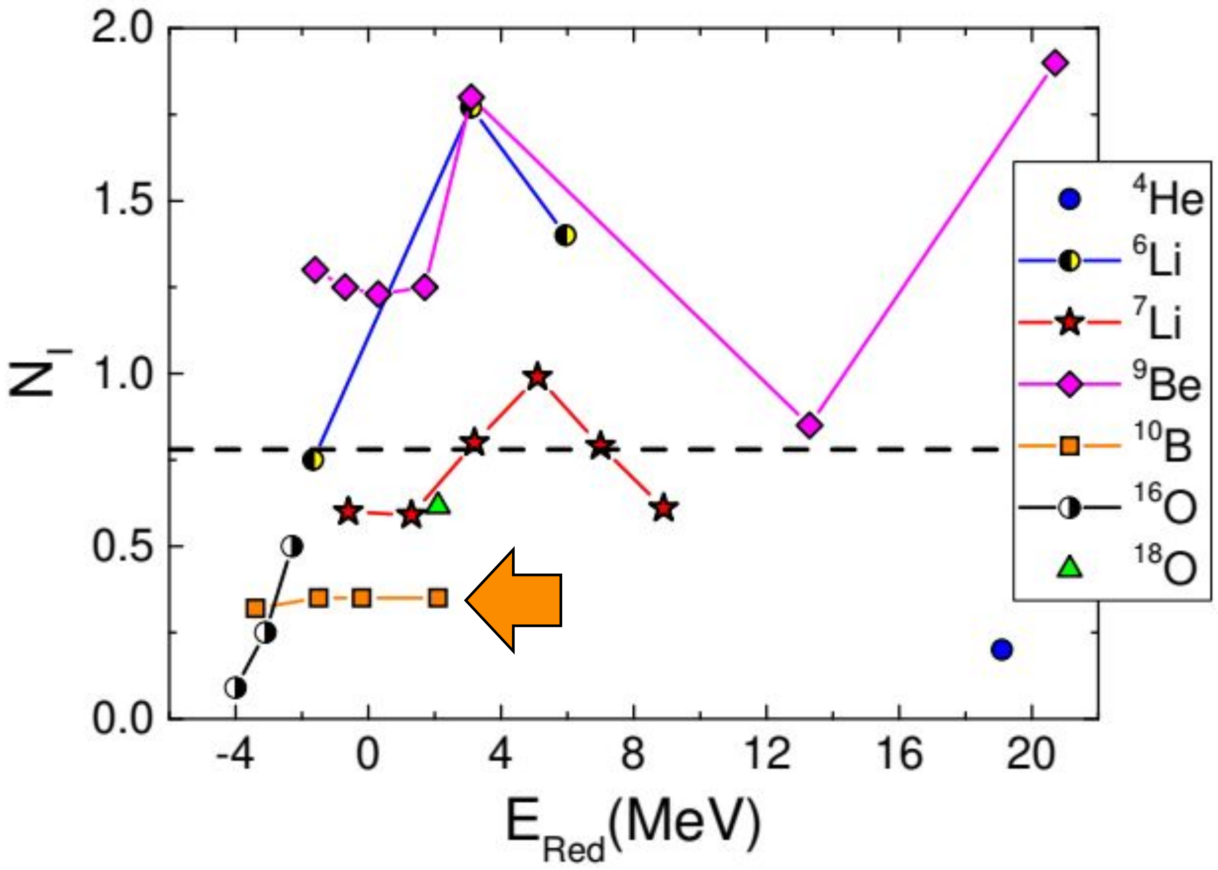

TABLE I. Break-up threshold of light stable and exotic nuclei.

system	cluster	ε_b (MeV)
^{11}Li	^{9}Li+2n	-0.396
^{11}Be	^{10}Be+1n	-0.501
^{6}He	^{4}He+2n	-0.975
^{6}Li	α+d	-1.473
^{9}Be	^{8}Be+1n	-1.574
^{9}Be	$\alpha+\alpha$+1n	-1.664
^{7}Li	α+t	-2.467
^{9}Li	^{7}Li+2n	-4.062
^{10}B	^{6}Li+α	-4.461
^{18}O	^{14}C+α	-6.228
^{16}O	^{12}C+α	-7.162
^{12}C$^{g.s.}$	^{8}Be+α	-7.367
^{12}C$^{H.s.}$	^{8}Be+α	-7.653
^{4}He	^{3}He+1n	-20.6

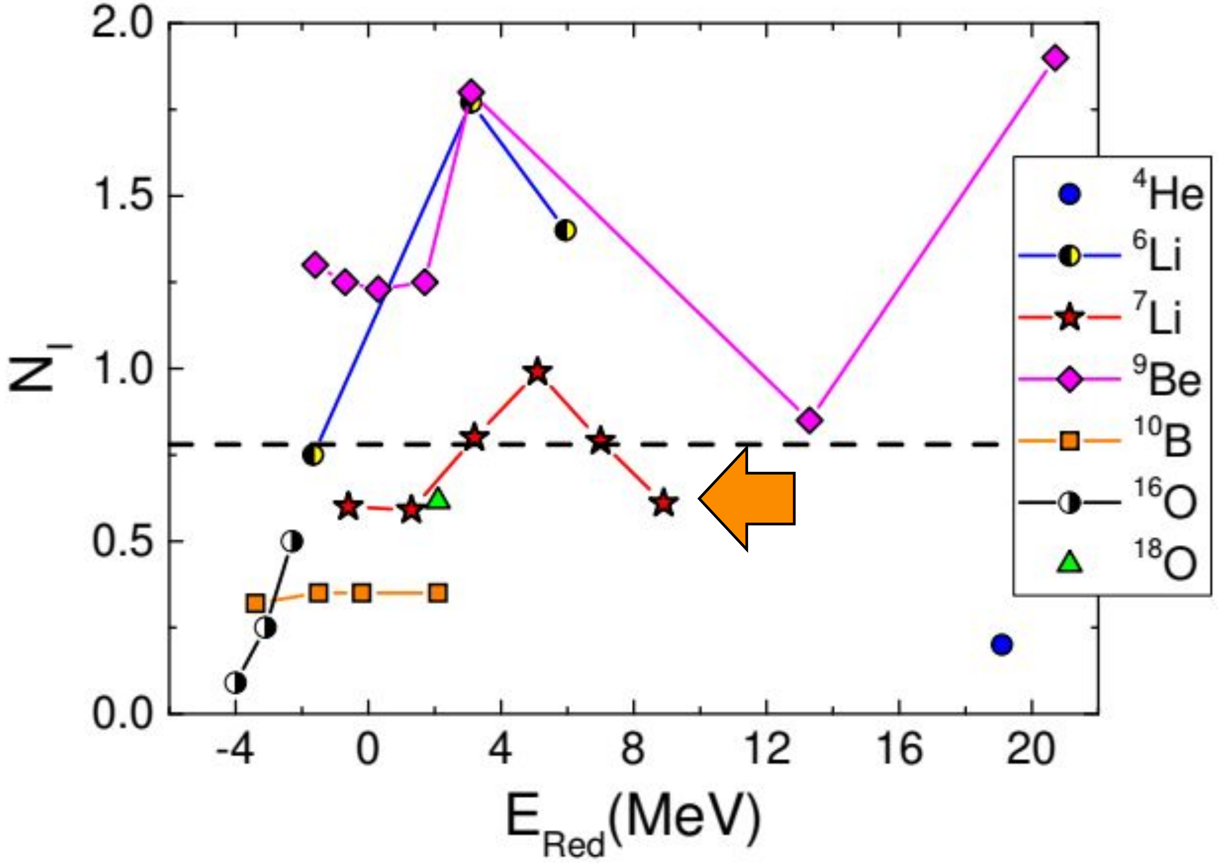

TABLE I. Break-up threshold of light stable and exotic nuclei.

system	cluster	ε_b (MeV)
^{11}Li	^{9}Li+2n	-0.396
^{11}Be	^{10}Be+1n	-0.501
^{6}He	^{4}He+2n	-0.975
^{6}Li	α+d	-1.473
^{9}Be	^{8}Be+1n	-1.574
^{9}Be	$\alpha+\alpha$+1n	-1.664
^{7}Li	α+t	-2.467
^{9}Li	^{7}Li+2n	-4.062
^{10}B	^{6}Li+α	-4.461
^{18}O	^{14}C+α	-6.228
^{16}O	^{12}C+α	-7.162
$^{12}C^{g.s.}$	^{8}Be+α	-7.367
$^{12}C^{H.s.}$	^{8}Be+α	-7.653
^{4}He	^{3}He+1n	-20.6

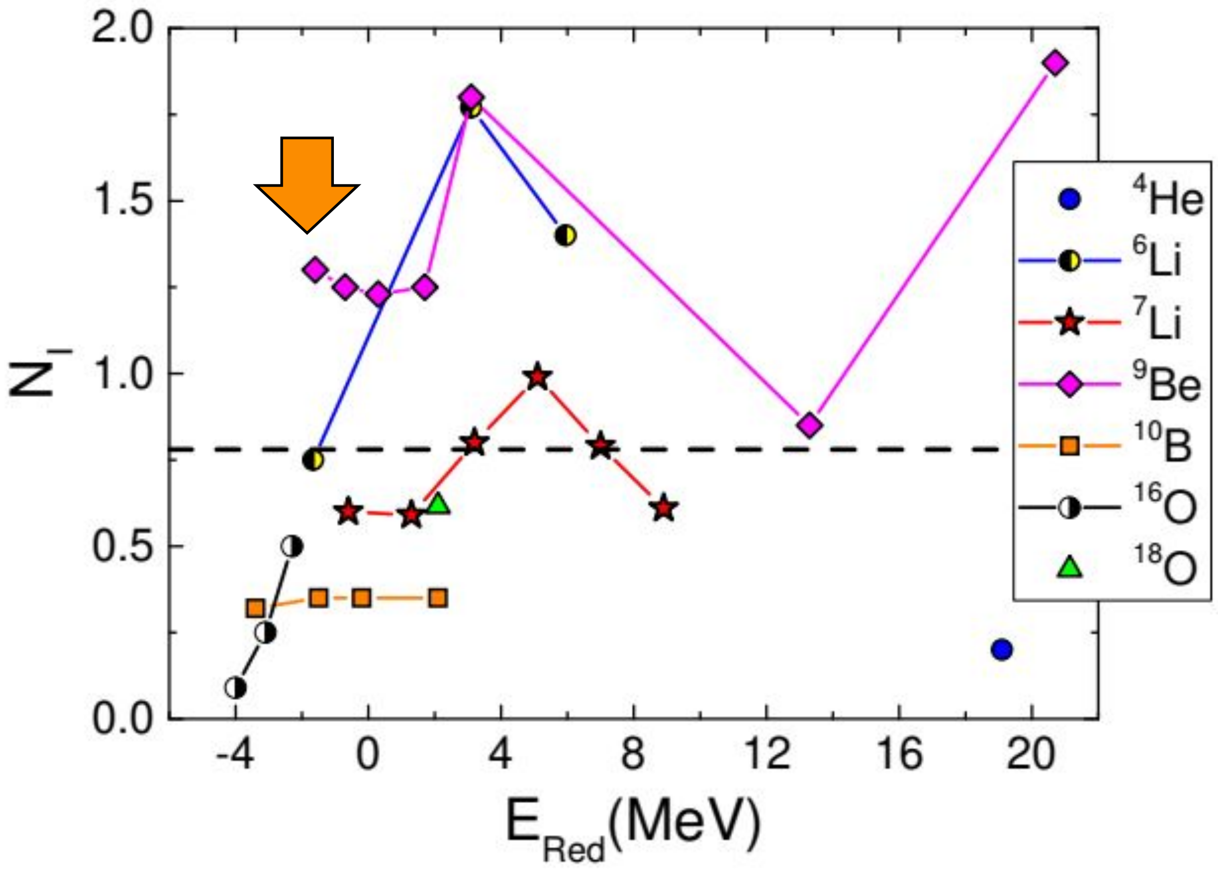

TABLE I. Break-up threshold of light stable and exotic nuclei.

system	cluster	ε_b (MeV)
^{11}Li	^{9}Li+2n	-0.396
^{11}Be	^{10}Be+1n	-0.501
^{6}He	^{4}He+2n	-0.975
^{6}Li	α+d	-1.473
^{9}Be	^{8}Be+1n	-1.574
^{9}Be	$\alpha+\alpha$+1n	-1.664
^{7}Li	α+t	-2.467
^{9}Li	^{7}Li+2n	-4.062
^{10}B	^{6}Li+α	-4.461
^{18}O	^{14}C+α	-6.228
^{16}O	^{12}C+α	-7.162
$^{12}C^{g.s.}$	^{8}Be+α	-7.367
$^{12}C^{H.s.}$	^{8}Be+α	-7.653
^{4}He	^{3}He+1n	-20.6

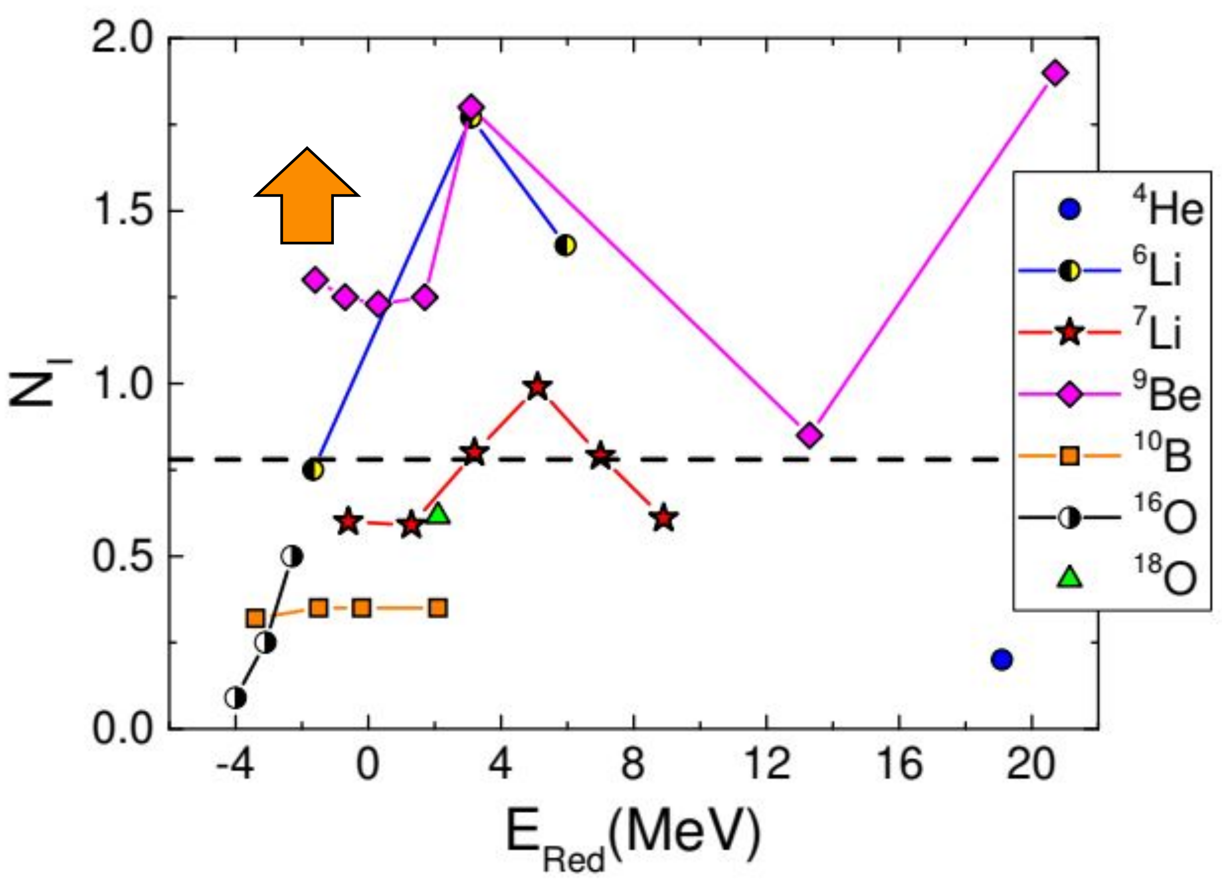

TABLE I. Break-up threshold of light stable and exotic nuclei.

system	cluster	ε_b (MeV)
^{11}Li	^{9}Li+2n	-0.396
^{11}Be	^{10}Be+1n	-0.501
^{6}He	^{4}He+2n	-0.975
^{6}Li	α+d	-1.473
^{9}Be	^{8}Be+1n	-1.574
^{9}Be	$\alpha+\alpha$+1n	-1.664
^{7}Li	α+t	-2.467
^{9}Li	^{7}Li+2n	-4.062
^{10}B	^{6}Li+α	-4.461
^{18}O	^{14}C+α	-6.228
^{16}O	^{12}C+α	-7.162
$^{12}C^{g.s.}$	^{8}Be+α	-7.367
$^{12}C^{H.s.}$	^{8}Be+α	-7.653
^{4}He	^{3}He+1n	-20.6

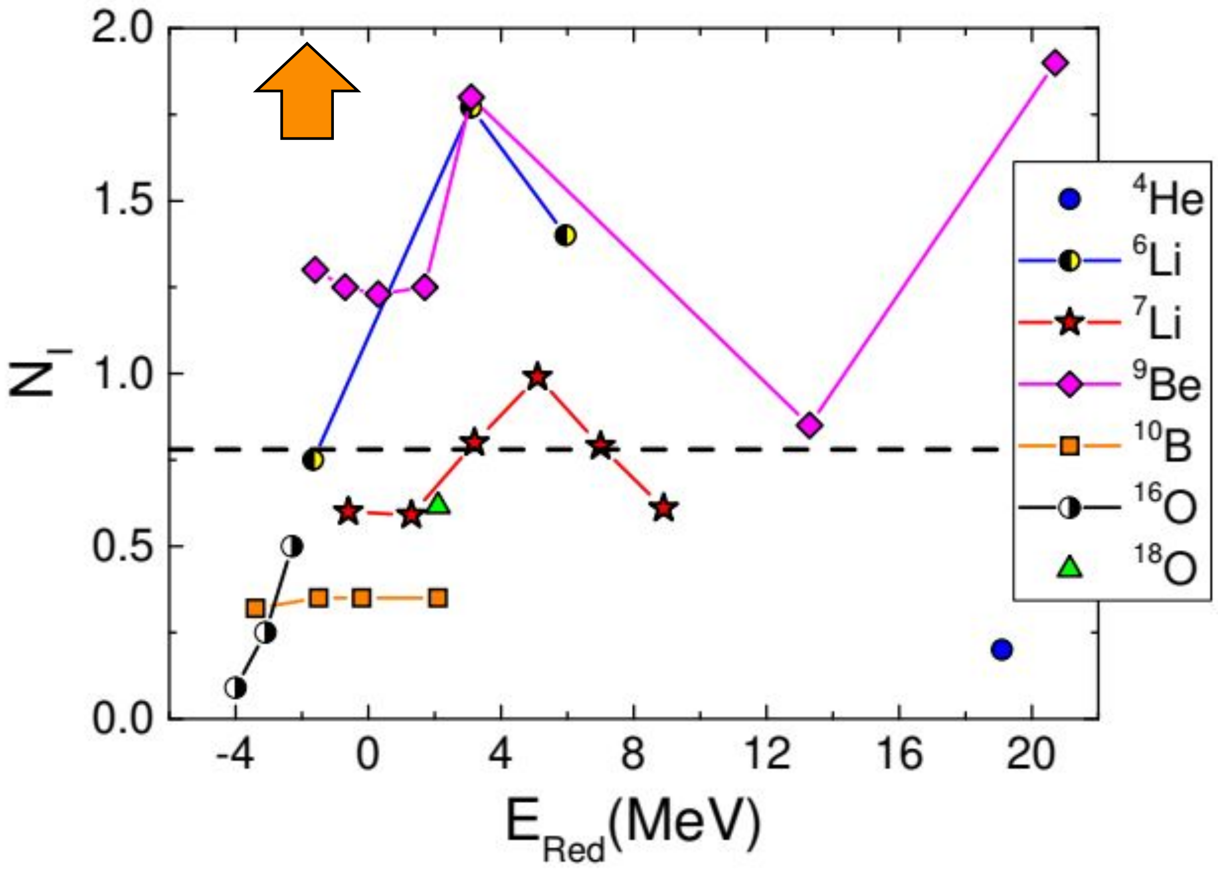

TABLE I. Break-up threshold of light stable and exotic nuclei.

system	cluster	ε_b (MeV)
^{11}Li	^{9}Li+2n	-0.396
^{11}Be	^{10}Be+1n	-0.501
^{6}He	^{4}He+2n	-0.975
^{6}Li	α+d	-1.473
^{9}Be	^{8}Be+1n	-1.574
^{9}Be	α+α+1n	-1.664
^{7}Li	α+t	-2.467
^{9}Li	^{7}Li+2n	-4.062
^{10}B	^{6}Li+α	-4.461
^{18}O	^{14}C+α	-6.228
^{16}O	^{12}C+α	-7.162
^{12}C$^{g.s.}$	^{8}Be+α	-7.367
^{12}C$^{H.s.}$	^{8}Be+α	-7.653
^{4}He	^{3}He+1n	-20.6

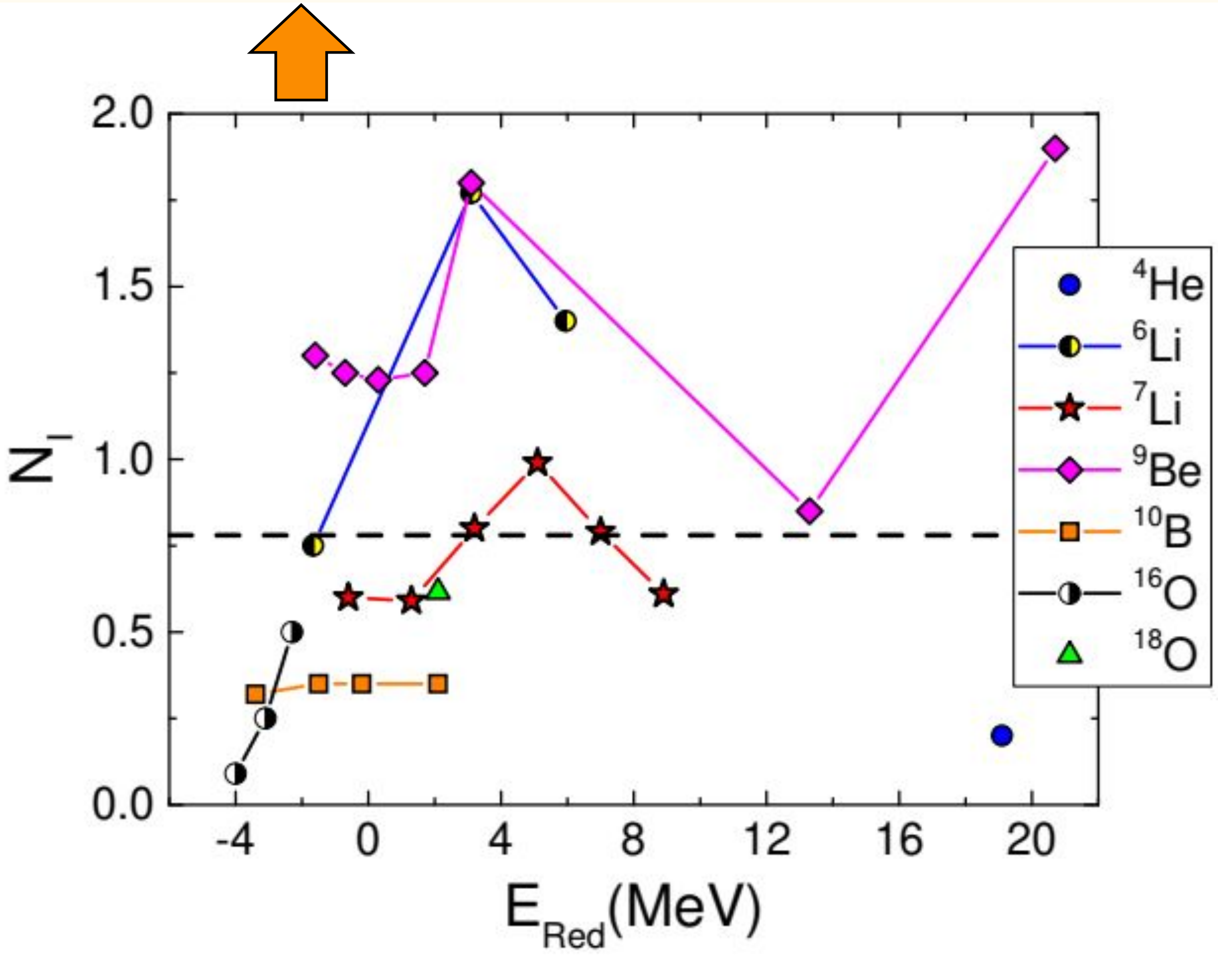

TABLE I. Break-up threshold of light stable and exotic nuclei.

system	cluster	ε_b (MeV)
^{11}Li	^{9}Li+2n	-0.396
^{11}Be	^{10}Be+1n	-0.501
^{6}He	^{4}He+2n	-0.975
^{6}Li	α+d	-1.473
^{9}Be	^{8}Be+1n	-1.574
^{9}Be	$\alpha+\alpha$+1n	-1.664
^{7}Li	α+t	-2.467
^{9}Li	^{7}Li+2n	-4.062
^{10}B	^{6}Li+α	-4.461
^{18}O	^{14}C+α	-6.228
^{16}O	^{12}C+α	-7.162
^{12}C$^{g.s.}$	^{8}Be+α	-7.367
^{12}C$^{H.s.}$	^{8}Be+α	-7.653
^{4}He	^{3}He+1n	-20.6

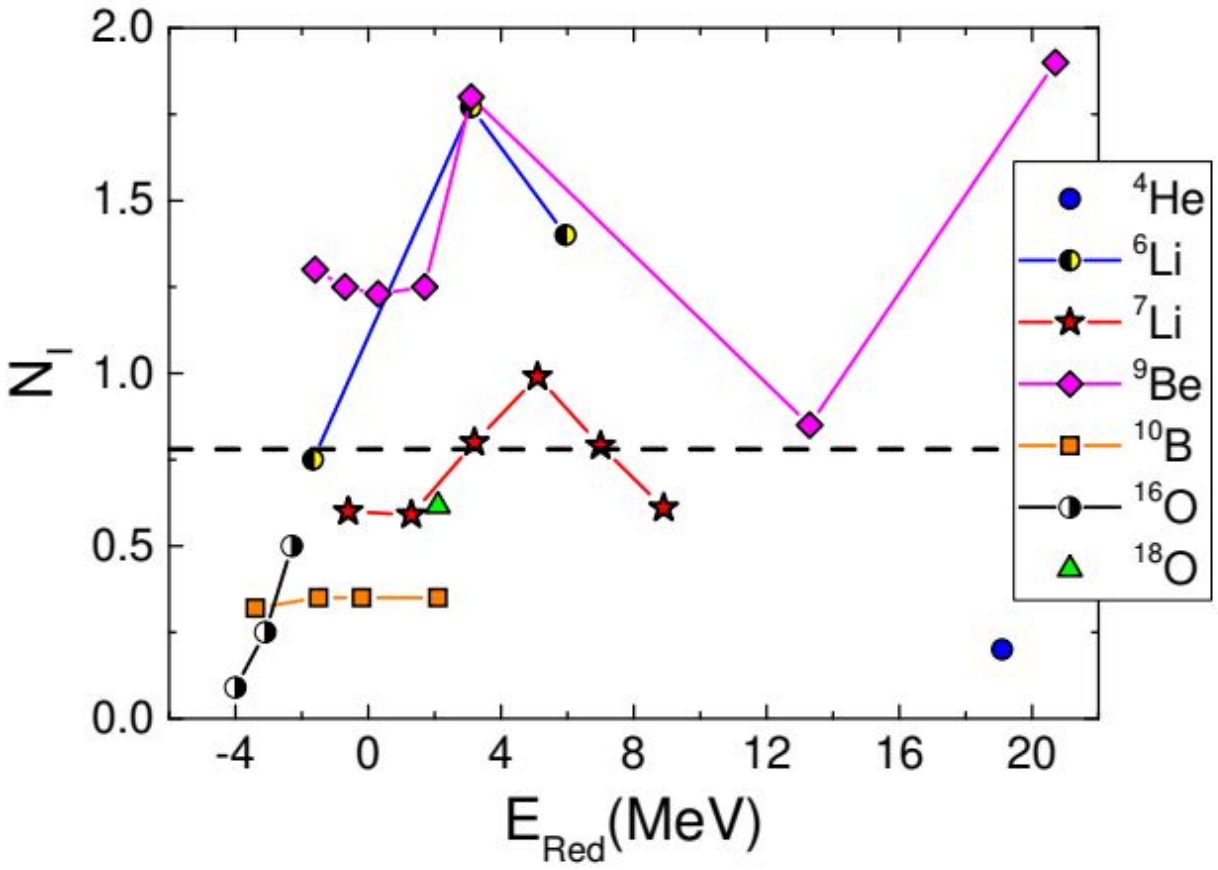

Coulomb dipole polarization effect

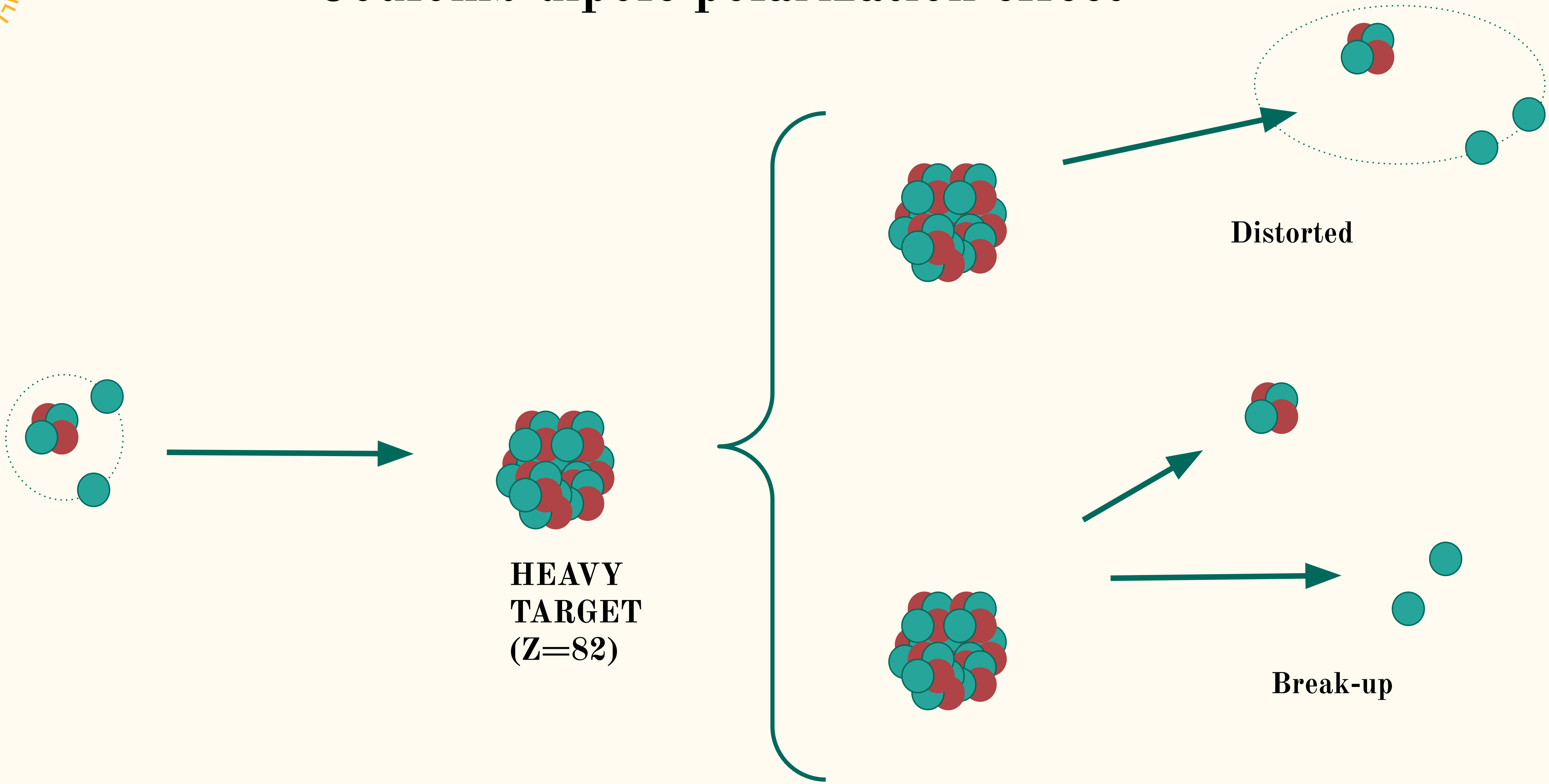

Coulomb dipole polarization effect

A simple analytical formula for the **Coulomb dipole polarization (CDP)** potential was derived in:

- M. V. Andrés et al., Nucl. Phys. A 579, 273 (1994).
- M. V. Andrés et al., Nucl. Phys. A 583, 817 (1995).

$$U_{pol} = -\frac{4\pi}{9}\frac{Z_t^2}{\hbar v}\frac{1}{(r-a_0)^2 r}\int_{\varepsilon_b}^{\infty} d\varepsilon \frac{dB(E1,\varepsilon)}{d\varepsilon}\left(g\left(\frac{r}{a_0}-1,\xi\right)+if\left(\frac{r}{a_0}-1,\xi\right)\right)$$

$\frac{dB(E1)}{d\varepsilon}$ is the probability distribution of the dipolar electric transition;

ε_b is the necessary energy to break up the projectile;

a_0 is the half of the distance of closest approach in the head-on collision;

f, g are analytic functions.

Coulomb dipole polarization effect

A simple analytical formula for the **Coulomb dipole polarization (CDP)** potential was derived in:

- M. V. Andrés et al., Nucl. Phys. A 579, 273 (1994).
- M. V. Andrés et al., Nucl. Phys. A 583, 817 (1995).

$$U_{pol} = -\frac{4\pi}{9}\frac{Z_t^2}{\hbar v}\frac{1}{(r-a_0)^2 r}\int_{\varepsilon_b}^{\infty} d\varepsilon \frac{dB(E1,\varepsilon)}{d\varepsilon}\left(g\left(\frac{r}{a_0}-1,\xi\right)+if\left(\frac{r}{a_0}-1,\xi\right)\right)$$

$\frac{dB(E1)}{d\varepsilon}$ is the probability distribution of the dipolar electric transition;

ε_b is the necessary energy to break up the projectile;

a_0 is the half of the distance of closest approach in the head-on collision;

f, g are analytic functions.

Coulomb dipole polarization effect

A simple analytical formula for the **Coulomb dipole polarization (CDP)** potential was derived in:

- **M. V. Andrés et al., Nucl. Phys. A 579, 273 (1994).**
- **M. V. Andrés et al., Nucl. Phys. A 583, 817 (1995).**

$$U_{pol} = -\frac{4\pi}{9}\frac{Z_t^2}{\hbar v}\frac{1}{(r-a_0)^2 r}\int_{\varepsilon_b}^{\infty} d\varepsilon \frac{dB(E1,\varepsilon)}{d\varepsilon}\left(g\left(\frac{r}{a_0}-1,\xi\right)+if\left(\frac{r}{a_0}-1,\xi\right)\right)$$

$\frac{dB(E1)}{d\varepsilon}$ is the probability distribution of the dipolar electric transition;

ε_b is the necessary energy to break up the projectile;

a_0 is the half of the distance of closest approach in the head-on collision;

f, g are analytic functions.

Coulomb dipole polarization effect

Experimental and theoretical B(E1) distributions

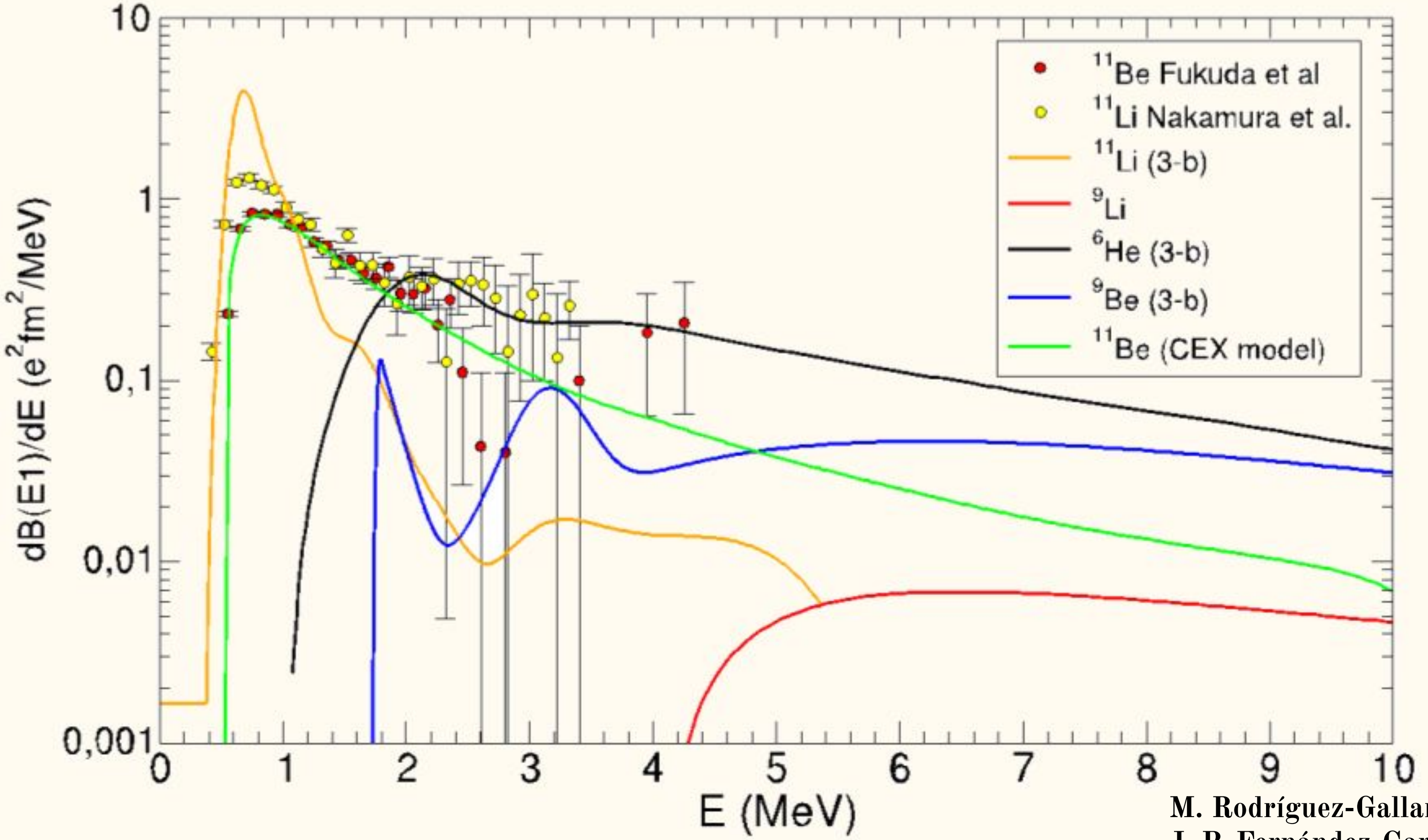

M. Rodríguez-Gallardo *et al.*, PRC 80, 051601 (R) (2009).
J. P. Fernández-García *et al.* PRL 110, 142701 (2013).
T. Nakamura et al., Phys. Rev. Lett. 96, 252502 (2006).
N. Fukuda et al., Phys. Rev. C 70, 054606 (2004).

Coulomb dipole polarization effect

$$U_{opt}(R) = V_{SPP}(R) + iN_I V_{SPP}(R) + V_{pol}(R) + iW_{pol}(R)$$

Coulomb dipole polarization potential

Coulomb dipole polarization effect

$$U_{opt}(R) = V_{SPP}(R) + iN_I V_{SPP}(R) + V_{pol}(R) + iW_{pol}(R)$$ **Coulomb dipole polarization potential**

$$U_{opt}(R) = V_{SPP}(R) + i0.78 V_{SPP}(R)$$

↕ **nuclear potential**

$$V_{\text{SPP}}(R) = V_{\text{Fold}}(R) e^{-4v^2/c^2}$$

$$V_{\text{Fold}}(R) = \int\int \rho_1(\vec{r}_1)\rho_2(\vec{r}_2)\nu_{NN}(\vec{R} - \vec{r}_1 + \vec{r}_2)\, d\vec{r}_1\, d\vec{r}_2$$

Coulomb dipole polarization effect

$$U_{opt}(R) = V_{SPP}(R) + iN_I V_{SPP}(R) + V_{pol}(R) + iW_{pol}(R)$$

Coulomb dipole polarization potential

$$U_{opt}(R) = V_{SPP}(R) + i0.78 V_{SPP}(R)$$

$$U_{pol} = -\frac{4\pi}{9}\frac{Z_t^2}{\hbar v}\frac{1}{(r-a_0)^2 r}\int_{\varepsilon_b}^{\infty} d\varepsilon \frac{dB(E1,\varepsilon)}{d\varepsilon}\left(g\left(\frac{r}{a_0}-1,\xi\right)+if\left(\frac{r}{a_0}-1,\xi\right)\right)$$

nuclear potential

$$V_{\mathrm{SPP}}(R) = V_{\mathrm{Fold}}(R) e^{-4v^2/c^2}$$

$$V_{\mathrm{Fold}}(R) = \int\int \rho_1(\vec{r}_1)\rho_2(\vec{r}_2)\nu_{NN}(\vec{R}-\vec{r}_1+\vec{r}_2)\, d\vec{r}_1\, d\vec{r}_2$$

Coulomb dipole polarization effect

$$U_{opt}(R) = V_{SPP}(R) + iN_I V_{SPP}(R) + V_{pol}(R) + iW_{pol}(R)$$ **Coulomb dipole polarization potential**

$$U_{opt}(R) = V_{SPP}(R) + i0.78 V_{SPP}(R)$$

nuclear potential

$$U_{pol} = -\frac{4\pi}{9}\frac{Z_t^2}{\hbar v}\frac{1}{(r-a_0)^2 r}\int_{\varepsilon_b}^{\infty} d\varepsilon \frac{dB(E1,\varepsilon)}{d\varepsilon}\left(g\left(\frac{r}{a_0}-1,\xi\right)+if\left(\frac{r}{a_0}-1,\xi\right)\right)$$

$$V_{\mathrm{SPP}}(R) = V_{\mathrm{Fold}}(R)e^{-4v^2/c^2}$$

$$V_{\mathrm{Fold}}(R) = \int\int \rho_1(\vec{r}_1)\rho_2(\vec{r}_2)\nu_{NN}(\vec{R}-\vec{r}_1+\vec{r}_2)\, d\vec{r}_1\, d\vec{r}_2$$

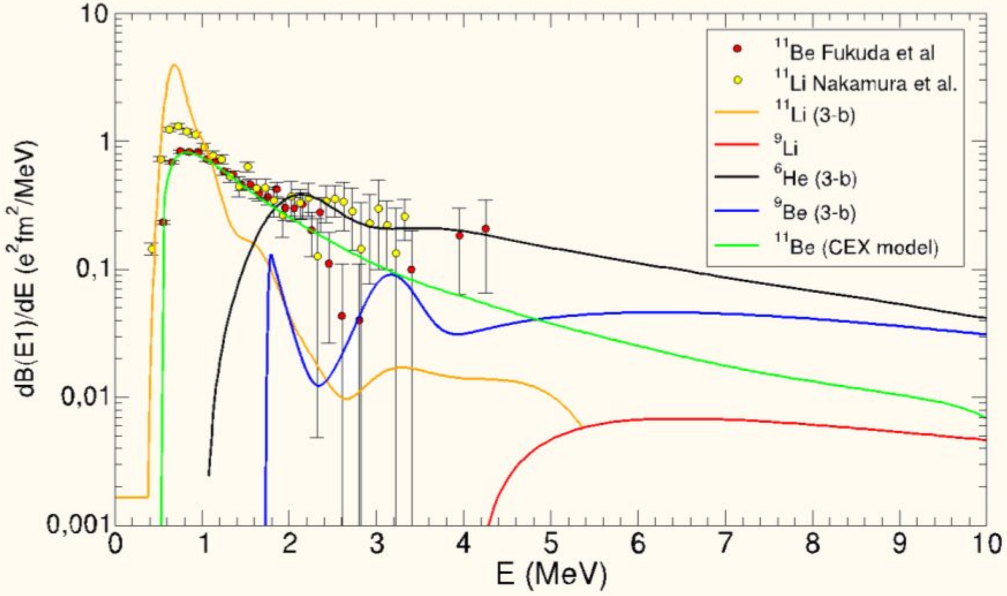

Coulomb dipole polarization effect

studying the intensity of
the imaginary CDP potential

TABLE I. Break-up threshold of light stable and exotic nuclei.

system	cluster	ε_b (MeV)
^{11}Li	^{9}Li+2n	-0.396
^{11}Be	^{10}Be+1n	-0.501
^{6}He	^{4}He+2n	-0.975
^{6}Li	α+d	-1.473
^{9}Be	^{8}Be+1n	-1.574
^{9}Be	$\alpha+\alpha$+1n	-1.664
^{7}Li	α+t	-2.467
^{9}Li	^{7}Li+2n	-4.062
^{10}B	^{6}Li+α	-4.461
^{18}O	^{14}C+α	-6.228
^{16}O	^{12}C+α	-7.162
$^{12}C^{g.s.}$	^{8}Be+α	-7.367
$^{12}C^{H.s.}$	^{8}Be+α	-7.653
^{4}He	^{3}He+1n	-20.6

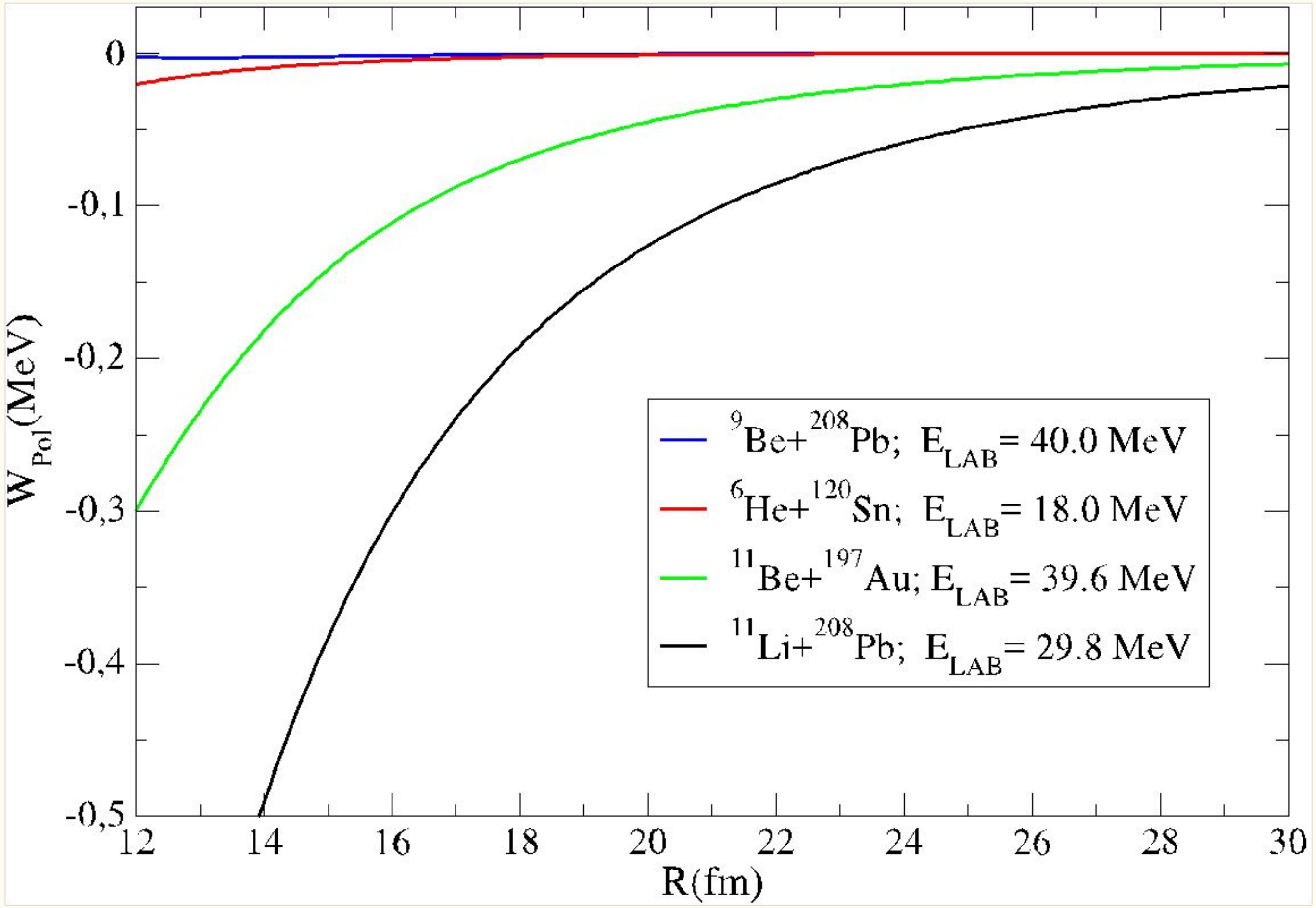

Coulomb dipole polarization effect

studying the intensity of
the imaginary CDP potential

TABLE I. Break-up threshold of light stable and exotic nuclei.

system	cluster	ε_b (MeV)
^{11}Li	^{9}Li+2n	-0.396
^{11}Be	^{10}Be+1n	-0.501
^{6}He	^{4}He+2n	-0.975
^{6}Li	α+d	-1.473
^{9}Be	^{8}Be+1n	-1.574
^{9}Be	$\alpha+\alpha$+1n	-1.664
^{7}Li	α+t	-2.467
^{9}Li	^{7}Li+2n	-4.062
^{10}B	^{6}Li+α	-4.461
^{18}O	^{14}C+α	-6.228
^{16}O	^{12}C+α	-7.162
$^{12}C^{g.s.}$	^{8}Be+α	-7.367
$^{12}C^{H.s.}$	^{8}Be+α	-7.653
^{4}He	^{3}He+1n	-20.6

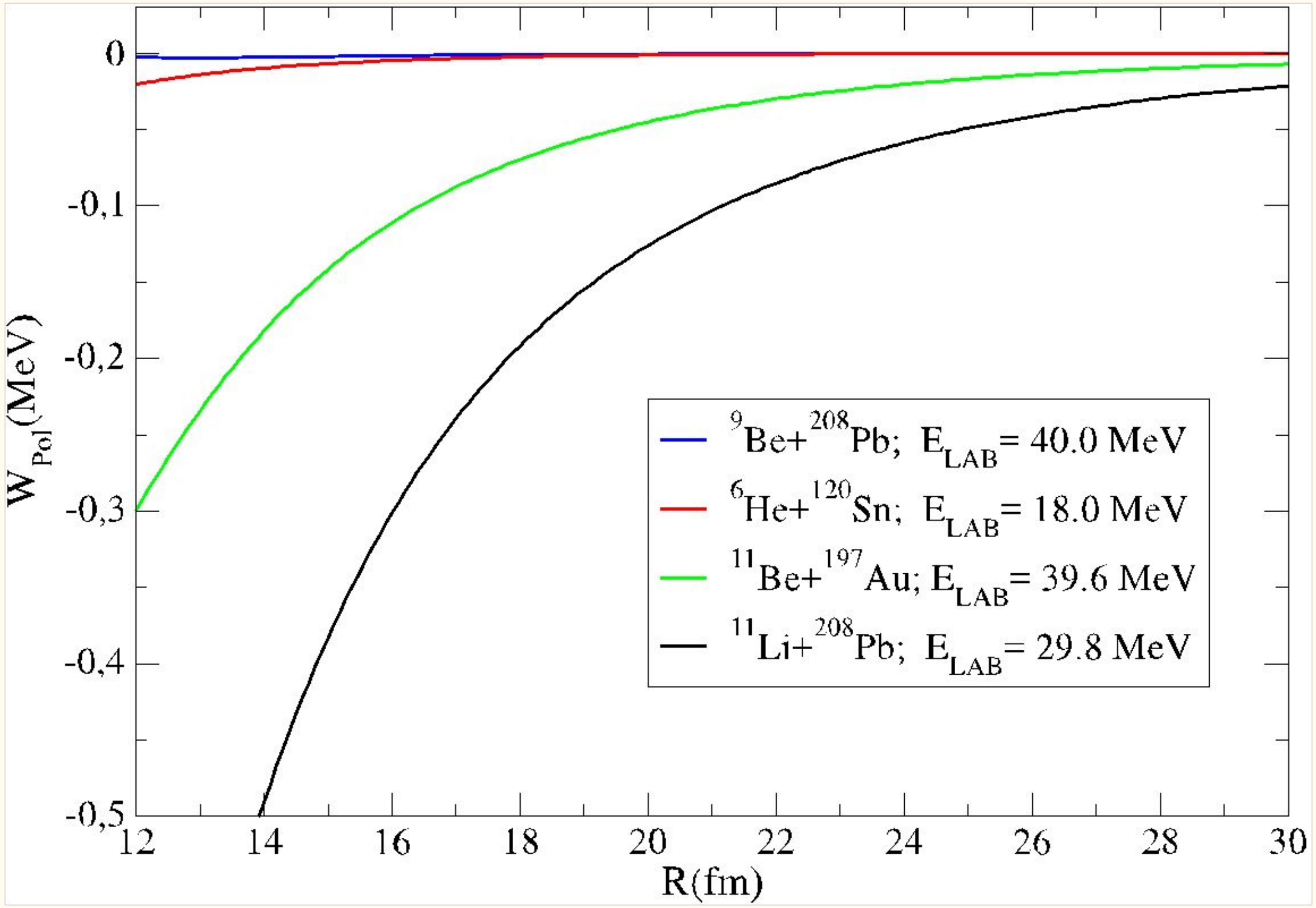

Coulomb dipole polarization effect

studying the intensity of
the imaginary CDP potential

TABLE I. Break-up threshold of light stable and exotic nuclei.

system	cluster	ε_b (MeV)
^{11}Li	^{9}Li+2n	-0.396
^{11}Be	^{10}Be+1n	-0.501
^{6}He	^{4}He+2n	-0.975
^{6}Li	α+d	-1.473
^{9}Be	^{8}Be+1n	-1.574
^{9}Be	$\alpha+\alpha$+1n	-1.664
^{7}Li	α+t	-2.467
^{9}Li	^{7}Li+2n	-4.062
^{10}B	^{6}Li+α	-4.461
^{18}O	^{14}C+α	-6.228
^{16}O	^{12}C+α	-7.162
$^{12}C^{g.s.}$	^{8}Be+α	-7.367
$^{12}C^{H.s.}$	^{8}Be+α	-7.653
^{4}He	^{3}He+1n	-20.6

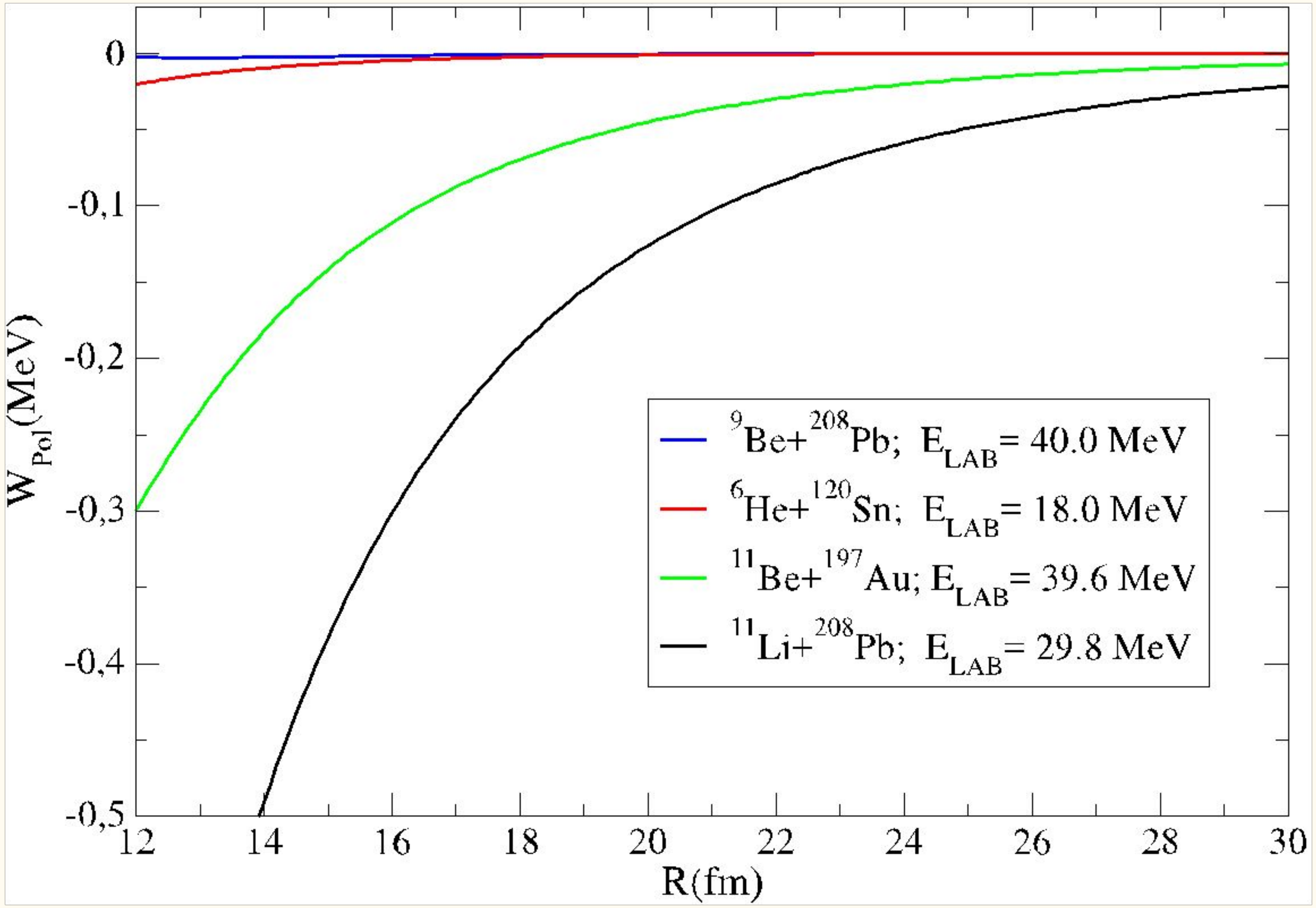

Coulomb dipole polarization effect

studying the intensity of
the imaginary CDP potential

TABLE I. Break-up threshold of light stable and exotic nuclei.

system	cluster	ε_b (MeV)
^{11}Li	^{9}Li+2n	-0.396
^{11}Be	^{10}Be+1n	-0.501
^{6}He	^{4}He+2n	-0.975
^{6}Li	α+d	-1.473
^{9}Be	^{8}Be+1n	-1.574
^{9}Be	$\alpha+\alpha$+1n	-1.664
^{7}Li	α+t	-2.467
^{9}Li	^{7}Li+2n	-4.062
^{10}B	^{6}Li+α	-4.461
^{18}O	^{14}C+α	-6.228
^{16}O	^{12}C+α	-7.162
^{12}C$^{g.s.}$	^{8}Be+α	-7.367
^{12}C$^{H.s.}$	^{8}Be+α	-7.653
^{4}He	^{3}He+1n	-20.6

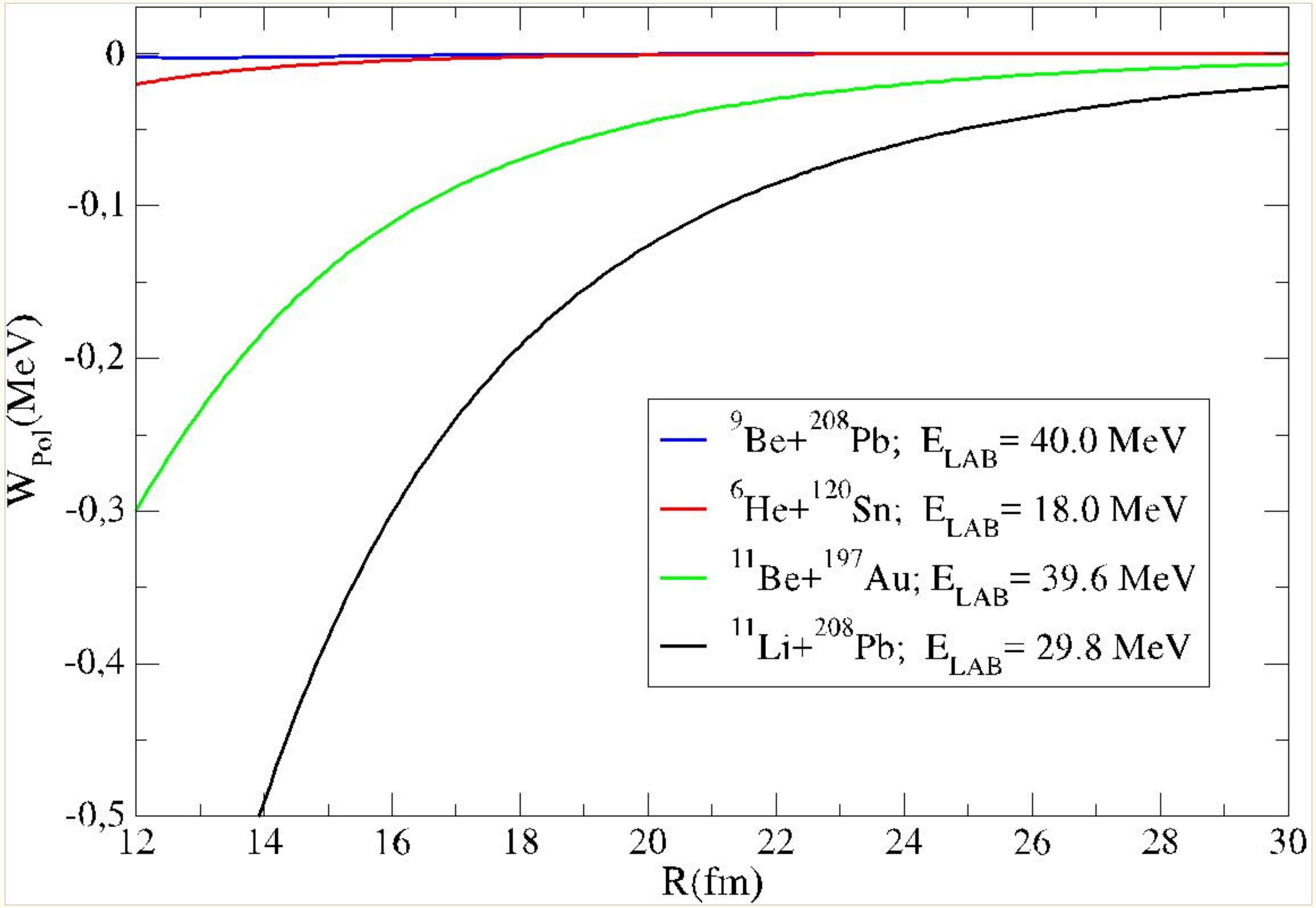

Coulomb dipole polarization effect

$$U_{opt}(R) = V_{SPP}(R) + iN_I V_{SPP}(R) + V_{pol}(R) + iW_{pol}(R)$$

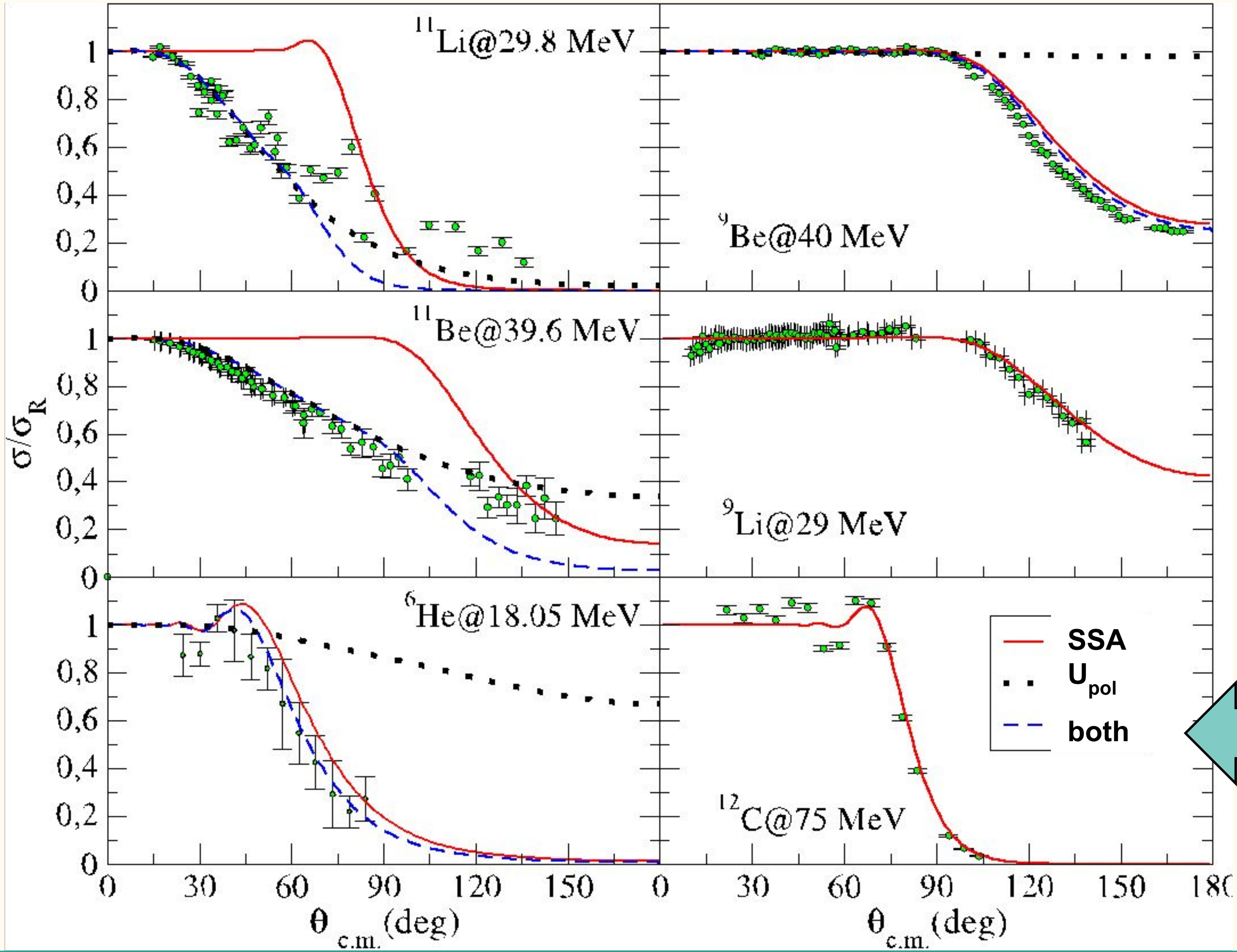

$^{12}C + ^{208}Pb$

Coulomb dipole polarization effect

$$U_{opt}(R) = V_{SPP}(R) + iN_I V_{SPP}(R) + V_{pol}(R) + iW_{pol}(R)$$

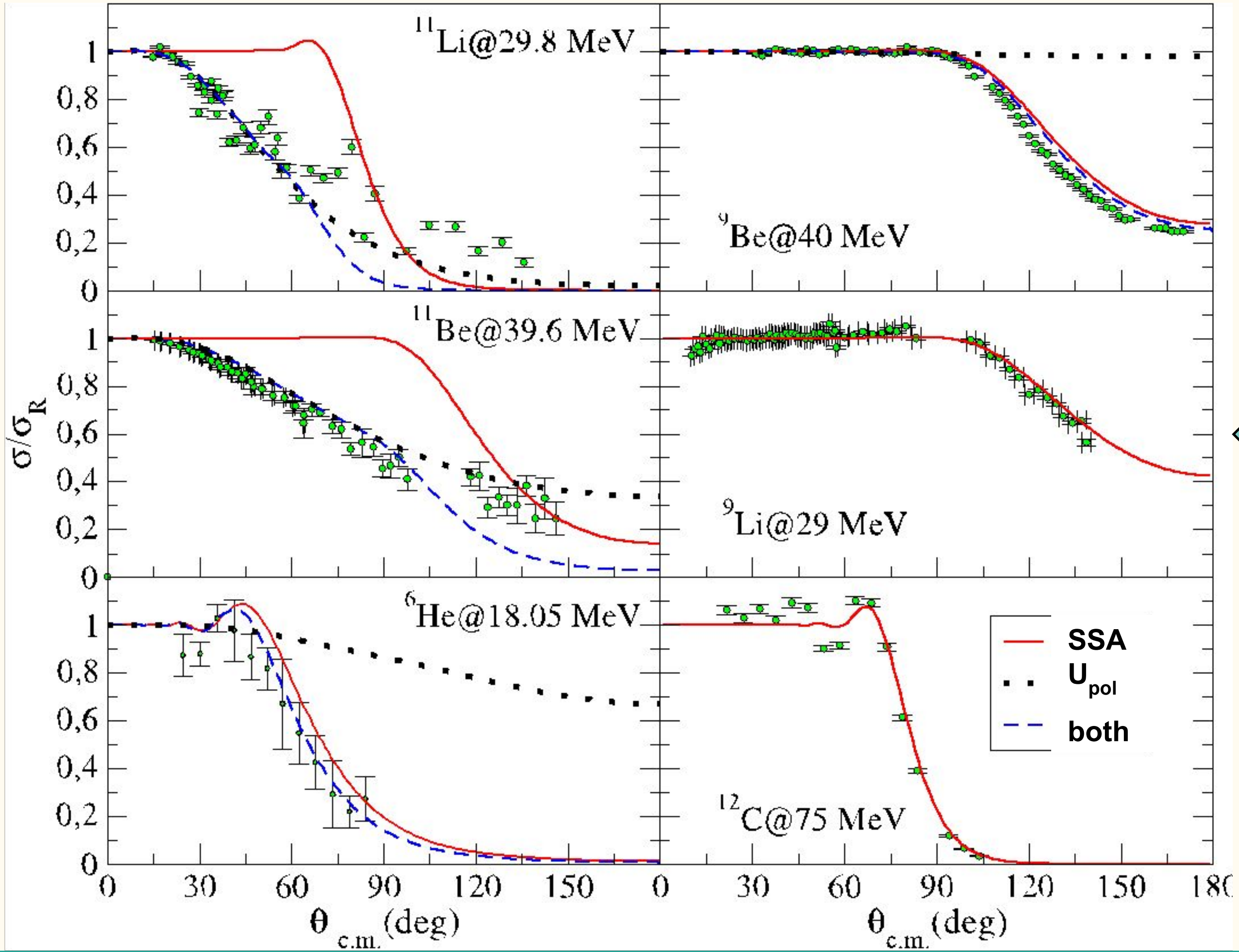

$^{9}Li + ^{208}Pb$

Coulomb dipole polarization effect

$$U_{opt}(R) = V_{SPP}(R) + iN_I V_{SPP}(R) + V_{pol}(R) + iW_{pol}(R)$$

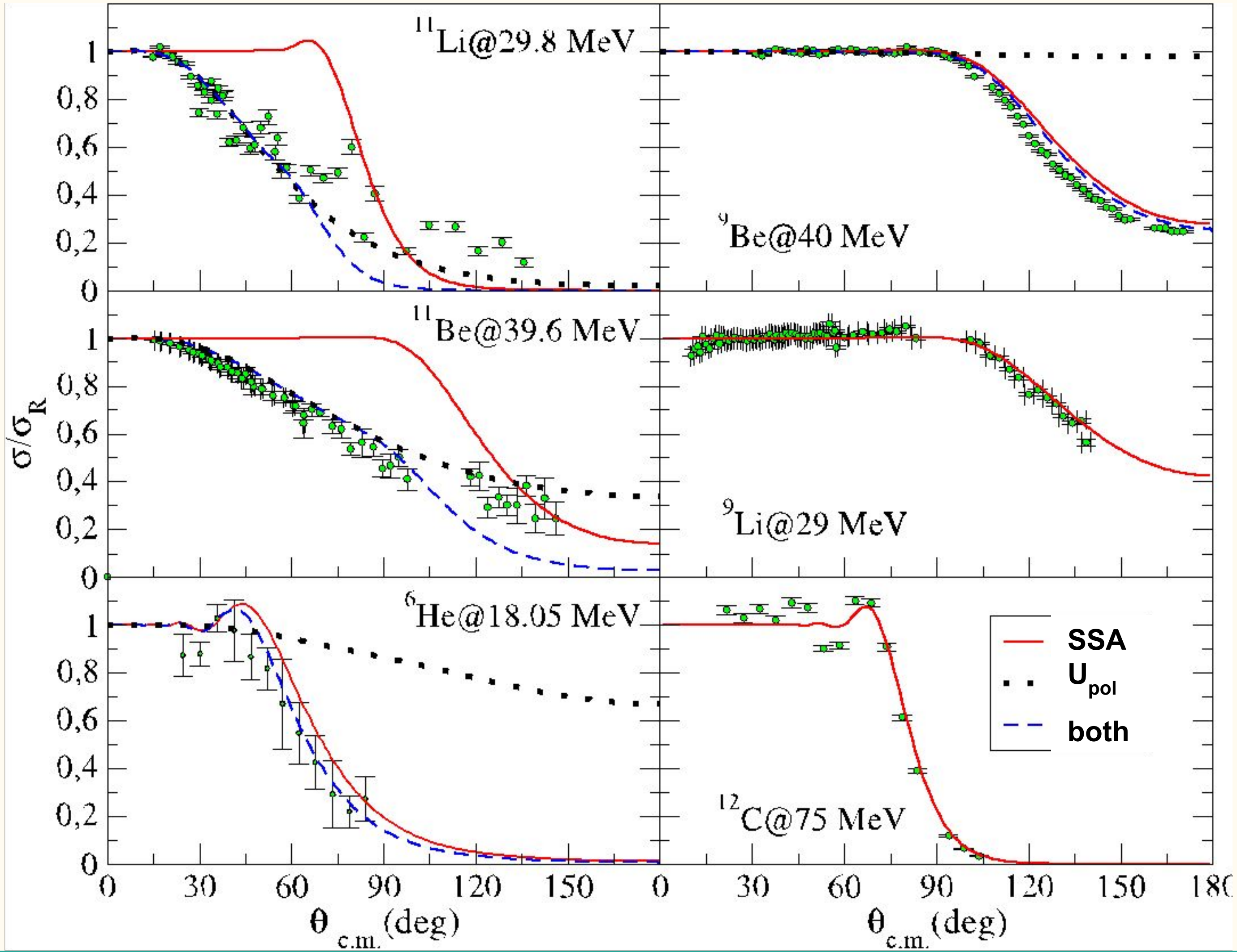

$^{9}Be + ^{208}Pb$

Coulomb dipole polarization effect

$$U_{opt}(R) = V_{SPP}(R) + iN_I V_{SPP}(R) + V_{pol}(R) + iW_{pol}(R)$$

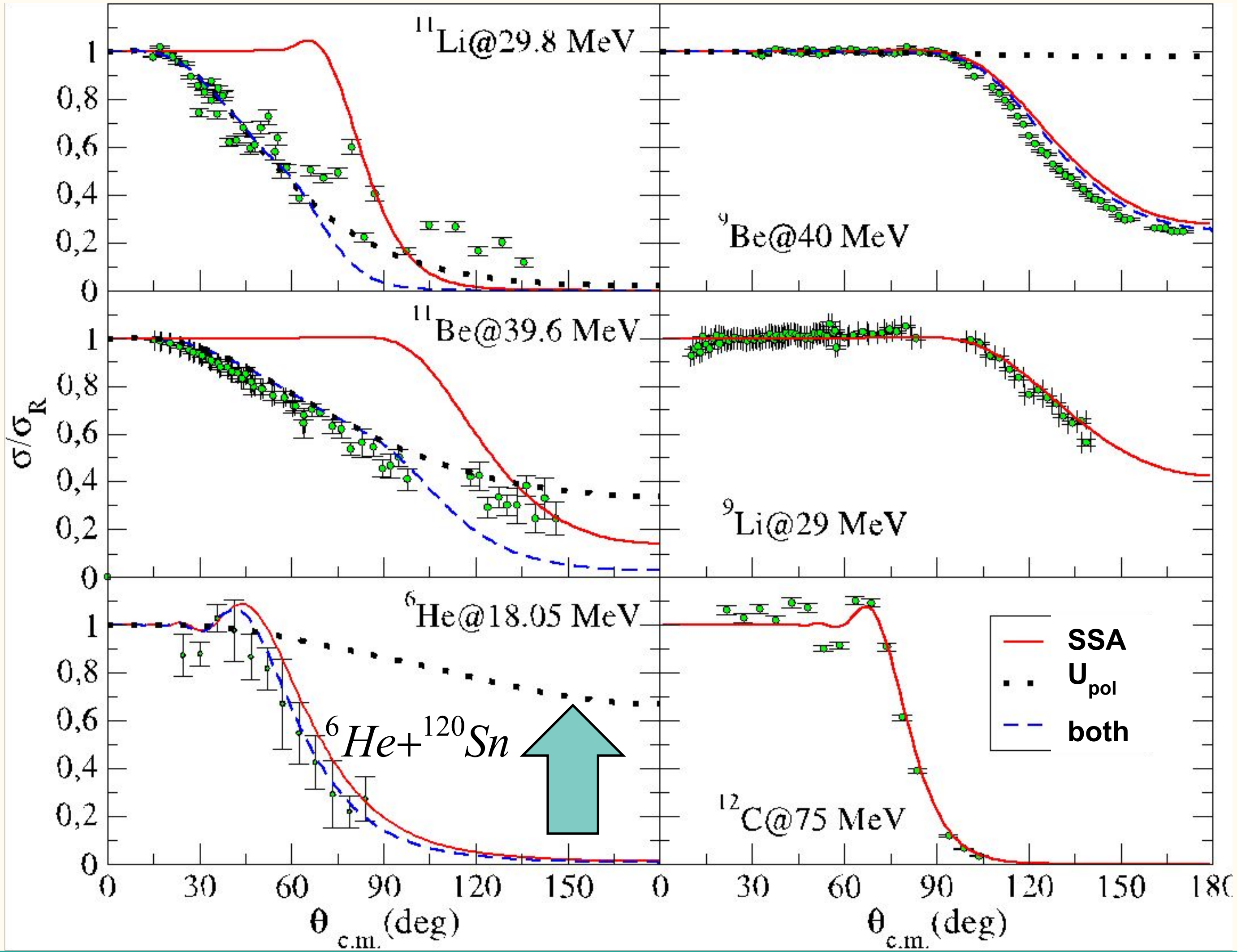

Coulomb dipole polarization effect

$$U_{opt}(R) = V_{SPP}(R) + iN_I V_{SPP}(R) + V_{pol}(R) + iW_{pol}(R)$$

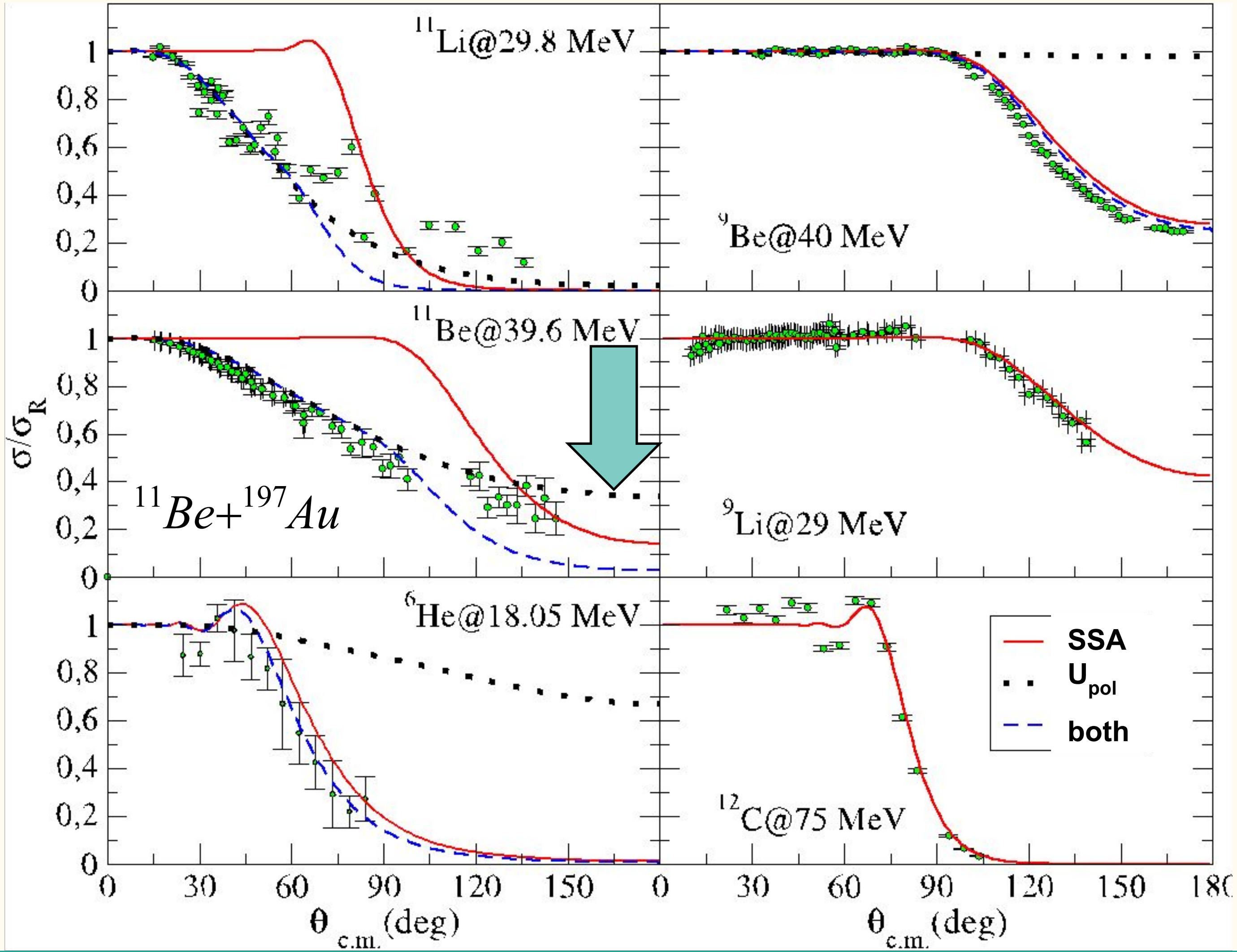

Coulomb dipole polarization effect

$$U_{opt}(R) = V_{SPP}(R) + iN_I V_{SPP}(R) + V_{pol}(R) + iW_{pol}(R)$$

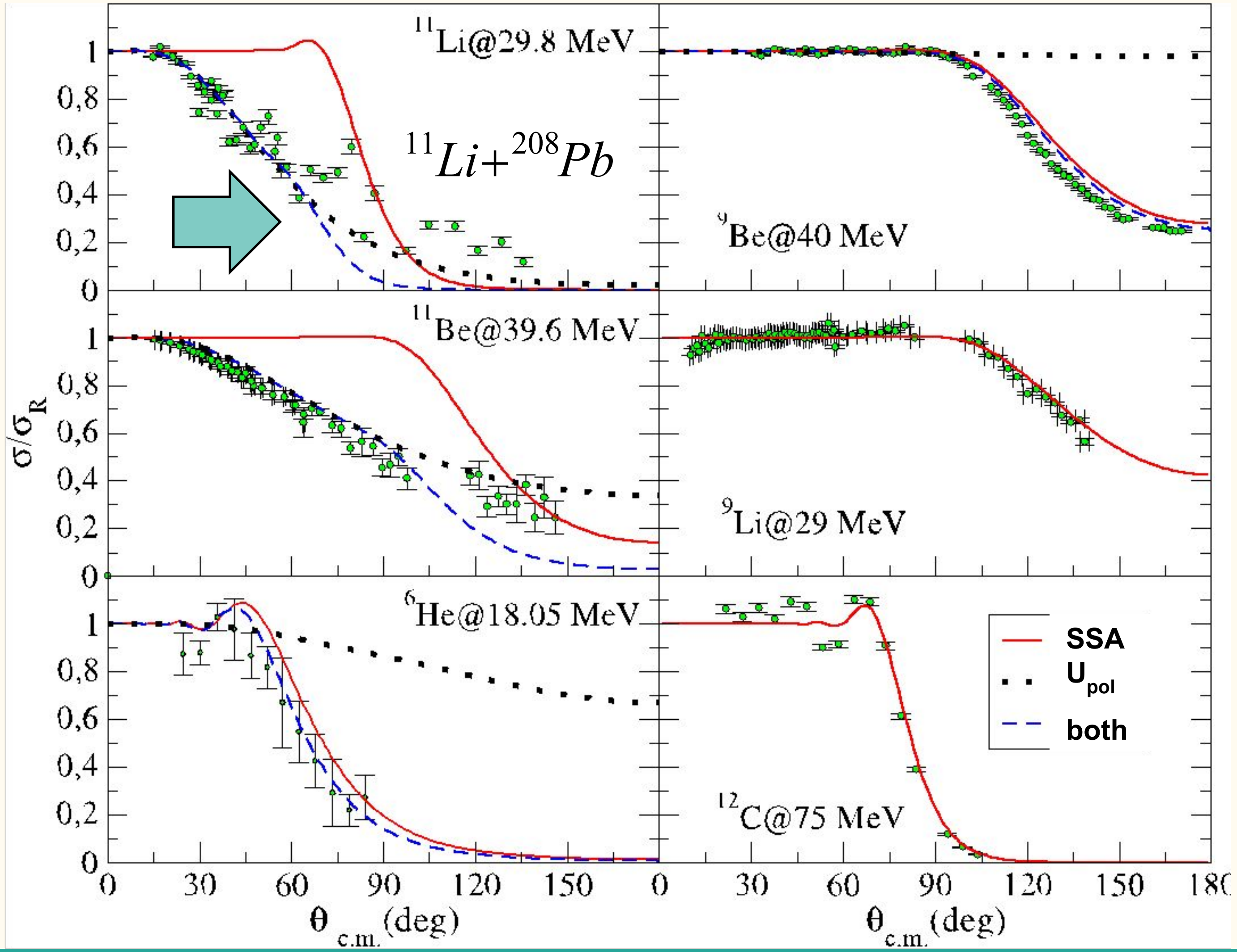

1. The Laboratories and SETUP´s

2. The Theoretical Optical Model

3. Experimental Data x Theoretical Calculations

4. Conclusions

CONCLUSIONS:

- We work on an international network based on using pelletron-tandem facilities.
- We have analysed 40 elastic scattering angular distributions of stable strongly bound, weakly bound and exotic nuclei, mainly on ^{120}Sn, at energies below, around and above the Coulomb barriers.
- We have analysed them with an OP based on the nuclear São Paulo Potential, allowing the most sensitive parameter to vary, which showed to be strongly connected to the projectile binding energy.
- Within this context, we have also showed the importance of the Coulomb dipole polarization potential, derived from the semi-classical theory of Coulomb excitation.
- We identified the evolution of ***long-range absorption*** as a function of the projectile binding energy, which, for more exotic nuclei, is dominated by the Coulomb interaction.
- The proposed approach shows to be a fundamental basis to study any nuclear reaction.

PHYSICAL REVIEW C **100**, 064602 (2019)

Systematic study of optical potential strengths in reactions on ^{120}Sn involving strongly bound, weakly bound, and exotic nuclei

M. A. G. Alvarez, J. P. Fernández-García, and J. L. León-García
Departamento FAMN, Universidad de Sevilla, Apartado 1065, 41080 Sevilla, Spain

M. Rodríguez-Gallardo
Departamento FAMN, Universidad de Sevilla, Apartado 1065, 41080 Sevilla, Spain
and Instituto Carlos I de Física Teórica y Computacional, Universidad de Sevilla, Spain

L. R. Gasques, L. C. Chamon, V. A. B. Zagatto, A. Lépine-Szily, and J. R. B. Oliveira
Universidade de Sao Paulo, Instituto de Fisica, Rua do Matao, 1371, 05508-090 Sao Paulo, SP, Brazil

V. Scarduelli
Instituto de Física, Universidade Federal Fluminense, 24210-340 Niterói, Rio de Janeiro, Brazil
and Instituto de Física da Universidade de São Paulo, 05508-090 São Paulo, SP, Brazil

B. V. Carlson
Departamento de Física, Instituto Tecnológico de Aeronáutica, São José dos Campos, SP, Brazil

J. Casal
Dipartimento di Fisica e Astronomia "G. Galilei" and INFN-Sezione di Padova, Via Marzolo, 8, I-35131 Padova, Italy

A. Arazi
Laboratorio TANDAR, Comisión Nacional de Energía Atómica, Av. Gral. Paz 1499, BKNA1650 San Martín, Argentina

D. A. Torres and F. Ramirez
Departamento de Física, Universidad Nacional de Colombia, Bogotá, Colombia

RECENT PUBLICATIONS:

- Physical Review C 101, 044604 (2020)
- Physical Review C 101, 044601 (2020)
- Physical Review C 100, 064602 (2019)
- Physical Review C 99, 054605 (2019)
- Physical Review C 99, 064617 (2019)
- Physical Review C 99, 014601 (2019)
- Physical Review C 98, 064601 (2018)
- Physical Review C 98, 034615 (2018)
- Physical Review C 98, 024621 (2018)
- Physical Review C 97, 034629 (2018)
- Physical Review C 95, 064614 (2017)

THANK YOU FOR YOUR ATTENTION